A FUNCTIONAL ANALYSIS OF LIVER- AND INTESTINAL-

FATTY ACID BINDING PROTEINS IN THE INTESTINAL

ENTEROCYTE: STUDIES IN NULL MICE

by

ANGELA MARIE GAJDA

A dissertation submitted to the

Graduate School-New Brunswick

Rutgers, The State University of New Jersey

In partial fulfillment of the requirements

For the degree of

Doctor of Philosophy

Graduate Program in Nutritional Sciences

Written under the direction of

Dr. Judith Storch

And approved by

_____

_____

_____

_____

_____

New Brunswick, New Jersey

May 2014

ABSTRACT OF THE DISSERTATION

A Functional Analysis of Liver- and Intestinal Fatty Acid Binding Proteins in the Intestinal

Enterocyte: Studies in Null Mice

By ANGELA MARIE GAJDA

Dissertation Director:

Dr. Judith Storch

The fatty acid binding protein (FABP) family consists of 14-15 kD cytoplasmic proteins, which are abundantly expressed in various mammalian tissues. In the enterocyte, two FABPs are present: Liver-type FABP (LFABP; FABP1), and Intestinal FABP (IFABP; FABP2). Previous studies in chow-fed mice did not reveal marked differences between IFABP or LFABP null mice, thus we hypothesized that feeding high-fat diets would provide a lipid overload to the intestine, perhaps revealing phenotypic differences that would provide insight into the individual functions of LFABP and IFABP. We directly compared IFABP$^{-/-}$, LFABP$^{-/-}$, and WT mice fed low or high fat diets. Changes in mucosal lipid metabolism were observed, with a decrease in FA incorporation into triacylglycerol (TG) relative to phospholipid (PL) in IFABP$^{-/-}$ mice, and reduced monoacylglycerol incorporation in TG relative to PL and reduced FA oxidation in LFABP$^{-/-}$ mice. Striking changes in whole body phenotypes were found: LFABP$^{-/-}$ mice fed a high-fat diet had greater weight gain and fat mass relative to WT, while IFABP$^{-/-}$ mice remained lean. Respiratory exchange ratios suggest that high-fat fed LFABP$^{-/-}$ mice preferentially oxidize lipids, while IFABP$^{-/-}$ mice preferentially metabolize carbohydrate as a fuel source. IFABP$^{-/-}$ mice are healthy with a lean phenotype, whereas LFABP$^{-/-}$ mice are obese but are otherwise metabolically normal. To further elucidate the individual and overlapping functions of enterocyte FABPs, we

generated a novel strain of mice that were null for both IFABP and LFABP (DKO). The phenotype

of DKO mice fed a high-fat diet was integrated between LFABP$^{-/-}$ and IFABP$^{-/-}$ mice, with body

weights and composition in between the single knockout mice. DKO mice fed a high-fat diet

were similar to IFABP$^{-/-}$ mice in primarily using carbohydrate for energy. It was also observed

that DKO mice were less active relative to WT mice. Importantly, there were no differences

between groups in fecal lipids, suggesting that LFABP and IFABP are not involved with bulk FA

uptake into the intestine. Overall, the results of these studies strongly suggest that IFABP and

LFABP have different functions in intestinal lipid metabolism, which result in downstream

alterations in whole body energy metabolism.

Acknowledgements

I would like to thank Dr. Judy Storch for being my graduate mentor. I feel very privileged to have had the opportunity to work in her lab and learn from her. I have also been very fortunate to have the assistance of helpful committee members for their support in my graduate process. I would like to thank Dr. Dawn Brasaemle for her very helpful advice, which has helped with my project, and which has helped me to complete the graduate program. I would like to thank Dr. Greg Henderson for always having an open door to very helpful discussions on exercise physiology. I would also like to thank Dr. Loredana Quadro for her thoughtful questions and suggestions, which have helped me throughout the process. I would like to thank Dr. Bill Blaner for providing additional expertise on my work.

The Storch laboratory has a wonderful group of people that I have been fortunate to work with. I would like to thank Yin Xiu Zhou for her expertise in animal surgery as well as her constant support. I would like to thank Sarala Kodukula for her patience with helping me learn laboratory techniques and for her continuous encouragement. I would also like to thank Dr. John Douglass and Dr. Leslie McCauliff for their advice and support through the last 6 years. We started out the program at the same time and I really enjoyed working with them throughout our doctoral studies. I would also like to thank the undergraduate students in the lab that had helped me including Khamoshi Patel, Melissa Boodoo, Valerie Lim, Ran Li, and Arete Pappas. Working with them gave me the opportunity to learn how to be a mentor and I hope their experience will help them in their future endeavors.

I would like to thank Dr. Anita Brinker from the Rutgers Institute for Food Nutrition and Health for her help for the LC/MS work and for her expertise with all of the analysis.

Table of Contents

Page

List of Tables

List of Figures

Chapter 3

Appendix

List of Abbreviations

2-AG	2-arachidonoylglycerol
2-MG	*sn*-2-monoacylglycerol
ACADL	Acyl CoA dehydrogenase, long chain
ACOX1	Acyl-CoA oxidase
AEA	Arachidonoyl ethanolamide
AFABP	Adipocyte fatty acid binding protein
AMPK	Adenosine monophosphate-activated protein kinase
ANOVA	Analysis of variance
ApoB48	Apolipoprotein B 48
ATGL	Adipose triglyceride lipase
AUC	Area under the curve
BL	Basolateral
CB1	Cannabinoid receptor type 1
BW	Body weight
CCK	Cholecystokinin
CCOX	Cytochrome c oxidase
CD36	Cluster of differentiation 36
CRBP	Cellular retinoid binding protein
DG	Diacylglycerol
DGAT	Diacylglycerol acyltransferase
DKO	Double knockout
DNA	Deoxyribonucleic acid
ER	Endoplasmic Reticulum
erGPAT	Glycerol-3-phosphate acyltransferase (GPAT3)
FA	Fatty acid
FAAH	Fatty acyl amide hydrolase
FABP	Fatty acid binding protein
FABPpm	Plasma membrane fatty acid binding protein
FATP	Fatty acid transfer protein
FFA	Free fatty acid
FM	Fat mass
FFM	Fat-free mass
FXR	Farnesoid X receptor

GI	Gastro-intestinal
GLP1	Glucagon-like peptide 1
GPAT	Glycerol-3-phosphate acyltransferase
h	Hour
HFABP	Heart fatty acid binding protein
HFS	High saturated fat diet
HFU	High unsaturated fat diet
HNF4α	Hepatic nuclear factor 4 alpha
IFABP	Intestinal fatty acid-binding protein
IFABP$^{-/-}$	Intestinal fatty acid-binding protein knockout
ILBP	Ileal lipid binding protein
KFABP	Keritinocyte fatty acid binding protein
KO	Knockout
LCFA	Long chain fatty acid
LC/MS	Liquid chromatography-coupled mass spectrometry
LFD	Low fat diet
LFABP	Liver fatty acid-binding protein
LFABP$^{-/-}$	Liver fatty acid-binding protein knockout
MCFA	Medium-chain fatty acid
MG	Monoacylglycerol
MGAT	Monoacylglycerol acyltransferase
MGL	Monoacylglycerol lipase
MHO	Metabolically healthy obese
min	Minute
mRNA	Messenger ribonucleic acid
MTP	Microsomal triglyceride transfer protein
mGPAT	Glycerol-3-phosphate acyltransferase (GPAT1)
NADHDe	Nicotinamide adenine dinucleotide dehydrogenase
NAE	N-acylethanolamines
NAPE	N-acetylphosphatidylethanolamines
NEFA	Non-esterified fatty acid
NPC1L1	Niemann-Pick C1-like 1
OEA	Oleoylethanolamide
PCTV	Prechylomicron transport vesicle

PEA	Palmitoylethanolamide
PL	Phospholipid
PPAR	Peroxisome proliferator-activated receptor
qPCR	Quantitative real time polymerase chain reaction
PYY	Peptide tyrosine tyrosine
RER	Respiratory exchange ratio
RNA	Ribonucleic acid
RXR	Retinoid X receptor
SEM	Standard error of the mean
SPA	Spontaneous physical activity
SRB1	Scavenger receptor class B1
SuccDe	Succinate dehydrogenase
TG	Triacylglycerol
t	Time
TLC	Thin layer chromatography
VCO2	Carbon dioxide production
VO2	Oxygen consumption
WT	Wild type

Chapter 1

Introduction and Review of the Literature

Introduction

Lipids are a diverse group of hydrophobic molecules including fatty acids (FA), triglycerides (TG), cholesterol, fat-soluble vitamins, ceremides, and phospholipids (PL), all of which can be extracted by organic solvents (1).   In particular, lipids provide an important source of energy in the diet because they have a higher caloric density per gram relative to carbohydrates and protein (2).   The typical American consumes about 33% of calories as dietary lipids, mostly in the form of TGs (3).   Concerns about lipid intake have grown in response to the increasing prevalence of obesity, hyperglycemia, hypertension, and high levels of blood lipids (triglycerides and cholesterol). A combination of these risk factors is associated with the metabolic syndrome, and Individuals having one of more of these risk factors have increased the chance for development of cardiovascular disease, diabetes, or stroke (4–6). Hence, it is important to understand how dietary lipids are processed in the human body in order to provide education and interventions to improve human health.

The overall aim of the research in this dissertation is to understand the functions of Intestinal–type (IFABP) and Liver-type fatty acid binding proteins (LFABP) in the intestinal enterocyte. They are structurally similar and are part of same family of intracellular lipid binding proteins (FABPs) that are known to have high affinity for binding to fatty acids. It is hypothesized that these proteins are involved in uptake and trafficking of lipids in the intestinal enterocyte for delivery into the circulation. LFABP and IFABP are highly expressed in the cytosol of the intestinal enterocyte and are known to bind to fatty acids, but it is not clear why two similar proteins are present in one cell type.   In these studies, transgenic mice that do not express each of these proteins were used to help elucidate the individual functions of IFABP and LFABP.

Previously, studies in our laboratory showed some changes resulting from ablation of these proteins, but a robust phenotype was not observed during regular chow feeding (7). The present work involves a high-fat diet-feeding regimen, thereby providing an overabundance of lipid to the intestine in order to characterize the phenotypes resulting from ablation of these proteins. Additionally, we have also developed a novel mouse strain in which both of these proteins have been simultaneously ablated so that we are able to compare these animals to each of the single IFABP and LFABP-null mice. The overall goal is to uncover the individual functions of these proteins in intestinal lipid metabolism, and secondary effects on systemic energy metabolism.

Dietary Triglycerides

Dietary triglycerides are the major source (>90%) of lipid in the human diet, of which consumption by Western societies can range to over 100 g per day (8). TGs consist of three FAs esterified to a glycerol molecule, which can be hydrolyzed by lipases to free fatty acids (FFA). The majority of TGs consumed in the human diet are rich in long chain saturated or unsaturated FA (LCFA), which contain 14 or more carbons. It is known that Americans and other Western populations consume high amounts of saturated LCFA, such as palmitate (C16:0) and stearate (C18:0) from animal-derived fat sources such as butter or lard (9). Consumption of high levels of long chain saturated fatty acid has been linked to higher risk of cardiovascular disease (10). In contrast, the Mediterranean diet is rich in unsaturated LCFA from plant oils and seems to promote a healthy cardiovascular profile (11, 12). Among the most common unsaturated LCFAs in the diet, linoleic acid (C18:2 n-6) and linolenic acid (C18:3 n-3) are present in plant oils and are actually required in the mammalian diet because they are not synthesized endogenously (13,

14) . Medium-chain FAs (MCFAs) also make up a small amount of the human diet. These FA

consist of 8-12 carbon chains, with coconut oil being a major source (15).

Digestion of Triglycerides

The gastrointestinal tract (GI) is made up of several organs in the body including the esophagus,

stomach, small intestine, and large intestine with the lumen of these organs being entirely

exposed to the outside environment. A primary responsibility of the GI tract is for digestion and

absorption of nutrients in the body, including lipids.   Digestion of TG begins in the stomach

where grinding and peristalsis in the stomach provides for emulsification of the lipids in the

bolus to form chyme (1). Hydrolysis of TG into DG and FA occurs by gastric lipase, an enzyme,

which is secreted by chief cells in the epithelium of the stomach, and unlike most peptides in the

body, is active at the low pH of the stomach (16). This lipase is largely responsible for hydrolysis

of TG to form sn-2,3-diacyglycerol (DG) and FA, which are transported past the pyloric sphincter

into the small intestine (1).

As the chyme travels into the small intestine, pancreatic lipase is secreted from the pancreas

into the intestinal lumen providing for further hydrolysis of diacylglycerols at the sn-3 position to

form into the primary endproducts of 2-monacylglycerol (2-MG) and FA in the lumen of the

small intestine (16). As the digesta travels through the intestinal lumen, the lipids are present in

a bulk fluid phase, which does not mix well with what is known as the "unstirred water layer"

which lies between the bulk fluid and the endothelial layer (16). Bile salts, synthesized in the

liver, are detergents that are secreted into the duodenum for emulsification of dietary lipids,

which then form micelles in the lumen (17). Micelles allow for movement of the lipids across

the unstirred water layer, allowing for monomeric uptake of lipids into intestinal cells, thereby

providing for efficient absorption (1). Any residual lipids enter the large intestine and are

exposed to the large microbiome and subsequently leave the body from the anus as a

constituent of feces.   The absorption process for lipids is highly efficient, with greater than 95%

uptake of the dietary fat ingested (18).

The Small Intestine

The small intestine is the major site of lipid absorption in the gastrointestinal tract.   Starting

from the stomach, the intestine forms a long tube from the stomach to the cecum, with three

regions that include the duodenum, jejunum, and the ileum (1). The ileum ends at the cecum

where the digesta is fermented by the large microbiome present in the large intestine. The

majority of lipid absorption occurs in the jejunum with bile acid uptake primarily occurring in the

ileum (16).

The intestine consists of several layers of cells including the mucosa, submucosa, muscularis

propia, and the serosal layer (16, 19). The mucosal layer consists of the cells with the important

role of nutrient absorption, as well as functioning as nutrient sensors (the latter will be

discussed in a separate section below). The mucosa forms small folds, known as villi, which

increase the surface area of the intestine to 200 m^2 for enhanced absorption (16).   The villi are

lined with epithelial cells, known as enterocytes, which are primarily involved with nutrient

uptake and absorption. These cells form a brush border (apical side of the cells), providing for

efficient absorption of nutrients (20). Goblet cells, also present in the villi, secrete glycoproteins

forming mucin that aid in reducing friction during transit of digesta through the intestine (21).

Between the villi, new epithelial cells are formed in the crypts (20). The cells are constantly being replenished; as the cells age, they travel towards the top of the villi before being sloughed off into the lumen (22, 23). Paneth cells also are located in the crypt region of the intestine and are involved with secretion of antimicrobial agents such as lysozyme and phospholipase A2 (24). These cells function to preserve a barrier between the exterior environment of the lumen and the rest of the body (16).

On the basolateral side of the enterocytes, lymphatic capillaries (lacteals) in the submucosal region absorb the chylomicrons formed in the enterocytes for subsequent delivery into the general circulation. The muscularis propia forms a layer of muscle cells around the submucosa, and is involved with peristalsis for movement of the digesta through the lumen, but also is innervated by the Vagus nerve for control of peristalsis and communication with the hindbrain for control of food intake (25). Finally, the mesothelial layer of cells forms the outer serosal layer of the intestine, providing a protective layer around this organ (16).

FA and MG Uptake into the Enterocyte

In the intestinal lumen, two FAs and one 2-MG form the main products of hydrolysis of TG in the intestinal lumen. Uptake of these lipids occurs via the apical membrane side of the intestinal enterocyte, also called the brush border membrane (26). The mechanism of uptake of these lipids is still not completely understood. It is known that lipids can cross the apical membrane by diffusion, but it is thought that membrane transport proteins are also involved in transport into the enterocyte because kinetic studies have shown that the uptake of FA is saturable (27). FATP4 (Fatty Acid Transport Protein 4), FABPpm (Plasma membrane FABP), and CD36 (Cluster of

Differentiation 36) are enterocyte membrane proteins which are known to have affinity for binding to FA and are thought to have a role in uptake (28, 29).

CD36 is a plasma membrane protein present in the proximal region of the small intestine and is known bind to FA, lipoproteins, collagen, among others (30). Some studies show that upon binding to a FA, this protein translocates into the cytosol where it is involved in a complex which forms prechylomicron transport vesicles (PCTV) that bud from the endoplasmic reticulum (ER) (31).   The importance of CD36 in chylomicron formation was evident when CD36-null mice were given a 6 hour lipid infusion resulting in increased TG in the intestine due to decreased transport into the lymph (32).   CD36 is likely involved with uptake of very long chain FA (>20 carbon) as it was observed that $CD36^{-/-}$ mice had an increase in fecal fat, but not when administered LCFA (12-20 carbon) (32, 33). Ultimately, total uptake of FA is not decreased in spite of ablation of CD36; it was observed that FA absorption shifts towards the distal regions of the intestine in $CD36^{-/-}$ mice (34).

Fatty acid transport protein 4 (FATP4) is also a membrane protein, and is found on the brush border of the enterocytes as well as the endoplasmic reticulum (35, 36). This protein also functions as an enzyme for conversion of FA into FA acyl CoAs (28).   Due to its affinity for binding FAs, it was thought this protein was involved with uptake. However, it was observed that FATP4-null mice do not have steatorrhea or reduced uptake into the intestine, suggesting that this protein does not likely play a large role in FA uptake (35).   Plasma membrane fatty acid binding protein (FABPpm), a 40 kD protein also has high affinity for FA and its expression is increased in response to fasting and also endurance training, suggesting that it is may also be involved in uptake of FA (37–39).

As found for FAs, 2-MGs are thought to be taken up into the enterocyte by a combination of passive diffusion and active transport via a membrane lipid binding protein, as studies in Caco-2 cells revealed that MG uptake is saturable (27, 40). Interestingly, when excess FA, but not DG was also added to the medium of Caco-2 cells, uptake of 2-MG was reduced, suggesting that that the same transport protein(s) may be involved with uptake of FA and 2-MG into the enterocyte (27, 41).

Intestinal Lipid Metabolism

When the FAs and 2-MG arrive into the intestinal enterocyte from the lumen, they undergo further processing for various functions. Importantly, FA accretion in the cell is toxic (42, 43), thus the cell has to process the FAs in order to prevent excess accumulation. The FAs are activated by Long-chain fatty acid acyl CoA synthetase (ACSL) in an ATP-dependent reaction to form FA acyl CoAs, with the primary isoform in the intestine known as ACSL5 (44). After activation, the acyl CoAs are then incorporated into TGs. The TGs are primarily included as constituents of chylomicrons, large ApoB48-containing lipoproteins that are secreted out of the basolateral side of the enterocyte and into the lymph and eventually into the general circulation (26). Indeed, FAs are also utilized for other functions in the cell (45).   The FAs and 2-MGs can be reincorporated into TGs and may be stored in lipid droplets. Fatty acyl CoAs can be incorporated into membrane phospholipids, which form selective barriers around the cells as well as cellular organelles. FAs can also be transported to the mitochondria or peroxisomes for oxidation. Additionally, FAs can play a role in regulation of gene expression by serving as ligands for RNA transcription factors (45).

In the intestinal enterocyte, TG synthesis occurs via 2 different pathways (Figure 1-1). The MGs can be formed into DG, by acylation of one FA by Acyl-CoA:monoacylglycerol acyl transferase-2 (MGAT2) in the endoplasmic reticulum, the first reaction of what is known as the MGAT pathway (46). An additional FA is acylated to the glycerol backbone to form TG by diacylyglycerol acyl transferase (DGAT) in the endoplasmic reticulum (47).   In the intestine, both DGAT1 and DGAT2 isoforms are present, with the former present on the inside of the ER, and the latter on the cytosolic side (29). The MGAT pathway is the predominant route (75%) for TG formation in the intestinal enterocyte, unlike other tissues, due to the very high abundance of MGs formed from dietary TGs in the intestinal lumen (48–50).

During times of limited MG availability, an alternative pathway for TG synthesis exists (51). The so-called glycerol-3-phosphate acyl transferase (GPAT) pathway is present in all cell types, including the intestinal enterocyte. The GPAT enzyme converts glycerol-3-phosphate to lysophosphatidic acid by addition of a FA CoA. 1-acylglycerol-3-phosphate acyltransferase (AGPAT) transfers a FA CoA to lysophosphatidic acid to form phosphatidic acid. Phosphatidic acid can then be formed into DG by phosphatidic acid phosphatase, and subsequently, the DGAT enzyme can acylate an FA to DG to form TG. In addition, DGs can be formed into phospholipids (PL) (52).

Figure 1-1
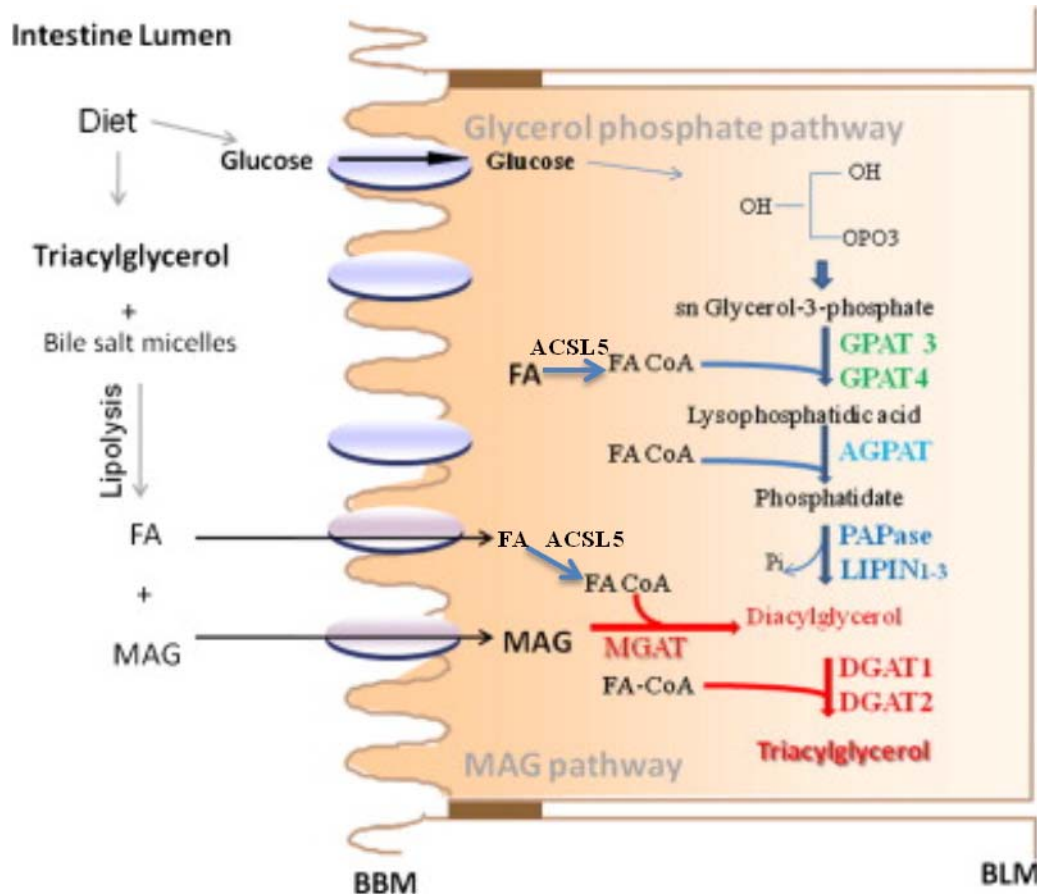
Figure 1-1. FA and MG uptake re-esterification in the intestinal enterocyte. Triglycerides are hydrolyzed by lipases into FA and MG in the lumen of the small intestine. FAs and MGs cross the brushborder membrane of the intestinal enterocyte. In the enterocyte, FAs are activated by ACSL5 to form FA CoAs. In the intestine, TGs are primarily resynthesized via the MGAT pathway, but the G3P pathway is an alternate route. *FA; Fatty acid*; *FA CoA, Fatty acid acyl coenzyme A*; *ACSL5 long-chain acyl-coenzyme A synthetase-5. GPAT, glycerol-3-phosphate acyltransferase; AGPAT, 1-acylglycerol-3-phosphate acyltransferase.; PAPase, phosphatidic acid phosphatase, MGAT,* Acyl-CoA:monoacylglycerol acyl transferase-2; *DGAT, diacylglycerol acyltransferase; MAG, monoacylglycerol, BBM, brushborder membrane; BLM, basolateral membane.*   Figure from Pan and Hussein (26). Adapted by permission from Elsevier: Biochimica et Biophysica Acta © 2012.

In addition to absorption, one of the major functions of the intestinal enterocyte is to shuttle lipids out of the cell and into the circulation for uptake by other tissues. In the endoplasmic reticulum (ER), TGs are transferred by microsomal triglyceride transport protein (MTP) to an apolipoprotein, known as ApoB48; this step initiates the process of lipoprotein assembly (28). MTP is intrinsic in this process as individuals with mutations of MTP have abetalipoproteinemia, resulting in increased levels of TG in the intestinal enterocytes with low levels in the blood (53). The TGs are packaged along with apolipoproteins, cholesterol, and fat soluble vitamins to form prechylomicrons in the endoplasmic reticulum. The pre-chylomicrons are enclosed in vesicles known as prechylomicron transport vesicles (PCTV). Budding of the PCTV from the ER to the Golgi apparatus requires a complex of proteins including CD36, apoB48, and Liver fatty acid binding protein (LFABP) (31, 54). The PCTV then fuse with the Golgi apparatus for final processing of a chylomicron. Chylomicrons are too large to be secreted into capillaries; instead they are secreted into the lymphatic system via the basolateral membrane of the enterocyte and then are subsequently delivered to the general circulation (55).

In addition to being incorporated into TG, intestinal FAs may also play a role in modulating gene expression by serving as ligands for peroxisome proliferator-activated receptors (PPARs). PPARs are a class of nuclear hormone receptors that regulate many genes involved with glucose and lipid metabolism (56). These cytoplasmic proteins are activated by ligands, which cause them to enter the nucleus where they form a heterodimer with Retinoid X receptor (RXR) and bind to PPAR response elements on the DNA promoter sequence, resulting in expression of their target genes (56). In particular, PPARα is highly expressed in the intestinal enterocytes and liver hepatocytes, and is associated with upregulation of genes involved with fatty acid oxidation (57).

Additionally, FA can be stored as triglycerides in lipid droplets, which serve as cellular reservoirs for lipid mobilization in the enterocyte and other tissues during times of increased demand, such as fasting.   Storing FA as TG also protects the cells from an overabundance of unbound FA, which is cytotoxic (42, 43). Indeed, lipid droplets are formed in intestinal enterocytes immediately following a high dietary lipid load, which decrease in concentration with increased fasting time (58). During fasting, stored TGs can be hydrolyzed by adipose tissue triglyceride lipase (ATGL). ATGL hydrolyzes a TG to a diacylglycerol and a free fatty acid. The importance of this protein in lipid mobilization from lipid droplets of intestinal enterocytes is highlighted by a recent study in which intestinal specific ablation of ATGL resulted in excess TG accumulation in the enterocytes (59). After DGs are formed, hormone sensitive lipase (HSL) hydrolyzes DGs into an MG and a FFA. The final step involves monoacylglycerol lipase (MGL) to yield a FFA and glycerol.   The intestine is not traditionally thought of as a lipid storage organ, but rather as one that takes up, processes, and exports lipids. However, recent reports using Coherent anti-Stokes Raman scattering (CARS) imaging have demonstrated that high-fat fed mice have greater numbers of lipid droplets containing stored TGs in the enterocytes relative to lean mice (58, 60).

While dietary lipids enter the enterocyte from the apical (luminal) side of the enterocyte, endogenous lipids from the bloodstream are also delivered to the cell via the basolateral side of the enterocyte (Figure 1-2). Interestingly, the site of entry into the enterocyte influences the metabolic fate of the lipids. Tracer studies using radiolabelled lipids have revealed that FA delivered from the apical side of the enterocyte are trafficked towards TG synthesis while bloodstream derived FA are more likely to be incorporated into PL or oxidized (61–64). This is the case for MG as well (62). Hence, the ratio of triglycerides to phospholipids is much lower for bloodstream-derived lipids relative to delivery via the apical side. These observations have led

to the idea of compartmentation of lipid metabolism in the enterocyte as two separate pools of

FA and MG for utilization by the cell (Figure 1-2).

It is worth noting that in addition to LCFAs, medium chain fatty acids (MCFA) are also consumed

in the human diet. Uptake of MCFAs differs from LCFA in that MCFAs do not require carriers

into the enterocyte and are more soluble than LCFAs in the hydrophilic cytosol. Interestingly,

MCFA are metabolized so that that they are not included in chylomicrons, but rather directly

enter the liver via the portal vein and therefore do not first enter the general circulation (65).

Diets containing MCFA are not as obesogenic as those containing LCFA (66–68).

Figure 1-2
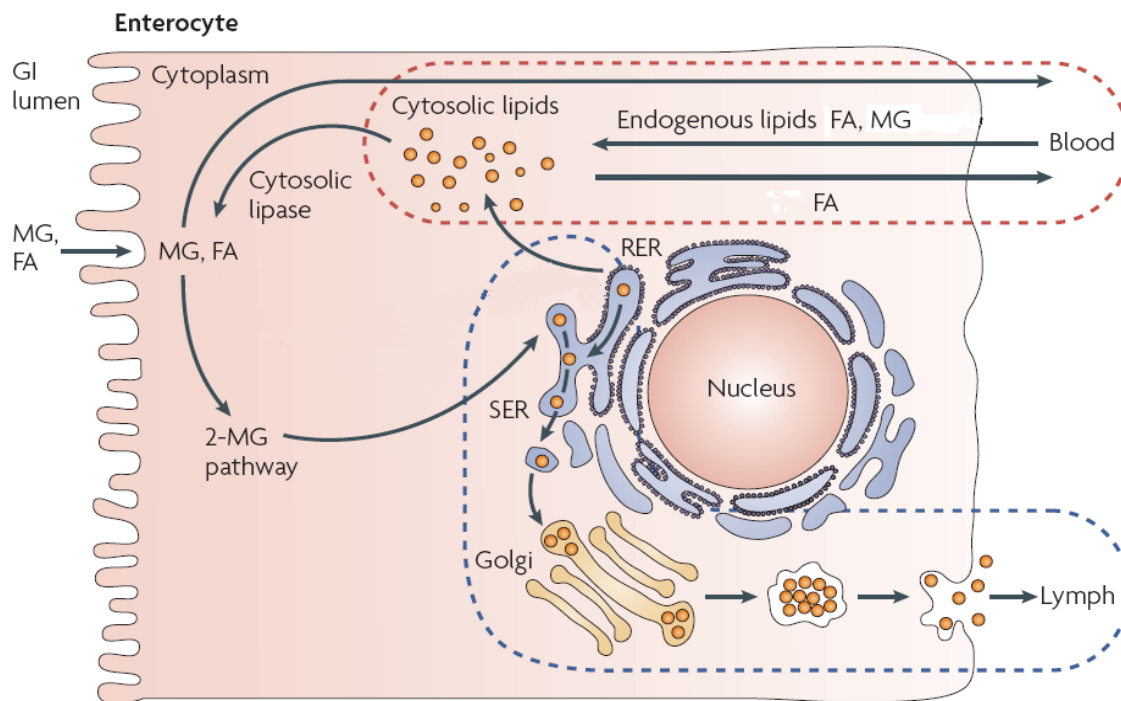
Figure 1-2. Lipid metabolism in the enterocyte. In the enterocyte, fatty acids (FA) and

monoacylglycerol (MG) enter the cell from the apical (luminal) side. Lumenal lipids are primarily

incorporated into TG via the MGAT pathway and then packaged into chylomicrons for delivery

into the lymphatic system. Alternatively, FA and MG can enter the basolateral side from the

circulation. FA delivered from the apical side of the enterocyte are trafficked towards TG

synthesis while bloodstream derived FA are more likely to be incorporated into PL or oxidized.

GI, gastrointestinal tract; MG, monoacylglycerol; FA, Fatty acid, SER, smooth endoplasmic

reticulum; 2-MG, 2-monoacylglycerol, RER, rough endoplasmic reticulum.   Graphic by Porter, et

al. (69). Adapted by permission from Macmillan Publishers Ltd: Nature Reviews Drug Discovery

© 2007.

Lipid Sensing in the Intestine

The small intestine is well known for being the major site of lipid absorption in the GI tract, but in addition to this important role, the intestinal cells also have an endocrine function involving sensing of nutrients. Throughout the intestine, endocrine cells are present which are involved with secretion of important gut hormones in response to nutrient availability. In particular, L cells secrete incretins such as Glucagon-like peptide 1 (GLP-1), a gut hormone that is released from the L cells in response to nutrients present in the small intestine (70). GLP-1 promotes insulin secretion from the beta cells of the pancreas, resulting in clearance of glucose from the blood and into the tissues (25). GLP-1 is also an inhibitor of glucagon (secreted from the alpha cells of the pancreas); therefore it is an important hormone for maintenance of glucose homeostasis (25, 71). Peptide tyrosine tyrosine (PYY) is another peptide hormone released by L cells in the distal intestine (72). It is secreted in response to a meal and slows gut motility, thereby assisting with efficiency of lipid uptake after a meal (73, 74).

Intestinal I cells are also present in the duodenum of the small intestine and secrete a peptide hormone known as cholecystokinin (CCK). Release of CCK from I cells is stimulated by lipids entering the small intestine (75). It acts by stimulating secretion of enzymes from the pancreas, which include proteinases and pancreatic lipase for digestion of nutrients as well as release of bile acids from the gall bladder that are necessary for emulsification of lipids in the lumen of the small intestine (18).   Lipid delivery into the gut prompts release of CCK and serotonin release and results in binding to their respective receptors, CCK1 and 5-HT3, which localize to the vagal efferent nerve cells (76, 77). Activation of these receptors results in a negative feedback of food intake (78). Additionally, the presence of lipids in the small intestine attenuates secretion of

ghrelin, a hormone produced by the stomach that increases in response to fasting, and therefore promotes food intake (79).

In addition to gut peptides, there has been increasing interest in lipids themselves as being important in the regulation of food intake. N-acetylphosphatidylethanolamines (NAPEs) are a group of lipids synthesized in the intestine and secreted into the plasma that have been shown to cause inhibition of food intake in response to dietary lipid (80). The N-acylethanolamines (NAEs) are formed by the hydrolysis of NAPEs by N-acylphosphatidylethanolamine-phophospholipase D and have also been shown to regulate food intake (81). Anandamide (arachidinoylethanolamide, AEA) was the first endocannabinoid identified in the NAE family of lipid signaling molecules. AEA was initially discovered in pig brain and found to have similar properties as Δ^9-tetrahydrocannabinoid, the active ingredient in cannabis, hence "ananda", (bliss in Sanskrit), was used for the name of this lipid (82). AEA is involved with regulation of food intake as an agonist of cannabinoid receptors 1 and 2 (CB_1 and CB_2) on the plasma membrane. Similarly to Δ^9-tetrahydrocannabinoid, increased concentrations of this lipid result in an acute increase in food consumption (83, 84).

Another member of this family includes oleoylethanolamide (OEA) which is derived from oleic acid (C18:1). OEA has the opposite effect of AEA, in that it promotes satiety and is increased in response to lipid infusions, but not carbohydrates or protein (85). However, unlike AEA, OEA is not a ligand for CB receptors, but does function as a ligand activator for PPARα (86). Intact vagal fibers are required for OEA- driven processes, hence capsacin administration, resulting in desensitization of vagal nerve fibers, attenuates the satiety effect of OEA administration (86). Along these lines, PPARα-null mice are not responsive to OEA infusion, and therefore do not

suppress their food intake (87). CD36 (discussed in a previous section) is another protein

hypothesized to be involved with lipid signaling pathways as demonstrated by studies in CD36-

null mice. These mice have been reported to have reduced OEA in the intestine and attenuated

food intake suppression relative to WT in response to a lipid infusion (85, 88).

Palmitoylethanolamide (PEA) is another NAE that is derived from palmitic acid (C16:0). Like

OEA, it also functions as a ligand activator for PPARα (89). The functions of PEA are proposed to

be quite different from the satiety effects shown upon OEA administration, as PEA is known for

its analgesic and anti-inflammatory effects (87, 90, 91).

Fatty acid amide hydrolase (FAAH), a highly expressed enzyme in the intestine, is responsible for

hydrolysis of the NAEs to a fatty acid and an ethanolamine as part of a regulatory process (92).

Hence, FAAH inactivates both AEA, which promotes hyperphagia, and OEA, which is opposite

and increases satiety.   Thus, these dual effects raise the question: which of these lipids has a

more powerful effect on energy balance? Indeed, ablation of FAAH results in increased food

intake and adiposity, suggesting that the effects of increases in AEA have a more robust effect

compared to OEA in regulation of food intake (93). Additional studies have revealed that FAAH

inhibition also can provide analgesia due to increased concentrations of PEA (94, 95).

2-arachidinoylglycerol (2-AG) is a 2-MG containing arachidonic acid (C20:4) esterified to a

glycerol, and is present in high concentrations in the intestine as well as the brain. Intestinal

concentrations of 2-AG increase in response to dietary lipids, but not carbohydrates or proteins

(96).   2-AG is similar to AEA in that it is an agonist for the CB_1 receptor and promotes food

intake, but it is present at much higher quantities than AEA (97, 98). Also, 2-AG is not hydrolyzed

by FAAH, but rather by MGL, which is responsible for hydrolysis of other MGs as well (99).

These data further support a role of intestinal lipids in the control of food intake, and in systemic

energy metabolism in response to nutrient availability.

Alterations in Intestinal Lipid metabolism Affect Whole Body Energy Balance in Null mice

Recent studies in which genetically modified mice have been generated have provided new

evidence regarding the link between intestinal lipid metabolism and whole body energy

homeostasis.   MGAT2 and MGAT3 are expressed in the ER of the intestinal enterocyte, but the

latter form is present in humans and not mice (100). MGAT2 is primarily found in the intestine,

with minimal (<1/100 of intestinal) expression in other tissues (50). DGAT1 and DGAT2 enzymes

are expressed in various tissues, but are markedly highly expressed in the intestine where they

are actively involved with TG synthesis (101, 102).   Studies of mice null for DGAT1 revealed that

these mice are resistant to diet-induced obesity and have increased TG stores in the intestines

due to blunted chylomicron transport out of the cell (103). Ablation of DGAT2 results in a more

severe phenotype; the mouse pups die within days after birth due to insufficiency of lipids

resulting in epidermal defects arising from water loss (103–106). Additionally, mice null for

MGAT2 are also lean in response to high-fat feeding and have reduced TG in the circulation

following an oral bolus of lipids. Interestingly, MGAT2$^{-/-}$ mice seem to have an increase in

energy expenditure relative to WT, suggesting that they are increasing lipid oxidation instead of

storing TG (50).

Studies using MGL-null mice revealed surprising findings; it was previously thought that in the

case of MGL ablation, elevations of 2-AG (2-arachidonoylglycerol) would occur, thereby resulting

in an increase in food intake and adiposity. However, the opposite was found; mice which have whole body ablation of MGL are lean relative to WT mice (107). Moreover, in mice which overexpress MGL in the intestine, 2-AG levels were low, as expected, but the animals were hyperphagic with a lower metabolic rate and greater adiposity (108).   Therefore, the actions of 2-AG in the intestine will need to be studied further in order to fully understand the functions of this lipid in regulation of energy intake. Based on these observations, the present studies examine not only the effects of enterocyte FABP ablation on the intestine, but also on whole body homeostasis.

Fatty Acid Binding Proteins

The fatty acid binding protein (FABP) family comprises of 14-15 kD size intracellular proteins which were initially discovered in the 1970s (109, 110). Presently, there are 9 known FABPs and cellular retinoid binding proteins (CRBP), of which are highly abundant (1-5%) in the cytosol of most tissues, with some FABPs present in more than one tissue (45, 111–114).   The names for the proteins came from the tissue in which they were initially identified, but since some proteins are expressed in multiple tissues, a newer nomenclature was introduced in which each FABP has a number (113).   The FABPs have high affinity for binding to long chain (>14 C) fatty acids (FA) in the hydrophilic cytoplasm of the cell. While these proteins have been studied for over 40 years, it remains uncertain why they are so highly expressed, and why there are so many FABPs; their specific functions are still being elucidated.

The FABPs have a highly conserved tertiary structure, consisting of 2 antiparallel β-helix sheets with 5 strands forming a forming a "clam shell" in which the ligands are bound.   In the barrel,

positively charged amino acids interact with the carboxylate groups of the FA (115). Despite the

tertiary structural similarities between these proteins, they only have about 20-70% amino acid

homology (116, 117), suggesting functional differences. The sheets are connected with a helix-

turn-helix motif, which has been shown to be important for the mechanism of ligand transfer

(118, 119).

Recently, the FABPs were identified as carriers of anandamide (arachidinoylethanolamide, (AEA)

(83, 84). As noted above, AEA is a member of the n-acyl ethanolamine (NAE) family of lipid

signaling molecules involved with regulation of food intake as an agonist of CB_1 and CB_2

receptors on the plasma membrane. It has been hypothesized that the FABPs are involved with

transport of NAEs to the ER where they are hydrolyzed by fatty acid amide hydrolase (FAAH),

which is a critical step in the regulation of these lipids. Since the NAEs are known to play

important roles in ingestive behavior, these observations raise the possibility that the FABPs

may play an important role in regulation of food intake.

FABPs in the Intestinal Enterocyte

The intestine is responsible for processing of dietary lipids of which >95% are absorbed; hence

these cells are able to uptake and process large quantities of dietary fat and it is though that the

presence of lipid binding proteins is critical for this capacity. In the intestinal enterocyte, two

FABPs are present, largely in the absorptive intestinal villi, but not in crypt cells (120, 121).

Liver-type FABP (LFABP; FABP1) was the first protein identified in the FABP family. As the name

suggests, it was initially discovered in the liver, but was later found in the intestine and also to a

lesser extent in the kidney (111). Intestinal FABP (IFABP; FABP2) is also present in the enterocyte

and is solely expressed in this tissue (111). Although these proteins have only about 29% amino

acid sequence homology, their tertiary structures are quite similar. Humans express more LFABP

than IFABP in the intestine (122, 123), however mice have similar levels of both of these

proteins in this tissue (122–124). Expression of these proteins occurs as early as 13 weeks of

gestation (122).

In addition to LFABP and IFABP, the Ileal lipid or Bile acid binding protein (ILBP or BABP; FABP6)

is present in the distal region of the small intestine and is known for having high affinity for

binding bile acids. ILBP can bind FA, but at lower affinity than for bile acids (125–129).

Moreover, expression of ILBP is increased in response to presence of bile acids (130–132). The

gene for this protein has a Farnesoid X receptor response element for binding to the Farnesoid x

receptor (FXR) transcription factor, of which bile acids serve as ligand activators. Mice null for

ILBP have increased excretion of bile acids and did not have any changes in protein expression of

LFABP in the intestine (133).

LFABP

LFABP is a highly abundant intracellular protein in the intestinal enterocyte (Figure 1-3). This

protein is present throughout the intestine, but it is most highly expressed in the duodenum and

jejunum (134). In vitro studies have shown that LFABP binds FA with high affinity, with K_d

values in the nanomolar range (135, 136). This protein is also unique among the FABPs in that it

has two FA binding sites, therefore it can bind up to two FA, and also other lipid species

including lysophospholipids, monoacylglycerols (MG), fatty acid acyl CoAs, and prostaglandins

(137–140). LFABP is also unusual in that, unlike most proteins in the FABP family, it transfers FA

to membranes via a diffusional mechanism rather than by a direct interaction with membranes (141, 142), LFABP is also proposed to play an important role in trafficking of lipids out of the enterocyte, in that it is involved with budding of prechylomicron transport vesicles (PCTVs) from the endoplasmic reticulum. These PCTVs form chylomicrons that leave the enterocyte and enter the lymph which are subsequently delivered into the general circulation for lipid delivery to other tissues (31, 54).

The promoter region of the DNA sequence for LFABP has a peroxisome proliferator receptor element (PPRE) and thus its expression is regulated by peroxisome proliferator activated receptor transcription factors (PPARs) (143). In particular, PPARα is present in the liver and intestine and when bound to ligands such as LCFA and fibrates, will promote transcription of genes involved with oxidation of lipids (144). Indeed, administration of PPARα agonists such as bezafibrate and clofibrate results in increased transcription of LFABP mRNA in the intestine and liver of mice (124, 145–147).   Interestingly, several studies have investigated a role for LFABP in the regulation of genes involved with lipid metabolism, by delivery of FA to transcription factors. It has been demonstrated that LFABP interacts with PPARα, and has more recently with HNF4α, a steroid hormone receptor known to promote transcription of genes involved with inflammation in the liver and intestine (148–151). Furthermore, this putative role of LFABP is further supported by evidence that oxidation of FA is reduced in the absence of LFABP in hepatocytes (149, 152). LFABP expression is also regulated by increased dietary intake of lipids, as high-fat feeding provides an excess of fatty acids to intestine and liver while also increasing expression of LFABP in these tissues (109, 145, 147, 153–155). Female rats express higher levels of LFABP in hepatocytes than males, suggesting that gender also influences expression of the protein (124, 156).

Polymorphism of LFABP

There have been no reported cases of deletion of the LFABP gene in humans, however a human polymorphism has been described in several recent reports (157–160). A substitution of alanine for threonine position 94 (T94A) of LFABP has been identified as a polymorphism in humans that is associated with increased plasma TG and FFA levels (158, 161).   Chang liver cells transfected with this variant form of LFABP had reduced uptake of FA, but additional accumulation of cholesterol compared to cells transfected with the wild-type protein (162). Interestingly, human subjects which carry the A94 allele of LFABP had a blunted response in plasma TG levels relative to carriers of the T94 allele when they were treated with fenofibrate (an activator of PPARα), therefore it is thought that the mutant form of LFABP is insufficient for delivery of fibrates to PPARα (158).   Indeed, human hepatocytes that express the A94 form of LFABP show reduced expression of PPARα regulated genes in response to fenofibrate than the WT form (163), therefore providing further evidence that LFABP is involved with PPARα-mediated lipid metabolic pathways.

Figure 1-3

A   B   C
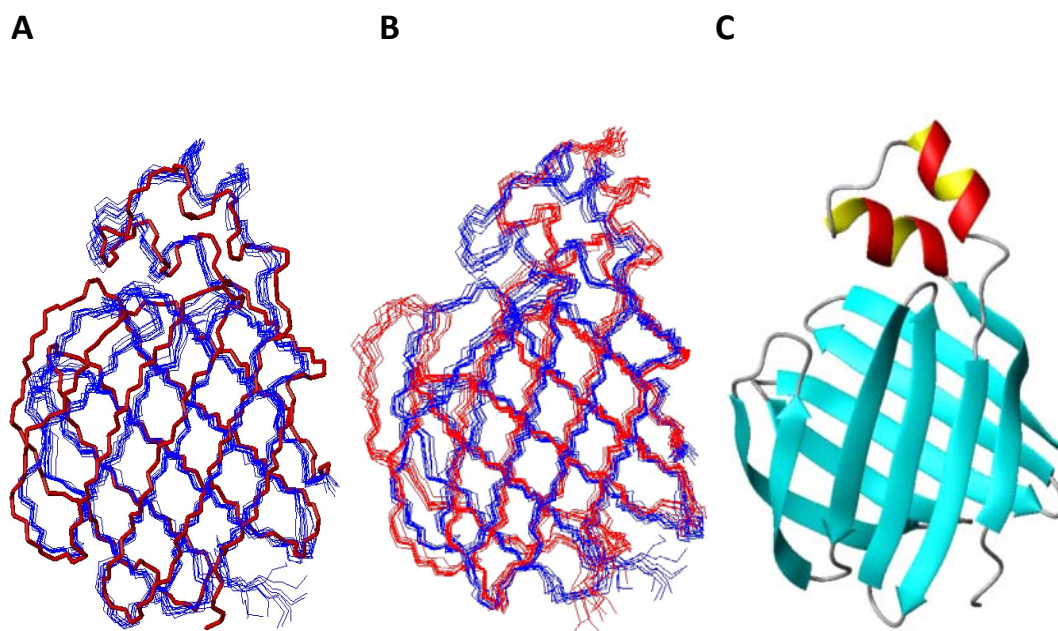
Figure 1-3. Structures of liver fatty acid binding protein (LFABP). A: The holo-LFABP solution structures are indicated in blue with the crystal structure shown with a thick red line; B: The lowest-energy apo- (red) and holo (blue) -LFABP structures. C: The ribbon diagram of the lowest-energy solution structure for apo-LFABP. Reprinted with permission from He et al (164). © 2007 American Chemical Society.

IFABP

Unlike LFABP, IFABP is solely expressed in intestinal enterocytes of mammals. While IFABP is present throughout the small intestine; its highest expression is in the jejunum (125). IFABP is found widely distributed throughout the cytosol of the enterocyte during the fed state, but is localized towards the apical side of the cell in the fasted state (120). IFABP has not been found to be involved with formation of chylomicrons (31, 54), hence IFABP has been proposed to be involved with uptake of FA from the lumen of the intestine and trafficking within the intestinal enterocyte to organelles. It is also thought that both FABPs may serve as a cytosolic reservoir for FA for various cellular functions, while also preventing accumulation of unesterified FA (114).

Several differences between LFABP and IFABP have been identified. For example, IFABP is typical among the members of the FABP family in that it has a single site where the ligand is bound. It has high affinity for binding saturated and unsaturated FA, but seems to have a slightly lower affinity for binding unsaturated FA relative to LFABP (135, 136, 165). Unlike LFABP, IFABP is similar to other proteins in the FABP family in that it transfers FA via a collisional mechanism with membranes with the alpha helix domain of the protein being necessary for this mechanism of FA delivery (118, 119, 142, 166). This portal region of the protein contains several positively charged residues that interact with negatively charged phospholipid head groups on membranes (167).   Fluorescence resonance energy transfer assays using a helix-less variant of IFABP, an engineered protein in which the alpha helices of IFABP are replaced with those of LFABP have shown reduced transfer rates and a diffusional mechanism of FA transfer. Hence, the alpha-helices of IFABP are required for direct interaction with membranes and for transfer of the ligands via collisional interaction (119, 142, 166–168).

Expression of IFABP in the intestine is influenced by PYY (peptide tyrosine tyrosine), a hormone which is released by intestinal cells in response to lipids in the gut (73). In mice, expression of IFABP in the intestine does not increase in response to ablation of LFABP and vice-versa (7, 169). Unlike LFABP, expression of IFABP is not regulated by PPARs, thus providing further evidence that these proteins may have different functions.

Polymorphism of IFABP

Deletion of the IFABP gene has not been detected in humans. However, a polymorphism of IFABP had been identified, in which threonine is substituted for alanine at amino acid 54 (A54T) (170). This amino acid substitution (frequency in the population of ~0.29) results in an increase in affinity for FA relative to the alanine-containing protein (141, 170). Individuals with the threonine-containing protein variant were found to have higher rates of insulin resistance and plasma triglycerides in several populations, including Pima Indians, a population with a high prevalence of diabetes (170–174). Additionally, diabetic subjects with the threonine allele have increased plasma triglycerides in response to an oral fat load (172). In vitro studies using Caco-2 cells showed increased secretion rates of radiolabelled FA into the media from cells transfected with the Thr54 variant relative to cells expressing the predominant Ala54 form of IFABP (175). Levy and coworkers used jejunal explants with the threonine-containing variant and compared with the WT alanine form of IFABP (176). They observed that when the tissues were incubated with radiolabeled FA, cells containing the Thr-form of IFABP had an increase in TG synthesis in the cells and also secretion of TG into the media, relative to the cells containing the Ala54 allele. It was also observed that chylomicron levels in the media were also markedly higher compared

to the cells with the Ala-form (176), consistent with the hyperlipemia observed in human studies

(172).

Figure 1-4
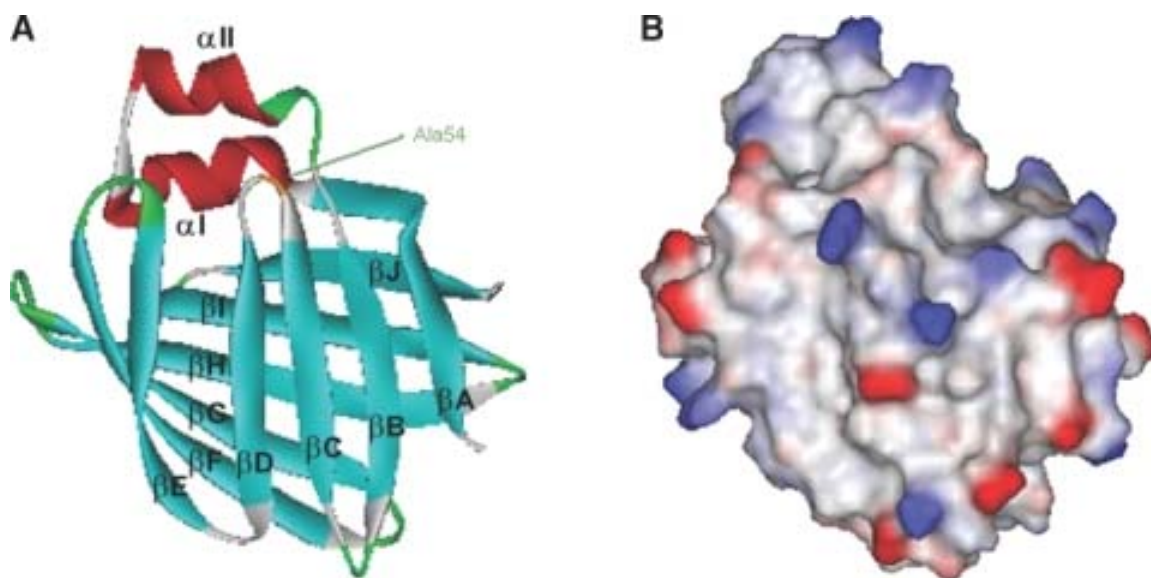
Figure 1-4. NMR-derived structure of intestinal fatty acid binding protein (IFABP). A. The flat ribbon structure of IFABP with the location of the polymorphism A54T indicated. B. The solvent surface structure is shown with the positive charged residues indicated in blue, negative charges in red, and neutral residues are shown in white. Adapted from Storch and McDermott (177). Reprinted with permission from the American Society for Biochemistry and Molecular Biology.

LFABP and IFABP in Intestinal Lipid Metabolism

It is unusual that one cell type expresses proteins with identical functions; therefore it is

generally believed that LFABP and IFABP have different roles in intestinal lipid metabolism. In

the intestine, dietary lipids from the lumen enter the enterocyte from the apical side of the

enterocyte, while endogenous lipids present in the bloodstream are delivered to the basolateral

side (69). The entry site into the enterocyte seems to impact the metabolic fate of the FAs.

Indeed, FAs delivered from the apical side of the enterocyte are trafficked towards TG synthesis

chylomicron formation. In contrast, FAs from the bloodstream are more likely to be formed into

mucosal phospholipids (PL) or oxidized (61–63). Therefore, the roles of LFABP and IFABP in the

delivery of FA from the apical or basolateral sites into the enterocyte have been examined.

Alpers et al (120) used an intestinal explant system in which FA were administered either on the

apical or basolateral side of the enterocyte to study the roles of IFABP and LFABP in binding of

FA. It was observed that LFABP bound more FA than IFABP, regardless of entry site.

Interestingly, IFABP bound more FA after apical administration than basolateral administration,

suggesting that this protein is more involved with transport of dietary derived FA, rather than

from the bloodstream (120). Using immunohistochemistry, they also found that both FABPs are

localized on the apical side of the enterocytes of fasted rats, but these proteins were located

throughout the cytoplasm in the fed state (120). Intestinal L-cell fibroblasts transfected with

IFABP or LFABP had increased incorporation of ^{3}[H]-oleic acid uptake into TGs relative to control

cells. However, cells containing LFABP had increased incorporation into PL, while IFABP

expressing cells had increased recovery of the radiolabel in neutral lipids (178).   In summary,

the evidence of differences in regulation, ligand binding specificities, and ligand transfer

mechanisms suggest that IFABP and LFABP have different roles in the enterocyte, but overall,

these functions are not clearly understood. Therefore, in vivo studies using mice null for IFABP
and LFABP have been conducted in order to directly compare the consequences of deleting each
of these proteins so as to further elucidate their functions.

LFABP$^{-/-}$ Mice

Two independent laboratories have generated individual lines of LFABP-null (whole body) mice
on the C57BL/6 background (179, 180). Martin and coworkers (Bert Binas and Friedhelm
Schroeder lab) published their first report on the LFABP$^{-/-}$ mouse in 2003 in which there was
complete deletion of all 4 exons of the LFABP gene along with the promoter region. These mice
were backcrossed 6 times to the C57BL/6N mouse strain (180). Newberry and coworkers
(Nicholas Davidson laboratory) also published a report in 2003 in which green fluorescent
protein was "knocked in" to exons 1 and 2 of the LFABP gene. These mice had a mixed
SV129/C57Bl6J background (179).

LFABP$^{-/-}$ mice have been shown by both laboratories to have defects in hepatic FA oxidation,
uptake, and VLDL secretion (152, 179, 181, 182). However, differences in body weight between
the two lines have been reported. Martin and coworkers (Bert Binas and Friedhelm Schroeder
laboratory) observed that male and female LFABP$^{-/-}$ mice were prone to obesity with increases in
fat mass relative to WT mice (183, 184). Interestingly, when the LFABP$^{-/-}$ mice were pair-fed a
high-fat diet (45 kcal% lard) to ensure equal caloric intakes, females gained more weight relative
to WT, but not males (182). Ad libitum feeding studies by the same laboratory showed that a
diet containing 25 kcal% fat promoted increases in fat mass of female LFABP$^{-/-}$ mice without
apparent changes in food intake (185). In addition to changes in body weight, they also

observed a reduction in ketone production, which suggests a perturbation in lipid oxidation. Interestingly, despite an obese phenotype, both high-fat fed male and female LFABP^{-/-} mice had lower liver weights as a percentage of body weight (182).

These body weight data are in contrast to observations by Newberry and coworkers in the Davidson laboratory. Newberry and coworkers did not observe a profound change in whole body phenotype in LFABP^{-/-}mice fed chow up to 14 weeks of age. However, they observed that the livers of 48-hour fasted KO mice had much lower deposition of TG relative to the WT, suggesting a defect in uptake of fatty acids in this tissue. VLDL secretion and ketone production rates were also lower in the knockouts (179, 181, 186), indicating that transport of lipids out of the liver and into the circulation is also affected by the absence of LFABP. Additionally, high-fat fed LFABP^{-/-} mice had elevated TG content in proximal intestinal mucosa, but not in distal sections, suggesting impaired trafficking out of the enterocytes (181). In several studies, female mice were fed diets containing high amounts of medium chain FA with C8 and C10 (as coconut oil) and it was observed that LFABP^{-/-} mice were resistant to obesity and hepatic steatosis (181, 187, 188). LFABP ablation resulted in lower lipid secretion rates from the intestine following an oral fat tolerance test with tyloxypol administration to inhibit lipoprotein clearance (181). In addition, these mice did not have any changes in fecal fat, suggesting that there are no changes in lipid uptake into the intestinal enterocytes (181, 186). This group has also observed that their female mice are resistant to obesity and hepatic steatosis when a Western diet containing 41 kcal% butter fat, a source which is rich in long chain FA (181, 186). However, they observed no differences in body weights between the knockout mice and WT when female mice were fed diets containing high levels of polyunsaturated FA (41 kcal% safflower oil) or containing high levels of trans fat with fructose (187, 189). They also measured IFABP mRNA and found that

there was no difference in IFABP levels in the intestinal enterocytes of LFABP$^{-/-}$ mice relative WT, suggesting that there is no compensatory upregulation (179). The differences in results between groups can be attributed to background strain differences (C57B6J versus C57BL6N), as well as the methods of gene ablation (210). Additionally, it is possible that environmental effects from differences in the animal facilities could affect the susceptibility to obesity (211).

IFABP$^{-/-}$ Mice

One line of IFABP$^{-/-}$ mice has been generated, which were backcrossed for 6 generations onto the C57BL/6J background by Vassileva and coworkers (190). Male mice fed diets with 35 kcal% fat as coconut oil and 1.25% cholesterol had an increase in body weight relative to wild-type mice (WT), and also developed fatty livers. Interestingly, female mice gained less weight than WT and did not exhibit any changes in hepatic lipid accumulation (190). Agellon and coworkers also reported that 30-40 week old IFABP$^{-/-}$ male mice fed 41 kcal% fat diets containing beef tallow or safflower oil for 14 days had higher body weights relative to WT. There were no differences in plasma TG for male or female IFABP$^{-/-}$ mice relative to WT mice, but IFABP$^{-/-}$ male mice had greater liver TG accumulation (191). Lipid malabsorption was not observed in IFABP-null mice, suggesting that like LFABP, that this protein is not required for bulk FA uptake into the enterocytes (190). Since these proteins are so abundant, it was hypothesized that each would compensate for the other, but it was found that LFABP expression was not increased in the intestinal mucosa of IFABP$^{-/-}$ mice (191).

Direct Comparison Between LFABP$^{-/-}$ and IFABP$^{-/-}$ mice

Studies using both LFABP and IFABP-null mice simultaneously have been conducted to further investigate the individual functions of these proteins. Lagakos and coworkers used LFABP null mice which were initially generated by Martin et al. (180). These mice, which had been backcrossed for another 6 generations onto the C57BL/6N strain, were backcrossed another 6 generations onto the C57BL/6J strain (7). IFABP$^{-/-}$ mice were derived from those used originally by Vassileva et al. without further backcrossing (190). No evidence of compensatory upregulation of IFABP was found in intestinal mucosa in response to ablation of LFABP, and vice versa (7). No differences in body weight were observed in chow-fed IFABP-null or LFABP-null male mice relative to WT mice (7). However, in response to a 48 hour fast, IFABP$^{-/-}$ mice lost more fat mass compared to WT mice. Intraduodenal administration of [^{14}C] FA in IFABP$^{-/-}$ mice showed an increase in recovery of radiolabel in PL in the mucosa relative to WT, resulting in a decrease in the TG/PL ratio. This suggests that IFABP directs FA towards synthesis of TG and away from PL.

In the same studies, it was observed that LFABP$^{-/-}$ mice lost less fat-free mass than WT in response to a 48 hour fast (7). It was also determined that delivery of [^{3}H]monoolein via the duodenum resulted in increases in [^{3}H] recovery in mucosal PL, MG, and DG, while recovery of [^{3}H] in TG was decreased in LFABP$^{-/-}$ mice relative to WT, suggesting that LFABP is involved in the transport of MG away from PL synthesis and toward TG synthesis. Also, LFABP ablation resulted in a reduction in mucosal oxidation of radiolabeled oleate. These results suggest that LFABP is involved with trafficking FA towards oxidative pathways and trafficking of MG towards TG, rather than PL (7).

Summary

The intestinal enterocytes serve the important function of dietary lipid uptake from the intestinal lumen. In particular, MGs and FAs, resulting from hydrolysis of TG, make up the highest quantities of lipids trafficked into the enterocytes. LFABP and IFABP are both highly abundant proteins that have high affinities for binding FAs, and are proposed to be involved with trafficking lipids in the intestinal enterocytes. In vitro studies have revealed that these proteins have differences in ligand binding, specificities, affinities and mechanisms of delivery of FA to membranes. Recently, it has been found that LFABP may be involved in the regulation of genes involved with intestinal lipid metabolism by association with PPARα, but this does not appear to be the case for IFABP, further suggesting that these proteins have different functions in intestinal lipid metabolism. Furthermore, in vivo studies that directly compared IFABP and LFABP null mice have shown that these mice have modest divergences in intestinal and whole body phenotypes, in response to low-fat chow diet feeding. To date, however, it is still not known why two structurally similar proteins are present in the same cell type. Therefore, it is of great interest to determine if a high-fat challenge to the enterocyte will reveal more profound changes in intestinal lipid metabolism, and perhaps result in more substantial changes in the whole body phenotypes of these mice. Therefore, the aims of this thesis project are:

Specific Aims

SPECIFIC AIM 1: To compare the effects of 3 months of low versus high-fat LCFA feeding on whole body metabolism and energy homeostasis in IFABP$^{-/-}$ and LFABP$^{-/-}$ mice.

Our laboratory was the first to directly compare both IFABP$^{-/-}$ and LFABP$^{-/-}$ mice fed chow diets (7). Body weight differences were not observed in either chow-fed knockout strain relative to WT. However, following a fast, LFABP$^{-/-}$ animals lost less fat free mass, while IFABP$^{-/-}$ animals lost more fat mass relative to WT mice, suggesting differences in whole body energy utilization during fasting. In the present study, we presented a high fat diet challenge to observe the whole body metabolic response of LFABP$^{-/-}$ and IFABP$^{-/-}$ mice relative to WT. Hence, we fed semipurified diets containing 10 or 45 kcal% fat. We also used diets containing high levels of either saturated or unsaturated LCFA because it has been shown that LFABP has a higher affinity for long chain unsaturated relative to saturated fatty acids relative to IFABP (136). We hypothesized that more distinct whole body phenotypic changes would occur in IFABP$^{-/-}$ and LFABP$^{-/-}$ mice, resulting from the lipid overload to the intestinal enterocytes. We hoped to uncover differences between IFABP$^{-/-}$ and LFABP$^{-/-}$ mice, which would suggest that these proteins have different functions in the intestinal enterocyte. The experiments that addressed this objective are described in Chapter 2.

SPECIFIC AIM 2: To compare the effects of low- and high-fat feeding on intestinal lipid metabolism and lipoprotein secretion in LFABP$^{-/-}$ and IFABP$^{-/-}$ mice.

In our previous work (7), intraduodenal administration of [^{14}C] fatty acid (FA) in IFABP$^{-/-}$ mice promoted an increase in recovery of radiolabeled phospholipids (PL) in the intestinal mucosa relative to WT, resulting in a decrease in the triacylglycerol:phospholipid (TG/PL) ratio. This suggests that IFABP directs FA towards synthesis of TG and away from PL. In LFABP$^{-/-}$ mice, delivery of [^{3}H]monoolein via the duodenum resulted in increases in [^{3}H] recovery in mucosal PL, monoacylglycerols (MG), and diacylglycerols (DG), while recovery in TG was decreased relative

to WT. This suggests that LFABP is involved with transport of MG away from PL synthesis and toward TG synthesis. LFABP$^{-/-}$ mice also had reduced oxidation of [^{14}C] FA to CO_2 and water soluble metabolites relative to WT, thus we believe that intestinal LFABP is involved in trafficking of FA towards oxidative pathways, as it has been previously found in liver. In this study, the three genotypes of mice were fed diets containing low or high levels of LCFA to determine if further changes in lipid metabolism in the enterocyte would be unmasked with high-fat feeding. The experiments that addressed this objective are described in Chapter 2.

SPECIFIC AIM 3. To determine the effect of simultaneous ablation of LFABP and IFABP on whole body energy homeostasis

We have crossed our IFABP$^{-/-}$ and LFABP$^{-/-}$ mice to create a novel double knockout mouse model (DKO), which does not express either protein. In this study, we compare WT and DKO and the single LFABP and IFABP-nulls fed diets containing low-fat or high saturated fatty acid levels, to determine the effects on the whole body energy metabolism of mice which do not express either of these proteins in the intestine (or in the liver). Since the enterocytes do not contain either of the FABPs that they normally express in high amounts, we anticipate that more striking changes will be found in these DKO mice relative to the single knockout mice, allowing us to further elucidate the individual and overlapping functions of these proteins. In vitro studies have suggested that IFABP and LFABP are involved with uptake of FA into the enterocytes, but we and others have not seen any evidence of malabsorption in the single knockout mice, though it is possible that one protein is still available for uptake in the absence of the other. Therefore, we hypothesize that there may be some dietary lipid malabsorption in mice which have

simultaneous ablation of these proteins. The experiments that addressed this objective are

described in Chapter 3.

Chapter 2

Direct Comparison of Mice Null for Liver or Intestinal Fatty Acid-binding Proteins Reveals Highly Divergent Phenotypic Responses to High Fat Feeding

Angela M. Gajda, Yin Xiu Zhou, Susan K. Fried, Luis B. Agellon, Sarala Kodukula,

Walter Fortson, Khamoshi Patel, and Judith Storch.

Abstract

The enterocyte expresses two fatty acid-binding proteins (FABP), intestinal FABP (IFABP; FABP2) and liver FABP (LFABP; FABP1). LFABP is also expressed in liver. Despite ligand transport and binding differences, it has remained uncertain whether these intestinally coexpressed proteins, which both bind long chain fatty acids (FA), are functionally distinct. Here, we directly compared IFABP$^{-/-}$ and LFABP$^{-/-}$ mice fed high fat diets containing long chain saturated or unsaturated fatty acids, reasoning that providing an abundance of dietary lipid would reveal unique functional properties. The results showed that mucosal lipid metabolism was indeed differentially modified, with significant decreases in FA incorporation into triacylglycerol (TG) relative to phospholipid (PL) in IFABP$^{-/-}$ mice, whereas LFABP$^{-/-}$ mice had reduced monoacylglycerol incorporation in TG relative to PL, as well as reduced FA oxidation. Interestingly, striking differences were found in whole body energy homeostasis; LFABP$^{-/-}$ mice fed high fat diets became obese relative to WT, whereas IFABP$^{-/-}$ mice displayed an opposite, lean phenotype. Fuel utilization followed adiposity, with LFABP$^{-/-}$ mice preferentially utilizing lipids, and IFABP$^{-/-}$ mice preferentially metabolizing carbohydrate for energy production. Changes in body weight and fat may arise, in part, from altered food intake; mucosal levels of the endocannabinoids 2-arachidonoylglycerol and arachidonoylethanolamine were elevated in LFABP$^{-/-}$, perhaps contributing to increased energy intake. This direct comparison provides evidence that LFABP and IFABP have distinct roles in intestinal lipid metabolism; differential intracellular functions in intestine and in liver, for LFABP$^{-/-}$ mice, result in divergent downstream effects at the systemic level.

Introduction

The small intestine is the primary site of dietary lipid absorption, and the quantity of dietary triacylglycerol (TG), which is absorbed following its luminal hydrolysis to fatty acid (FA) and monoacylglycerol (MG), is high in Western diets, ranging to over 100 g per day (8). Soluble carrier proteins are thought to be required for the intracellular trafficking of hydrophobic lipid species within the hydrophilic cytoplasmic environment. The fatty acid binding protein (FABP) family is composed of >10 distinct ~15 kD cytosolic proteins. Initially discovered in the 1970s (110, 192), these proteins are highly expressed in various tissues, with some tissues containing more than one FABP.   Interestingly, the proximal intestinal absorptive cell expresses two FABPs: Liver FABP (LFABP; FABP1), which is also highly expressed in liver and to some extent in kidney, and Intestinal FABP (IFABP; FABP2), which is solely expressed in the small intestine (122, 193). Both have been suggested by in vitro studies to be involved in FA uptake from the intestinal lumen, as well as the bloodstream, into the intestinal enterocyte (120, 194).

Although the individual functions of LFABP and IFABP in the intestine have not been elucidated, several lines of evidence indirectly suggest that they may function differentially within the same cell type.   For example, although all of the FABPs have a highly conserved tertiary structure containing a 10 strand β-barrel within which the ligands are bound, IFABP is typical of the FABP family in that it has a single high affinity binding site for FA, whereas LFABP can bind two FA as well as other lipids including lysophospholipids, prostaglandins, and MG (137, 138)   In vitro FA transfer mechanisms are also different, with LFABP transferring FA to membranes via an aqueous diffusional mechanism, while FA transfer from IFABP occurs during direct protein-membrane collisional interactions (119, 142, 166). Finally, while both IFABP and LFABP bind

saturated fatty acids with similar affinity, LFABP binds unsaturated FA with a 5 to 10 fold greater

affinity than IFABP (136). Thus, it is hypothesized that differences in the ligand binding and

transfer properties of IFABP and LFABP may give rise to individual, if not entirely disparate, roles

in lipid trafficking in the enterocyte.

In this study, we directly compare LFABP$^{-/-}$ and IFABP$^{-/-}$ male mice, both on the C57BL/6

background, to gain further insight into functional similarities and differences between the two

enterocyte proteins. Two laboratories have generated independent lines of LFABP$^{-/-}$ mice on the

C57BL/6 background (179, 180).   Both lines of mice have been shown to have defects in hepatic

FA oxidation, uptake, and VLDL secretion (152, 179, 181, 182). LFABP$^{-/-}$ mice from one line have

been observed to gain more weight relative to WT mice when fed chow or high-fat diets (182,

184, 185), while female mice from the other line were shown to gain less weight following chow

or high saturated fat feeding (181, 195, 196). One line of IFABP$^{-/-}$ mice has been generated and it

was found that male, but not female, mice gained more weight and exhibited

hypertriglyceridemia and hyperinsulinemia in response to high-fat high-cholesterol feeding,

relative to wild type mice (190, 191).

We recently reported the first direct comparison of mice null for LFABP and IFABP (7). We

observed no body weight differences in chow-fed mice of either knock-out line relative to WT.

Subtle phenotypic differences were noted, however. Intraduodenal administration of [^{14}C] FA in

IFABP$^{-/-}$mice showed an increase in recovery of mucosal radiolabel in PL relative to WT, resulting

in a decrease in the TG/PL ratio. As this was not accompanied by changes in gene expression of

lipid synthesis enzymes, it suggests that IFABP directs FA towards synthesis of TG. It was also

found that in LFABP$^{-/-}$ mice, relative to WT, duodenal delivery of [^{3}H] monoolein resulted in

increased [3H] recovery in mucosal PL, MG, and DG, whereas recovery of [3H] in TG was decreased, suggesting that LFABP is involved in the transport of MG away from PL synthesis and toward TG synthesis. We also found significantly decreased intestinal mucosal oxidation of [14C] FA in the LFABP^{-/-} mice, similar to what has been reported in the LFABP^{-/-} liver (7, 149, 152).

The objective of the current study was to test the hypothesis that challenging the LFABP^{-/-} and IFABP^{-/-} mice with high-fat diets would reveal more profound effects of FABP ablation. We reasoned that a chow diet would not necessarily exceed the capacity of the abundant intracellular FABPs, but that high fat feeding could potentially provoke greater phenotypic changes, and perhaps exacerbate and reveal further differences between the two FABPs. The type of dietary lipid is also an important factor as IFABP and LFABP have different binding affinities for saturated and unsaturated fatty acids (136). Thus, we compared a low fat semipurified (10% kcal) diet to two high fat (45% kcal) diets, one containing high long-chain saturated (HFS) and the other high monounsaturated (HFU) long chain FA (LCFA), to further elucidate the individual functions of LFABP and IFABP in the intestinal enterocyte, and in whole body energy homeostasis.

Experimental Procedures

Animals and Diets

LFABP^{-/-} mice on a C57BL/6N background were generously provided by Binas and coworkers (180). As described previously, the mice were additionally back-crossed with C57BL/6J mice from The Jackson Laboratory (Bar Harbor, ME) for six generations to create congenic LFABP mice (7). IFABP^{-/-} mice used in the present studies are a substrain bred by intercrossing of the original

IFABP$^{-/-}$ mice (190), and are also on a C57BL/6J background. Wild type C57BL/6J mice from The

Jackson Laboratory were used as controls. Mice were maintained on a 12-hour light/dark cycle,

and allowed *ad libitum* access to standard rodent chow (Purina Laboratory Rodent Diet 5015).

At 2 months of age, male LFABP$^{-/-}$, IFABP$^{-/-}$, and WT (C57BL/6J) mice (3x3 factorial design) were

housed 2-3 per cage and fed one of the following diets for 12 weeks: a low fat diet (LFD)

containing 10 kcal% fat, a 45 kcal% fat diet with high saturated fat (HFS) , or a 45 kcal% fat diet with

mostly unsaturated fat (HFU) . Product numbers are D10080401, D10080402, and D10080403,

respectively (Research Diets, Inc., New Brunswick, NJ) and are detailed in Table 2-1; the fatty acid

compositions (provided by the manufacturer) are listed in Table 2-2. The three diets used were

isocaloric, balanced so that only the carbohydrate and fat sources were modified between low

and high-fat treatments. The level of fat, 45% by calories, is commonly used to promote obesity

in rodents without lowering carbohydrates to levels which would promote ketogenesis.

Nevertheless, differences obtained between low fat and high fat feeding may be due, as well, to

reciprocal differences in carbohydrate content (Table 2-1).

Table 2-1

	LFD		HFS		HFU	
	Grams	Kcal	grams	kcal	grams	Kcal
Casein	200	800	200	800	200	800
L-Cystine	3	12	3	12	3	12
Corn starch	315	1260	72.8	291	72.8	291
Maltodextrin	35	140	100	400	100	400
Sucrose	350	1400	172.8	691	172.8	691
Cellulose	50	0	50	0	50	0
Soybean Oil	10	90	10	90	10	90
Lard	8.5	77	0	0	0	0
Cocoa Butter	26.5	239	192.5	1733	0	0
High Oleic Safflower Oil	0	0	0	0	192.5	1733
Mineral Mix, S10026	10	0	10	0	10	0
Dicalcium Phosphate	13	0	13	0	13	0
Calcium Carbonate	5.5	0	5.5	0	5.5	0
Potassium Citrate, 1H2O	16.5	0	16.5	0	16.5	0
Vitamin mix, V10001	10	40	10	40	10	40
Choline Bitartrate	2	0	2	0	2	0
FD&C Yellow Dye #5	0.05	0	0	0	0.025	0
FD&C Red Dye #40	0	0	0.05	0	0	0
FD&C Blue Dye #1	0	0	0	0	0.025	0
Total	1055.05	4057	858.15	4057	858.15	4057

Table 2-1. Diet compositions of low-fat (LFD), high saturated fat (HFS) or high unsaturated fat (HFU) diets.

Table 2-2

	LFD	HFS	HFU
grams/4057 kcal			
C16	8.2	49.9	11.1
C16:1	0.1	0.4	0.0
C18	9.3	64.3	3.7
C18:1	17.7	65.2	152.6
C18:2	7.3	10.7	32.7
C18:3	0.8	1.0	0.8
%			
Saturated fatty acids	40.8	60.0	7.8
Monounsaturated fatty acids	40.9	33.9	75.6
Polyunsaturated fatty acids	18.1	6.1	16.5

Table 2-2. Fatty acid compositions of low-fat (LFD), high saturated fat (HFS) and high-unsaturated fat (HFU) diets (as provided by the manufacturer).

Body weights were measured weekly. The food pellets were weighed each week to determine weekly

food intakes for each cage. Grams per week was divided by the number of animals per cage and then

divided by 7 days to determine the daily food intake; independent measures were taken as the number

of cages. Daily caloric intake was determined using the caloric densities of 3.9 kcal/g for the LFD or 4.7

kcal/g for HFS and HFU (Research Diets, Inc.). At the end of the experiment, the mice were fasted

for 24 hours and anesthetized with ketamine/xylazine/acepromazine (80:100:150mg/kg,

intraperitoneally, respectively), prior to collection of blood and tissues. Rutgers University

Animal Care and Use Committee approved all animal experiments.

Body Composition

Fat mass and fat-free mass measurements were taken by MRI (Echo Medical Systems, LLC.,

Houston, TX) 2-3 days prior to starting the feeding protocol and 2-3 days prior to sacrifice. The

instrument was calibrated each time according to the manufacturer's instructions. Two

measurements for fat and fat-free mass were taken for each mouse and averaged.

Energy Expenditure and Activity

Energy expenditure and activity were assessed using the Oxymax system (Columbus Instruments,

Columbus, OH). Mice were placed in an indirect calorimetry chamber for a total of 48 h, which

includes a 24-h period for adaptation prior to measurements. VO_2 and VCO_2 (VCO_2/VCO_2) were

used to determine the respiratory exchange ratio (RER) as an estimation of the Respiratory

Quotient.   Energy expenditure was assessed using the gas exchange measurements as

follows: $(3.815 + 1.232 \times RER) \times VO_2$ (197, 198). Energy expenditure (EE) data were analyzed

using the multiple regression model (least squares, JMP 10.0) that statistically adjusts for the

differences in fat free mass (LBM) among genotypes (199). The number of IR-beam breaks in a

plane was recorded as spontaneous activity. The number of *X* axis IR beam breaks during the

24-h period (X Total), successive X-axis IR beam breaks (X ambulatory), and number of vertical IR

beam breaks (Z total) were counted over the 24-h period.

Preparation of Tissues and Plasma

At sacrifice, blood was drawn and glucose (Accu-chek, Hoffmann-La Roche) and TG levels

(Cardiochek, Polymer Technology Systems, Inc.) were measured. Plasma was extracted after

centrifugation for 6 min at 4000 rpm and stored at -80°C. Livers and inguinal, perirenal, and

epididymal fat pads were removed and immediately placed on dry ice, and subsequently stored

at -80°C for further analysis. The intestine from stomach to cecum was removed and measured

lengthwise, rinsed with 60 mL ice-cold 0.1M NaCl, opened longitudinally and mucosa scraped

with a glass microscope slide into tared tubes in dry ice. Mucosal samples were subsequently

diluted with 10 X volume of PBS pH 7.4 per gram wet weight, and homogenized using 20 strokes

with a Potter-Elvejhem homogenizer on ice. Protein concentration was determined (200), and

lipid extraction performed on samples containing 1 mg protein/mL using the Folch procedure

(62, 201). Lipids were extracted twice with 10 mL chloroform/methanol (2:1) and the aqueous

phase non-lipid fractions discarded. The organic lipid layer was dried under a nitrogen stream

and resuspended in chloroform/methanol (2:1) for further analysis.

LC/MS Analysis

Monoacylglycerol species, including 2-AG, and ethanolamines from intestinal mucosa were

analyzed by LC/MS as described previously, at the core facility of the Rutgers Institute for Food,

Nutrition, and Health (108)

Plasma Analyses

At time of sacrifice, plasma was collected and stored at -80°C for further analyses as noted

above. ELISA kits were used to measure plasma leptin, adiponectin, and insulin (Millipore).

Plasma total cholesterol and FA levels were also analyzed (Wako Diagnostics, Inc.). Adiponectin

and leptin indices (202) were calculated as the plasma adiponectin or leptin levels divided by the

total fat mass determined by MRI. Homeostatic Model Assessment (HOMA-IR) was determined

using fasting glucose (mg/dl) X fasting insulin (µU/mL)/405 (203).

Oral Fat Tolerance Tests

After 3 months of high-fat feeding, mice were fasted for 24 h. Time 0 blood was taken from

conscious mice via the tail vein and then an intraperitoneal injection of Tyloxapol (500 mg/kg

BW) was administered to prevent lipoprotein TG uptake via inhibition of lipoprotein lipase.

After 30 min, an orogastric gavage of 300 µL of olive oil was given. Blood was taken at t = 60,

120, 180, and 240 min. Blood TG levels were measured using 15 µl of whole blood using a

Cardiochek instrument (Polymer Technology Systems, Inc. Zionsville, IN).

Mucosal FA and MG Metabolism

Preparation of lipids for bloodstream and intraduodenal administration was as follows. For

intravenous FA administration, 15 µCi [^{14}C] oleate (275 nmol) was dried under a nitrogen stream

and then 0.5% ethanol (final volume) and 150 µl of a solution containing 0.1M NaCl and mouse

serum (1:1) were added sequentially. For duodenal FA administration, 1.5 µCi [^{3}H] oleate (34

nmols) was dried under a nitrogen stream and then 150 of 10mM sodium taurocholate in 0.1 M

NaCl was added. For intraduodenal administration of [^{3}H] monolein, [^{3}H] monoolein 7.3 µCi

(0.122 nmol) was dried under a nitrogen stream and then 150 µl of 10mM sodium taurocholate

in 0.1M NaCl was added.   Eight-week-old WT, IFABP$^{-/-}$, and LFABP$^{-/-}$ male mice (n=6/group) were

fed LFD or HFS for 3 months and were then fasted 24 h and anesthetized as indicated above

prior to the experiment. Surgical procedures for intravenous and intraduodenal administration,

collection of mucosa at t = 2 minutes following introduction of lipids, lipid extraction, and

analysis of mucosal lipid metabolites by TLC and phosphorimaging (for [^{14}C]-labeled oleate) or

scraping and scintillation counting (for [^{3}H]-labeled oleate and monoolein), were performed as

described in detail previously (7, 62).

Fatty Acid Oxidation

Fatty acid oxidation measurements on mucosa from mice administered [^{14}C]-oleate were carried

out as described previously (7, 62).

Fecal Lipid Content

Fecal lipids were measured to determine if there were any alterations in total lipid absorption in

the gene-ablated mice. Feces were collected from the cages between 4 and 10 weeks during the

12 week period and then dried overnight at 60°C and weighed. 0.5 g (dry weight) was dissolved

in water overnight and lipid extracted using the Folch method (201). The extracted lipids in 2:1

chloroform:methanol were placed in pre-weighed glass tubes and dried down completely under

a nitrogen stream. They were weighed again to determine recovered lipid. The weight of the

extract was divided by original weight of the feces to determine percent of lipid in the feces.

Quantitative RT-PCR for mRNA Expression Analysis

The protocol for mRNA acquisition and analysis was adapted from Chon *et al.* (204). Briefly,

tissues were homogenized in 4M guanidiniumthiocyanate,25mM sodium citrate, 0.1M β-

mercaptoethanol using several strokes of a Polytron. Total RNA was further purified by phenol

extraction and the RNeasy cleanup kit (Qiagen,Valencia, CA) along with DNase treatment to

minimize genomic DNA contamination. Reverse transcription was performed using 1µg of RNA,

random primers, an RNase inhibitor, and reverse transcriptase (Promega Madison, WI) in a total

volume of 25 µl. Primer sequences were obtained from Primer Bank (Harvard Medical School

QPCR primer data base) and are presented in Table 2-3. The efficiency of PCR amplifications

was analyzed for all primers to confirm similar amplification efficiency. Real time PCR reactions

are performed in triplicate using an Applied Biosystems 7300instrument. Each reaction

contained 80 ng cDNA, 250 nM of each primer, and 12.5 µl of SYBR Green Master Mix

(AppliedBiosystems, Foster City, CA) in a total volume of 25 µl. Relative quantification of mRNA

expression is calculated using the comparative Ct method normalized to β-actin.

Table 2-3

Gene	Primer	Sequence
β-actin	Forward	5'- GGCTGTATTCCCCTCCATCG-3'
	Reverse	5'- CCAGTTGGTAACAATGCCATGT-3'
MGAT2	Forward	5'- TGGGAGCGCAGGTTACAGA-3'
	Reverse	5'- CAGGTGGCATACAGGACAGA-3'
erGPAT (GPAT3)	Forward	5'-TATCCAAAGAGATGAGTCACCCA-3'
	Reverse	5'-CACAATGGCTTCCAACCCCTT-3'
mtGPAT (GPAT1)	Forward	5'- CTGCTTGCCTACCTGAAGACC- 3'
	Reverse	5'- GATACGGCGGTATAGGTGCTT- 3'
DGAT1	Forward	5'-TCCGTCCAGGGTGGTAGTG-3'
	Reverse	5'-TGAACAAAGAATCTTGCAGACGA3'
DGAT2	Forward	5'- TTCCTGGCATAAGGCCCTATT- 3'
	Reverse	5'- AGTCTATGGTGTCTCGGTTGAC-3'
MGL	Forward	5'- CAGAGAGGCCAACCTACTTTTC-3'
	Reverse	5'- ATGCGCCCCAAGGTCATATTT-3'
PPARα	Forward	5'- TCGGCGAACTATTCGGCTG-3'
	Reverse	5'- GCACTTGTGAAAACGGCAGT-3'
ACADL	Forward	5'-GAGAAGTGAGTAGAGAGGTCTGG-3'
	Reverse	5'-AACTGCTGTTGAGAGCAAGTC-3'
ACOX1	Forward	5'-ATATTTACGTCACGTTTACCCCGG-3'
	Reverse	5'-GGCAGGTCATTCAAGTACGACAC-3'
CCOX	Forward	5'- TCAACGTGTTCCTCAAGTCGC-3'
	Reverse	5'- AGGGTATGGTTACCGTCTCCC-3'
NADHDe	Forward	5'- GGTACTTTGCTTGCTTGATGAGA-3'
	Reverse	5'- TGGGAAGATATACGGCTGAGG-3'
SUCCDe	Forward	5'-CATGAACATCAACGGAGGCAA-3'
	Reverse	5'-CTCCTGGGACTCATCCTCTT-3'
CD36	Forward	5'- TCCCCCTACTAGAAGAAGTGGG-3'
	Reverse	5' TCCAACAGATTGGTTTCGTTCA-3'
SRB1	Forward	5'- TTTGGAGTGGTAGTAAAAAGGGC-3'
	Reverse	'5- TGACATCAGGGACTCAGAGTAG-3'
NPC1L1	Forward	5'- GCTTCTTCCGCAAGATATACACTCCC-3'
	Reverse	5'- GAGGATGCAGCAATAGCCACATAAGAC-3'
LFABP	Forward	5'-GGGGGTGTCAGAAATCGTG -3'
	Reverse	5'-CAGCTTGACGACTGCCTTG-3'
IFABP	Forward	5'-GTGGAAAGTAGACCGGAACGA-3'
	Reverse	5'-CCATCCTGTGTGATTGTCAGTT-3'
FAAH	Forward	5'-GAGGCTCCCCTCTGGGTTTA-3'
	Reverse	5'-GCCAGGCTATCCACATCCC-3'
CB1	Forward	5'- GGGCACCTTCACGGTTCTG-3'
	Reverse	5'- GTGGAAGTCAACAAAGCTGTAGA-3'

Table 2-3. Primer sequences for qPCR.

Statistical Analysis

Data are presented as mean ± S.E.M. Statistical comparisons for body weights were made by two-way repeated measures ANOVA (genotype X time). For OFTT tests, comparisons were made by Student's t-test (IFABP^{-/-} or LFABP^{-/-} versus WT) for each time point. The effect of genotype within each diet was made by one-way ANOVA followed by Tukey's post-hoc test using JMP statistical software (version 10, SAS Institute). Multiple linear regression (least squares analysis, JMP) was used to assess effects of diet and genotype, adjusted for FFM, on energy expenditure.

Results

Ablation of LFABP or IFABP Differentially Affects Body Weight, Body Composition, and Food Intake

The BW and body fat mass (FM) of IFABP^{-/-} and LFABP^{-/-} mice were similar to WT prior to the start of feeding, but percentage of fat-free mass (FFM) of LFABP^{-/-} mice were slightly lower than WT ($p<0.05$) (data not shown),

After 12 weeks of high-fat feeding, different BW phenotypes were readily evident between the IFABP^{-/-} and LFABP^{-/-} mice. IFABP^{-/-} mice fed the 10 kcal% low fat diet (LFD) had similar BW relative to WT over the 12-week study (Figure 2-1A), however IFABP^{-/-} mice fed diets containing 45 kcal% high-saturated fat (HFS) and high-unsaturated fat (HFU) had lower BW relative to WT ($p<0.05$) (Figure 2-1B, C). Total weight gain for IFABP^{-/-} mice was similar to WT when fed the LFD, but weight gain was significantly lower after HFS diet feeding ($p <0.05$) and a similar trend was observed for mice fed the HFU (Figure 2-1D). Notably, IFABP^{-/-} mice were found to have lower %

of FM and a higher % of FFM on all dietary treatments (p <0.05) (Figures 2-1E, F). The food

intake of IFABP$^{-/-}$ mice was somewhat higher when they were consuming the LFD, but was lower

than WT in response to the HFS diet (p<0.05). Caloric intakes were similar between WT and

IFABP$^{-/-}$ fed the HFU diet (Figure 2-1G). Food efficiency (g of BW gained per kcal consumed) was

similar to WT mice during HFS feeding (Figure 2-1H). Importantly, fecal fat measurements were

similar between IFABP$^{-/-}$ and WT mice (Figure 2-1I), thus lipid absorption was not affected, in

agreement with previous results for chow-fed mice (7). The body weight phenotype for the

present substrain of IFABP null mice differs from what we found in the original strain, where

male mice showed increased weight gain relative to WT mice (190, 191).

Remarkably, the results showed that LFABP$^{-/-}$ mice displayed an opposite phenotype to the

IFABP$^{-/-}$ mice. Weekly body weights of LFABP$^{-/-}$ mice were similar to WT when fed the LFD, but

net weight gain over the 12 weeks of feeding was significantly greater (p <0.05) (Figures 2-1A, D).

Moreover, in marked contrast to IFABP$^{-/-}$ mice, LFABP$^{-/-}$ had significantly higher BW relative to

WT when fed HFS or HFU during the 12 week feeding study, resulting in substantially greater

weight gains (p <0.05) (Figure 2-1B, C, D). The LFABP$^{-/-}$ had a higher % of FM and lower % of FFM

when fed either high fat diet (p < 0.05) (Figures 2-1E, F), indicating that high-fat feeding caused

increased adiposity relative to WT. In further contrast to the IFABP nulls, the food intake of

LFABP$^{-/-}$ mice was higher on the HFS diet (p <0.05) (Figure 1G), and significantly higher food

efficiency was observed when LFABP$^{-/-}$ were fed HFS and HFU (p <0.05)(Figure 2-1H). In

agreement with previous reports (7, 181), no differences in fecal fat were found (Figure 2-1I),

thus there is no indication of lipid malabsorption in the LFABP$^{-/-}$ knockout mice.

Figure 2-1
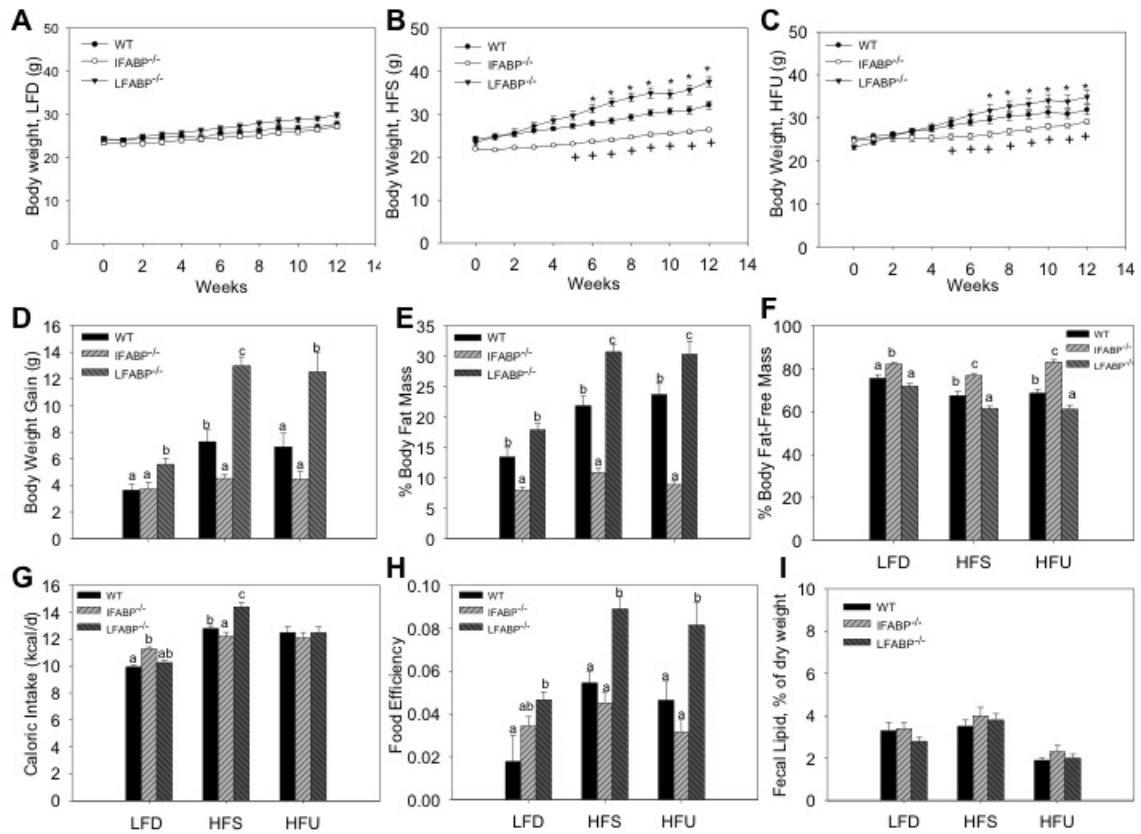
Figure 2-1. Body weight and composition for WT, IFABP$^{-/-}$ and LFABP$^{-/-}$ mice after 12 weeks on a low-fat (LFD), high saturated fat (HFS) or high unsaturated fat (HFU) diet. A. Body weights on LFD (n=15-16); B. Body weights on HFS (n=13-14); C. Body weights on HFU (n=12-16); D. BW gains (n=12-16); E. Percent Fat Mass (n=12-16); F. Percent Fat-free mass (n=12-16); G. Food intake for mice fed LFD (n=5-7), HFS (n = 5-6), HFU: (n = 5-7); H. Food efficiency (g BW gained/kcal food intake) for mice fed LFD (n=5-7), HFS (n = 5-6), HFU (n= 5-7).   I. Fecal fat% for mice fed LFD (n=5-7), HFS (n = 5-6), HFU (n= 5-7). For Figures A–C data are mean ± SEM, analyzed using two way ANOVA using repeated measures with post-hoc Tukey's test (genotype x time) *p<0.05 for LFABP$^{-/-}$ vs WT $^+$p<0.05 for IFABP$^{-/-}$ vs WT. For Figures D - H, data are mean ±

SEM, analyzed using one way ANOVA with a Tukey's post-hoc test. Results with different letters within diet treatment are significantly different ($p < 0.05$).

Overall, the present direct comparison of LFABP$^{-/-}$ and IFABP$^{-/-}$ mice reveals divergent

phenotypes when fed high LCFA diets. After 12 weeks of feeding, LFABP$^{-/-}$ mice display greater

increases in body weight and FM, and lower FFM compared to WT, with more pronounced

changes occurring during HFS feeding compared to HFU. In contrast, IFABP$^{-/-}$ mice gain less

weight than WT and have a smaller amount of FM, regardless of the amount or type of dietary

fat.

IFABP$^{-/-}$ Mice Have Greater Reductions in FM After Fasting

Since body composition differed between the two enterocyte FABP null mice, we further

examined the effects of fasting on changes in FM and FFM, using MRI (Table 2-4). When fed the

LFD, the IFABP$^{-/-}$ mice lost a larger percent of BW after fasting relative to WT ($p < 0.05$).

Additionally, while LFD-fed IFABP$^{-/-}$ mice had lower FM than WT in both fed and fasted states,

the loss of fat mass following the fast was almost double for the IFABP$^{-/-}$ mice compared to WT

($p < 0.05$). Similarly, on both the HFS and HFU diets, the percent change in FM for the IFABP$^{-/-}$

mice was approximately twice that of the WT mice ($p < 0.05$) (Table 2-4). These results are in

agreement with our recent observations for IFABP$^{-/-}$ mice of this substrain fed laboratory chow

(7), indicating that a large loss of fat mass during fasting occurs under all dietary regimens

examined. HFU-fed but not HFS- or LFD-fed IFABP$^{-/-}$ mice also lost more FFM than WT mouse

during the fast.

In contrast to the IFABP$^{-/-}$ mice, the LFABP$^{-/-}$ mice did not differ from WT in the percent of fat

mass lost following a 24-h fast, although as noted above the LFABP$^{-/-}$ mice had much greater

absolute fat mass (Table 2-4). This, too, is in keeping with our previous results for chow-fed

mice. No changes in the loss of FFM were found following fasting for the LFABP$^{-/-}$ mice,

regardless of dietary treatment.

Table 2-4

|	LFD			HFS			HFU		
	WT	IFABP^{-/-}	LFABP^{-/-}	WT	IFABP^{-/-}	LFABP^{-/-}	WT	IFABP^{-/-}	LFABP^{-/-}
Fed BW, g	27.5 ± 0.4	27.0 ± 0.6	27.6 ± 0.6	33.6 ± 0.7[b]	28.5 ± 0.7[a]	37.2 ± 1.2[c]	32.7 ± 2.0[a]	29.8 ± 1.0[a]	40.6 ± 2.2[b]
Fasting BW, g	24.8 ± 0.4	23.7 ± 0.6	24.8 ± 0.5	31.0 ± 0.7[b]	25.4 ± 0.7[a]	34.3 ± 1.1[c]	30.6 ± 1.9[a]	26.7 ± 0.5[a]	37.5 ± 2.2[b]
% Change	9.9 ± 0.5[a]	12.4 ± 0.6[b]	10.0 ± 0.4[a]	8.0 ± 0.4[a]	10.8 ± 0.6[b]	7.8 ± 0.4[a]	-6.7 ± 0.4[a]	-10.4 ± 0.5[b]	-7.9 ± 0.8[a]
Fed FM, g	4.1 ± 0.2[b]	2.6 ± 0.1[a]	4.5 ± 0.3[b]	7.8 ± 0.5[b]	3.1 ± 0.3[a]	11.3 ± 0.8[c]	9.1 ± 1.4[b]	3.2 ± 0.6[a]	15.1 ± 1.7[c]
Fasting, FM, g	3.1 ± 0.2[b]	1.5 ± 0.1[a]	3.5 ± 0.3[b]	6.0 ± 0.5[b]	2.2 ± 0.3[a]	10.4 ± 0.8[c]	7.7 ± 1.3[b]	2.0 ± 0.5[a]	13.8 ± 1.6[c]
% Change	-24.8 ± 2.2[a]	-44.5 ± 3.1[b]	-22.7 ± 2.5[a]	-17.1 ± 2.5[a]	-30.2 ± 4.9[b]	-9.0 ± 0.9[a]	-15.9 ± 2.7[a]	-40.5 ± 4.0[b]	9.3 ± 1.7[a]
Fed FFM, g	21.3 ± 0.5	21.7 ± 0.6	20.5 ± 0.3	23.2 ± 0.6	22.4 ± 0.6	23.0 ± 0.5	21.4 ± 0.6[a]	24.5 ± 0.5[b]	22.8 ± 0.6[ab]
Fasting, FFM, g	19.4 ± 0.4	19.8 ± 0.5	18.9 ± 0.2	22.3 ± 0.5	20.7 ± 0.5	21.6 ± 0.5	20.8 ± 0.5	22.3 ± 0.5	22.5 ± 0.6
% Change	-8.3 ± 1.5	-8.7 ± 0.3	-7.9 ± 0.4	-3.5 ± 1.6	-7.4 ± 0.9	-6.3 ± 0.9	-2.9 ± 1.1[a]	-9.0 ± 0.7[b]	-1.45 ± 0.8[a]

Table 2-4. Fed and 24 hour fasted body weight and composition for WT, LFABP^{-/-} and LFABP^{-/-} mice after 12 weeks on a low-fat (LFD), high saturated fat (HFS) or high unsaturated fat (HFU) diet. LFD, n=15-24; HFS, n=18-25; HFU, n=6-9. Data are mean ± SEM, analyzed

using one way ANOVA with a Tukey's post-hoc test.   Results with different letters within a dietary treatment are significantly different

(p<0.05).

IFABP$^{-/-}$ and LFABP$^{-/-}$ Mice have Different Metabolic Fuel Source Utilization, 24-h Energy

Expenditure, and Activity

The ratio of VCO2/VO2 (RER) was higher in IFABP$^{-/-}$ mice fed HFS or HFU, suggesting increased utilization of carbohydrate for oxidation (p <0.05) (Figure 2-2C). By contrast, the LFABP$^{-/-}$ mice had a lower RER on LFD and HFS compared to WT (p <0.05) (Figure 2-2C), indicating that these mice utilized more lipids as an energy source.

Multiple regression analysis indicated that there was a statistically significant interaction of metabolic rates with diet and genotype, therefore we analyzed the genotype effect within each diet. When fed the HFS or HFU diets, there were no genotype effects on 24-h EE per mouse (data not shown). In mice fed the LFD, however, 24-h energy expenditure (kcal/h) was higher in IFABP$^{-/-}$ than WT (Figure 2-2A) (p <0.005). After adjusting for variations in FFM, there was also no difference in the 24-h EE in mice fed HFS. However, in mice fed HFU, 24h EE adjusted for FFM was higher in the LFABP$^{-/-}$. Furthermore, when fed the LFD, the IFABP$^{-/-}$ group had higher energy expenditure than WT after adjustment for FFM.

Surprisingly, we found that despite their increased adiposity and body weight, the LFABP$^{-/-}$ mice had increased activity compared to WT mice after HFS feeding (p < 0.05), and higher total X activity than the IFABP$^{-/-}$ group on both HFS and HFU (Figure 2-2, D-F). Thus, the greater adiposity of the LFABP$^{-/-}$ mice appears to be due to greater feed efficiency (Figure 2-1H).

Figure 2-2
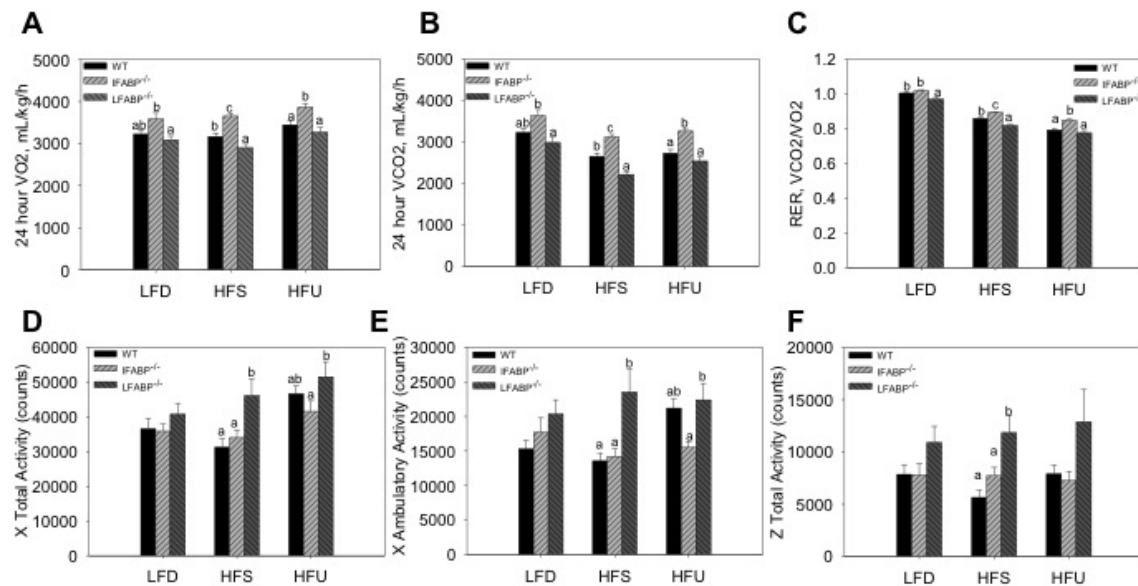
Figure 2-2. Indirect calorimetry and 24 hour activity for WT, IFABP$^{-/-}$ and LFABP$^{-/-}$ mice after 12 weeks on a low-fat (LFD), high saturated fat (HFS) or high unsaturated fat (HFU) diet. A. 24 hour VO2 B. 24 hour VCO2; C. 24 hour RER; D. 24 hour X activity; E. 24-hour ambulatory total activity; F. 24-hour Z total activity. LFD, n=15-16; HFS, n= 13-14; HFU, n=12-17. Data are given as mean ± SEM, analyzed using one-way ANOVA with a Tukey's post-hoc test. Results with different letters within a diet treatment are significantly different (p<0.05).

IFABP^{-/-} and LFABP^{-/-} Mice Display Differences in Markers of Whole Body Energy Metabolism

Plasma and tissue analyses are presented in Table 2-5. IFABP^{-/-} mice had lower fasting blood glucose levels relative to WT mice when fed LFD and HFS (p<0.05), but no changes in insulin or TG levels were found. Total cholesterol and non-esterified FA (NEFA) levels were not different, except after HFU feeding, where both were lower for IFABP^{-/-} relative to WT mice (p <0.05). Plasma leptin levels were lower in the IFABP^{-/-} mice fed HFU (p<0.05), presumably reflecting their lower FM (Figure 2-1). For the same reason we were surprised to find that IFABP^{-/-} mice had lower adiponectin levels following LFD and HFU feeding, however the adiponectin index, which takes into account the total fat mass of the animals (plasma adiponectin/ g of FM) showed that IFABP^{-/-} had higher values than WT after HFU feeding (p <0.05). Livers weights per g BW of IFABP^{-/-} mice were similar to WT, although this finding is in contrast to the increased liver weights found in male IFABP^{-/-} mice from the original line (23). In keeping with the lower FM shown by MRI, the epididymal, perirenal, and inguinal fat pads were smaller for IFABP^{-/-} on LFD or HFU (p<0.05), and a similar trend was found on the HFS diet.

Despite the markedly greater fat mass of the LFABP^{-/-} mice relative to WT, no changes were observed in fasting blood glucose, insulin, cholesterol, NEFA, or adiponectin levels on any of the dietary regimens (Table 2-5). Plasma TGs were higher in LFABP^{-/-} mice fed a LFD, but somewhat lower when fed a HFU (p<0.05). Leptin levels of LFABP^{-/-} mice on HFS were strikingly higher than WT (p<0.05), in keeping with the large increases in FM (Figure 2-1). Correspondingly, the LFABP^{-/-} mice had larger epididymal, perirenal, and inguinal fat pads when fed HFS (p<0.05). The absolute liver weights of LFD and HFU-fed LFABP^{-/-} mice were lower than WT mice, and were also lower (p<0.05) when expressed per g BW.

Table 2-5

	LFD			HFS			HFU		
	WT	IFABP$^{-/-}$	LFABP$^{-/-}$	WT	IFABP$^{-/-}$	LFABP$^{-/-}$	WT	IFABP$^{-/-}$	LFABP$^{-/-}$
Glucose, mg/dl	169 ± 15^b	92 ± 9^a	147 ± 16^b	156 ± 25^b	87 ± 5^a	159 ± 19^b	149 ± 20^{ab}	101 ± 9^a	169 ± 22^b
Insulin, ng/ml	0.18 ± 0.02	0.20 ± 0.02	0.28 ± 0.01	0.21 ± 0.01	0.26 ± 0.06	0.25 ± 0.01	0.25 ± 0.01	0.24 ± 0.00	0.35 ± 0.07
HOMA, IR	1.9 ± 0.2	1.2 ± 0.1	1.6 ± 0.3	2.0 ± 1.4	1.4 ± 0.4	2.5 ± 0.4	2.2 ± 0.3	1.4 ± 0.1	2.7 ± 0.5
Total cholesterol, mg/dl	95 ± 5	86 ± 7	94 ± 4	99 ± 5^{ab}	86 ± 4^a	109 ± 7^b	108 ± 3^b	76 ± 5^a	105 ± 11^b
TAG, mg/dl	75 ± 9^a	83 ± 11^a	148 ± 10^b	99 ± 11	114 ± 10	90 ± 9	97 ± 6^b	80 ± 5^b	73 ± 5^a
NEFA, mEq/liter	0.30 ± 0.04	0.34 ± 0.06	0.42 ± 0.06	0.26 ± 0.04	0.36 ± 0.03	0.43 ± 0.13	0.40 ± 0.04^b	0.24 ± 0.04^a	0.38 ± 0.07^b
Leptin, ng/ml	3.1 ± 0.6^{ab}	0.4 ± 0.3^a	5.7 ± 1.7^b	3.2 ± 0.6^a	1.1 ± 0.2^a	13.4 ± 1.9^b	3.3 ± 0.8^{ab}	0.2 ± 0.2^a	10.2 ± 3.3^b
Leptin index	0.8 ± 0.1^b	0.2 ± 0.1^a	0.9 ± 0.2^b	0.6 ± 0.1^a	0.3 ± 0.0^a	1.2 ± 0.1^b	1.9 ± 0.4^b	0.1 ± 0.1^a	1.3 ± 0.3^b
Adiponectin, ng/ml	10.7 ± 0.7^b	6.4 ± 0.4^a	10.6 ± 0.6^b	10.8 ± 1.1^{ab}	8.3 ± 0.4^a	12.6 ± 1.2^b	10.3 ± 0.8^b	5.9 ± 0.4^a	11.8 ± 1.0^b
Adiponectin index	3.0 ± 0.4^{ab}	4.0 ± 0.4^b	2.3 ± 0.2^a	2.6 ± 0.3^{ab}	2.8 ± 0.4^b	1.3 ± 0.2^a	1.7 ± 0.1^a	3.0 ± 0.2^b	1.4 ± 0.1^a
Liver WT, g	0.94 ± 0.03^b	0.84 ± 0.02^a	0.86 ± 0.01^a	0.90 ± 0.04^{ab}	0.79 ± 0.02^a	1.00 ± 0.06^b	0.99 ± 0.03^b	0.93 ± 0.02^{ab}	0.85 ± 0.03^a
Liver, g/g BW	0.035 ± 0.001^{ab}	0.036 ± 0.001^b	0.033 ± 0.001^a	0.034 ± 0.001	0.031 ± 0.001	0.035 ± 0.003	0.034 ± 0.001^b	0.0037 ± 0.002^b	0.029 ± 0.001^a
Epididymal fat, g	0.49 ± 0.06^b	0.14 ± 0.04^a	0.60 ± 0.05^b	0.74 ± 0.07^b	0.28 ± 0.04^a	1.50 ± 0.14^c	0.93 ± 0.14^b	0.18 ± 0.05^a	1.01 ± 0.14^b
Perirenal fat, g	0.17 ± 0.03^b	0.05 ± 0.01^a	0.18 ± 0.02^b	0.21 ± 0.02^a	0.09 ± 0.02^a	0.45 ± 0.05^b	0.32 ± 0.05^b	0.07 ± 0.05^a	0.36 ± 0.06^b
Inguinal fat, g	0.32 ± 0.05^b	0.12 ± 0.04^a	0.36 ± 0.03^b	0.45 ± 0.04^a	0.25 ± 0.10^a	1.04 ± 0.14^b	0.56 ± 0.10^b	0.14 ± 0.03^a	0.69 ± 0.09^b

Table 2-5. Plasma and Tissue Analyses for WT, IFABP$^{-/-}$ and LFABP$^{-/-}$ mice after 12 weeks on a low-fat (LFD), high saturated fat (HFS) or high unsaturated fat (HFU) diet. Data are mean ± SEM, analyzed using one-way ANOVA with Tukey's post-hoc test. Results with different letters within a dietary treatment are significantly different (p<0.05). n=6-9 for all groups.

IFABP$^{-/-}$ Mice have Increased Chylomicron Secretion Rates

Oral fat tolerance tests were performed on 24 hour fasted mice treated with Tyloxypol to prevent clearance of circulating TG-rich lipoproteins (Figure 2-3). We found little or no differences between the LFABP$^{-/-}$ and WT mice except on the LFD at baseline and 1 h, where TG levels were slightly but significantly higher ($p < 0.05$), as also shown above (Table 2-5 and Figure 2-3A). The IFABP$^{-/-}$ fed the LFD showed a trend toward increased TG secretion, with values significantly different than WT at t = 2h ($p < 0.05$). On the HFS diet, the IFABP$^{-/-}$ mice showed significantly higher TG levels at 2 hours following the oral fat bolus ($p < 0.05$), which continued throughout the 4-hour measurement period (Figure 2-3B). Similar but smaller increases were seen for IFABP$^{-/-}$ mice fed HFU, however differences were not statistically significant (Figure 2-3C). For the LFABP$^{-/-}$ mice, no changes were found on the HFU diet, and HFS-fed LFABP$^{-/-}$ mice tended to have greater plasma TG levels following the oral fat bolus, with differences significant at t = 3h (Fig. 2-3A-C) ($p < 0.05$).

Figure 2-3
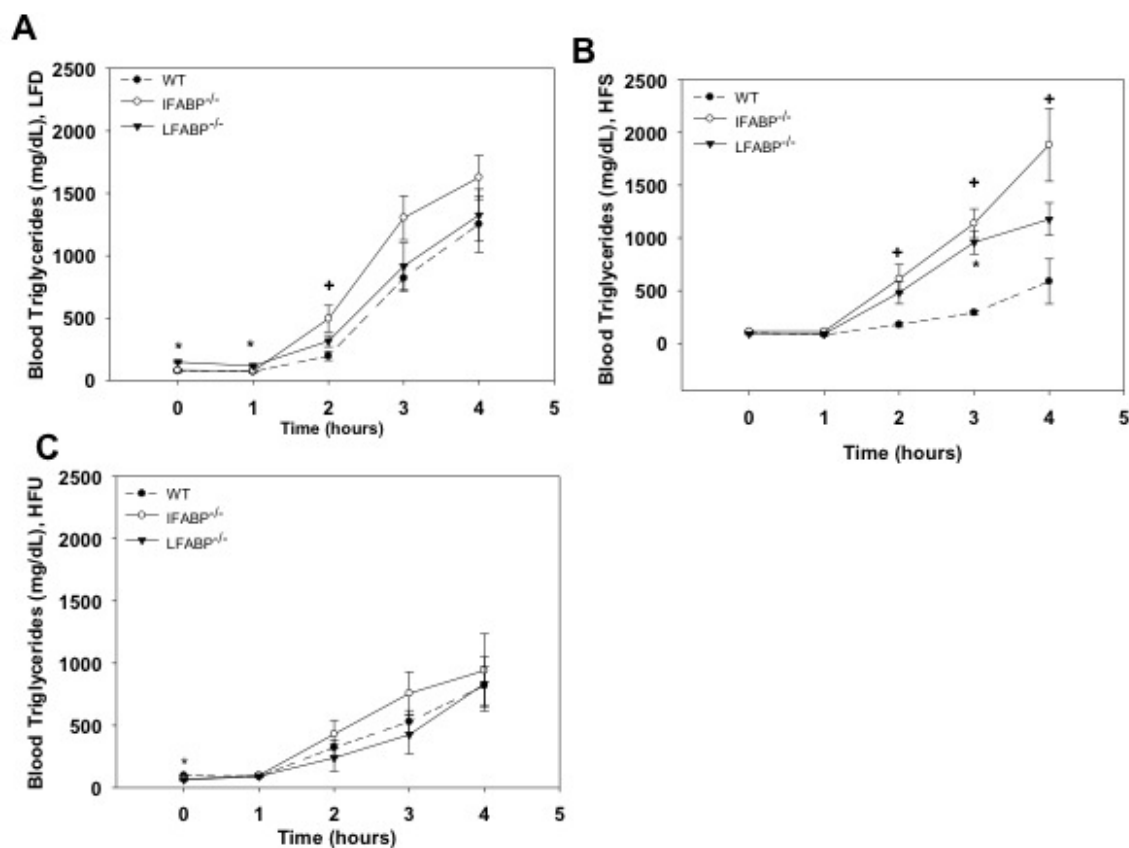
Figure 2-3. Oral fat tolerance tests following a 24-hour fast for WT, IFABP$^{-/-}$ and LFABP$^{-/-}$ mice after 12 weeks on a low-fat (LFD), high saturated fat (HFS) or high unsaturated fat (HFU) diet. Blood TG levels for A. LFD-fed mice (n=6-9); B. HFS-fed mice (n=5-6); C. HFU-fed mice. **(**n=6-9). Data are given as mean ± SEM, analyzed using Student's t-test. *$p<0.05$ for LFABP$^{-/-}$ vs WT at the same timepoint $^{+}p<0.05$ for IFABP$^{-/-}$ vs WT at the same timepoint.

Altered FA and MG Metabolism in the Intestinal Enterocyte by IFABP⁻ or LFABP Ablation

[^{14}C]-labeled oleate was administered intravenously while simultaneously introducing [^{3}H]-labeled oleate into the duodenum, in 24h fasted mice, to examine the metabolic fate of bloodstream-derived and diet-derived FA, respectively. As detailed in "Experimental Procedures", small intestinal mucosa was harvested after 2 min, and lipids were extracted and separated by TLC to measure recovery of both dietary and bloodstream-derived FA in specific lipid species (Figure 2-4). Data were expressed as the percent of label recovered in each lipid species, and as the ratio of label recovered in TG relative to PL (7). No significant differences from WT were found for IFABP$^{-/-}$ or LFABP$^{-/-}$ mice fed the LFD (Figure 2-4, A and B). However, HFS feeding resulted in a lower recovery of the [^{14}C]-oleate label in TG for the IFABP$^{-/-}$ mice ($p < 0.05$). In contrast, LFABP$^{-/-}$ mice had an increase in recovery of [^{14}C]-oleate in PL (Figure 2-4C). This resulted in a lower TG/PL ratio for both knockouts (Figure 2-4D) ($p < 0.05$), indicating that in mice fed high-fat diets, both proteins are involved in trafficking FA from the bloodstream toward TG synthesis. Administration of duodenal oleate did not result in changes in the IFABP$^{-/-}$ during LFD or HFS feeding (Figure 2-4E, G). However, we observed that LFABP$^{-/-}$ mice fed LFD had a lower TG/PL ratio (Figure 2-4E, H) ($p < 0.05$). In separate experiments, we measured the oxidation of duodenally-administered [^{14}C]-labeled oleate, and found that on both the LFD and HFS diet, LFABP$^{-/-}$ mice had lower mucosal FA oxidation ($p < 0.05$) (Figure 2-4I). This is in agreement with previous experiments in chow fed mice (7), as well as studies of liver FA oxidation (152, 179, 182, 186).

Figure 2-4
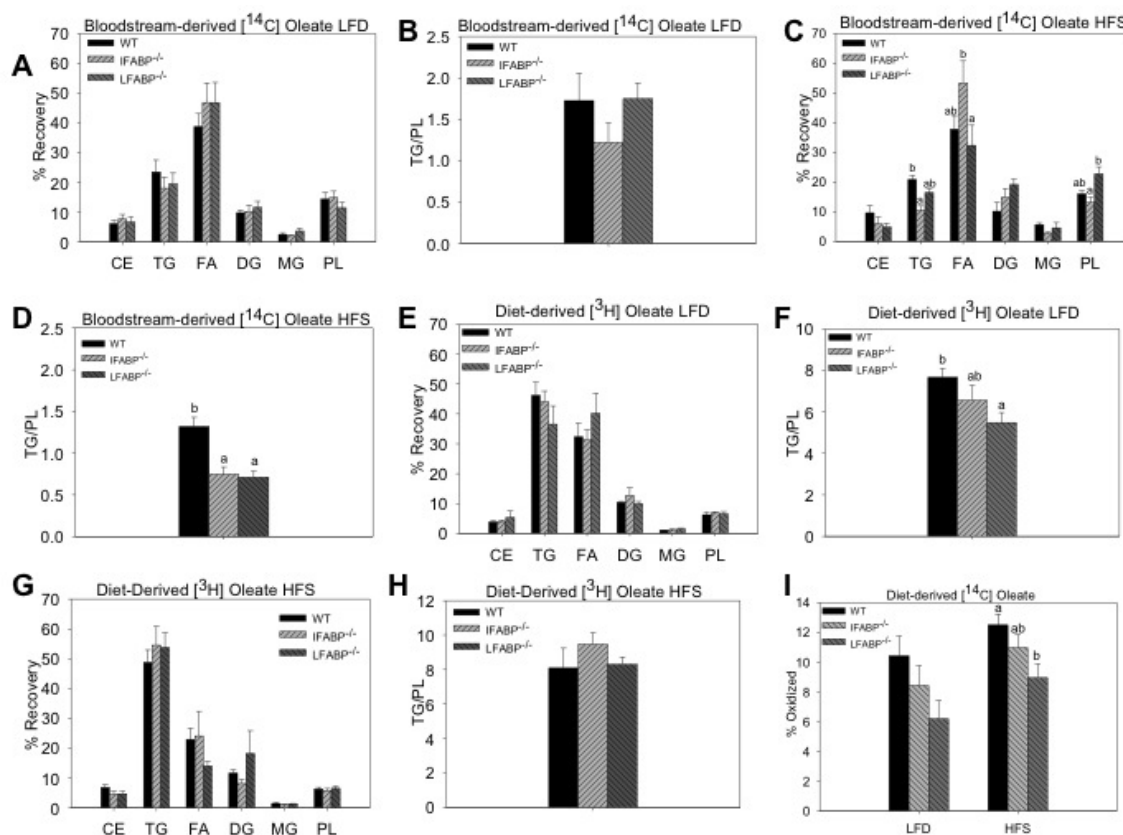
Figure 2-4. Intestinal fatty acid metabolism in WT, IFABP^{-/-} and LFABP^{-/-} mice after 12 weeks on a low-fat (LFD), high saturated fat (HFS) or high unsaturated fat (HFU) diet. A. Bloodstream-derived [14C] Oleate LFD (n=6-7); B. Bloodstream-derived [14C] Oleate TG/PL ratio LFD (n=6-7); C. Bloodstream-derived [14C] Oleate HFS (n=6); D. Bloodstream-derived [14C] Oleate TG/PL ratio HFS (n=6); E. Diet-derived [3H] Oleate LFD (n=6-7); F. Diet-derived [3H] Oleate TG/PL ratio LFD (n=6-7); G. Diet-derived [3H] Oleate HFS (n=6); H. Diet-derived [3H] Oleate TG/PL ratio HFS (n=6); I. Oxidation of Diet-Derived [14C] Oleate for LFD and HFS-fed mice (n=8); Data are given as mean ± SEM, analyzed using one-way ANOVA with Tukey's post-hoc test. Results with different letters are significantly different (p<0.05).

Studies from our laboratory have shown that LFABP, but not IFABP, is a 2-MG binding protein *in vitro* and *in vivo* (138, 139). In keeping with this binding function, we found alterations in intestinal 2-MG metabolism in chow-fed LFABP$^{-/-}$ mice, but not in the IFABP$^{-/-}$ mice (7). Here, we determined whether altered MG metabolism would also be manifested under the HFS feeding regimen (Figure 2-5). Indeed the results showed that LFD-fed LFABP$^{-/-}$mice had an increase in recovery of 'dietary' [^{3}H]-monoolein PL, relative to WT, resulting in a significantly lower TG/PL ratio ($p < 0.05$) (Figure 2-5A, B), and that the HFS feeding resulted in lower recovery in TG, and a higher recovery in PL, relative to WT, also resulting in a lower TG/PL ratio ($p < 0.05$) (Figure 2-5C, D).

Figure 2-5
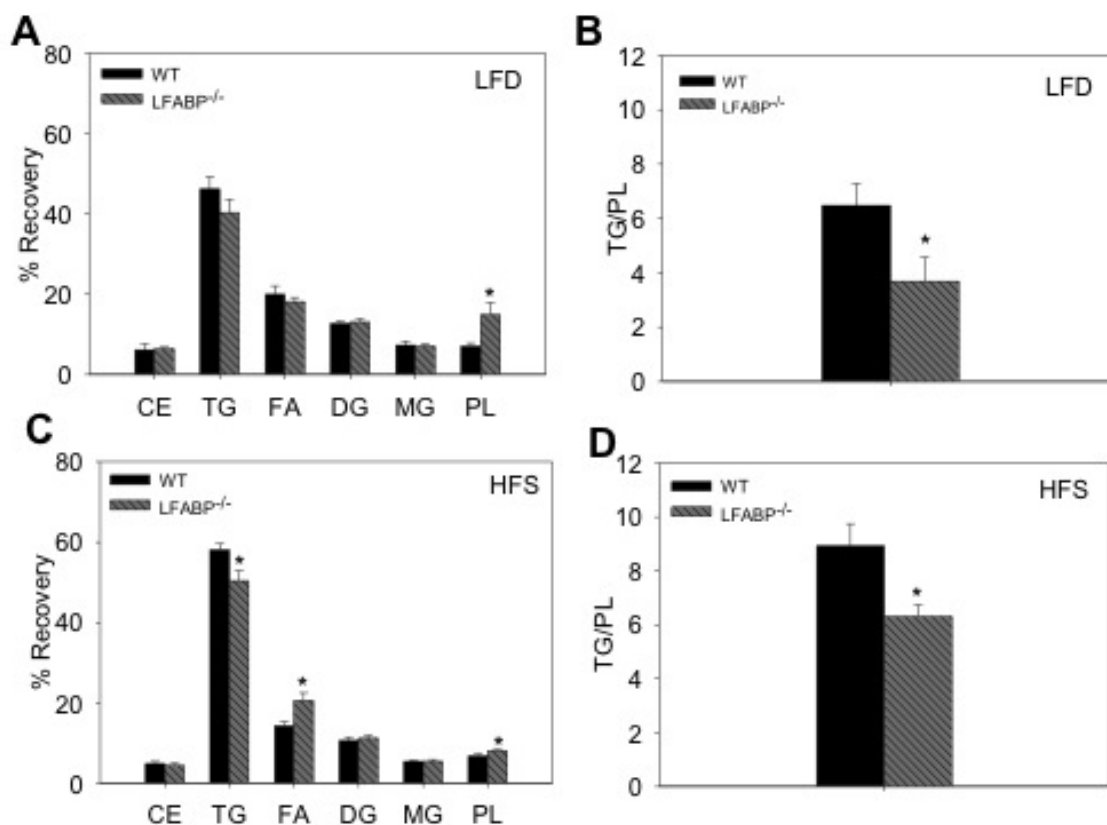
Figure 2-5. Intestinal 2-monoacylglycerol metabolism in WT and LFABP$^{-/-}$ mice after 12 weeks on a low-fat (LFD) or high saturated fat (HFS) diet. A. Diet-derived [^{3}H] Monoolein LFD (n=6-7); B. Diet-derived [^{3}H] Monoolein TG/PL ratio LFD (n=6-7); C. Diet-derived [^{3}H] Monoolein HFS (n=6-7); D. Diet-derived [^{3}H] Monoolein TG/PL ratio HFS (n=7).   Data are given as mean ± SEM, and are analyzed using Student's t-test. *p<0.05 vs WT.

Effects of IFABP and LFABP ablation on Expression of Genes Involved in Intestinal Lipid

Metabolism

As noted above, few changes, compared to WT mice, were found in mucosal expression of genes related to lipid metabolism and transport for IFABP^{-/-} or LFABP^{-/-} mice on a chow diet, suggested that alterations in lipid metabolism were not due to changes in gene expression but were rather, more likely, due to changes in lipid transport (7). Here we further examined lipid-related gene expression to determine whether feeding high fat compared with low fat diets resulted in differential regulation of mucosal gene expression in the IFABP^{-/-} or LFABP^{-/-} mice. In keeping with prior observations, high fat feeding resulted in increased expression of several genes in WT mouse mucosa. In particular the HFS diet resulted in significantly increased expression of LFABP, IFABP, MGL, and FAAH, and the HFU diet resulted in increased expression of these genes as well as MGAT and PPARα (46, 204, 205)(Figure 2-6A). With almost no exception, the responses to high-fat feeding in the WT mice were also found in the two knockout strains. For example, the HFS diet caused a 9-fold increase in LFABP expression in WT and an 8-fold increase in LFABP expression in the IFABP^{-/-} mouse; the HFU diet resulted in 3 to 4-fold increases in FAAH expression in all three genotypes, etc. (Figure 2-6B, C). Thus, the present differences found in FA and MG metabolism in the IFABP^{-/-} and LFABP^{-/-} mice appear to be primarily caused by nontranscriptional effects, most likely via alterations in intracellular lipid binding capacity and transport. A small but significant increase (50%) in PPARα expression was found in HFU-fed WT mouse mucosa which was not found in LFABP^{-/-} mucosa, perhaps related to the proposed direct interaction between LFABP and PPARα (137, 148, 149). Importantly, no compensatory increase was found in LFABP expression in the IFABP^{-/-} mucosa, or in IFABP in the LFABP^{-/-} mucosa, on any of the three diets used, supporting the hypothesis that these two enterocyte proteins have unique functional roles.

Figure 2-6
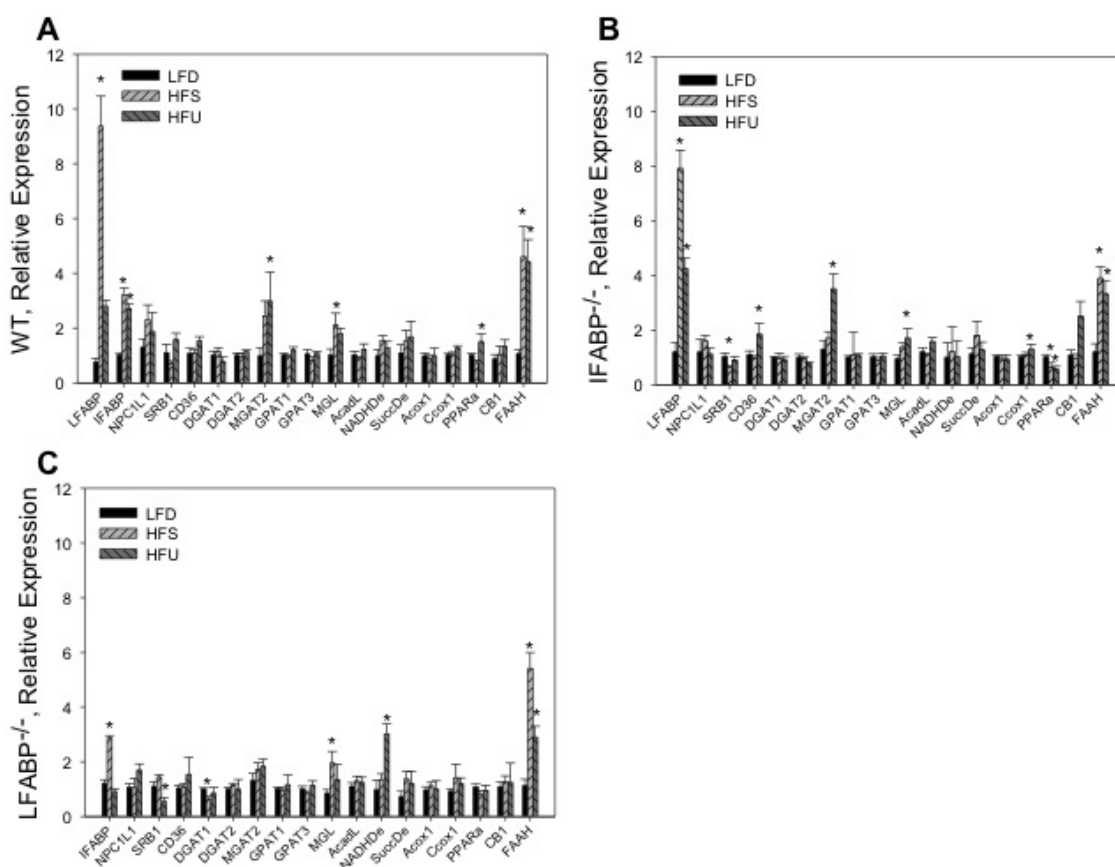
Figure 2-6. Relative quantification of mRNA expression of intestinal lipid metabolic and transport genes for WT, IFABP$^{-/-}$ and LFABP$^{-/-}$ mice after 12 weeks on a low-fat (LFD), high saturated fat (HFS) or high unsaturated fat (HFU) diet. A. WT fed HFS or HFU relative to WT fed LFD (n=5-9) B. IFABP$^{-/-}$ fed HFS or HFU relative IFABP$^{-/-}$ fed LFD (n=5-9). C. LFABP$^{-/-}$ fed HFS or HFU relative LFABP$^{-/-}$ fed LFD (n=5-9). Data are given as mean ± SEM, and are analyzed using Student's t-test. *p<0.05 vs same genotype on LFD.

Intestinal Mucosal Endocannabinoid Levels in IFABP$^{-/-}$ and LFABP$^{-/-}$ Mice.

Recent reports have shown that several FABPs can bind the endogenous cannabinoid receptor

ligand anandamide (arachidinoylethanolamine, (AEA)) (83, 84). 2-arachidonoylglycerol (2-AG) is

also an endocannabinoid, and we have shown that LFABP binds 2-monoacylglycerols (138).

Because the endocannabinoid system is involved in appetite regulation, we hypothesized that

changes in food intake observed in the two FABP null mice could perhaps be related to changes

in intestinal endocannabinoid levels. Hence, we measured mucosal levels of AEA and 2-AG as

well as several other monoacylglycerol species, and of oleoylethanolamine and

palmitoylethanolamine, which are ligands for the PPARα transcription factor and may also play a

role in food intake (87, 90). We found that both 2-AG (p = 0.053) and AEA levels showed a trend

to be elevated in LFABP$^{-/-}$mucosa, as was 2-linoleoylglycerol (p < 0.05); Oleoylethanolamine and

palmitoylethanolamine levels were not changed (Figure 2-7). 2-AG levels showed an opposite,

lower, trend in the IFABP$^{-/-}$ mucosa on LFD and HFS; lower levels of 2-monopalmitin were also

found in IFABP$^{-/-}$ mucosa (Figure 2-7). Notably, no differences in the mRNA expression of MGL

or FAAH, enzymes that degrade 2-AG and AEA, respectively, were found between genotypes

(Figure 2-6).

Figure 2-7
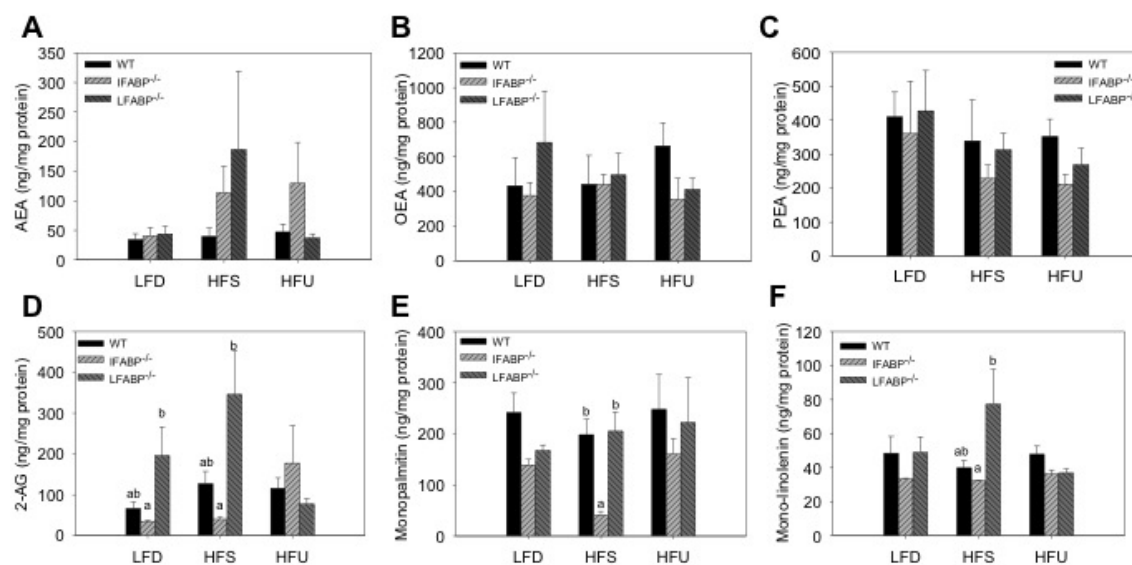
Figure 2-7. Intestinal ethanolamine and 2-monoacylglycerol Levels for WT, IFABP^{-/-} and LFABP^{-/-} mice after 12 weeks on a low-fat (LFD), high saturated fat (HFS) or high unsaturated fat (HFU) diet. A. AEA (n=6); B. OEA (n=6); C. PEA (n=6); D. 2-AG (n=6); E. Monopalmitin (n=6); F. Monolinolenin (n=6). Data are mean ± SEM, analyzed using one-way ANOVA with Tukey's post-hoc test. Results with different letters within dietary treatment are significantly different (p<0.05).

Discussion

The human intestine can process large quantities of dietary lipid, averaging up to 100 g in adult males on a daily basis, with a remarkable absorption efficiency of >95%. The co-expression of two members of the FABP family of lipid-binding proteins, IFABP and LFABP, has generally been thought to be related to the large lipid processing needs of the enterocytes, however it has not been entirely clear why two related proteins, both of which bind long chain FA, are present. In this regard, the ileal lipid binding protein, another FABP family member found in the distal small intestine, may also contribute to fat absorption in view of the fact that this protein can also bind fatty acids (125, 127). Indeed, the FABP protein family differs from many other classes of lipid-binding proteins in having more than 10 separate genes, each with a different tissue distribution, in contrast to the more typical expression of the same gene in many or all tissues, for other classes of lipid-binding proteins (111).

Because there are some ligand binding differences between IFABP and LFABP (135, 136) and since we demonstrated differences in in vitro FA transport properties (119, 142, 166), we directly compared mice null for each of these genes to determine whether physiological differences would be observed. Our initial studies, using male mice fed laboratory chow, showed a modest FA trafficking defect for the IFABP$^{-/-}$ mice, a modest MG trafficking defect for the LFABP$^{-/-}$ mice, and defective mucosal FA oxidation in the LFABP$^{-/-}$ but not IFABP$^{-/-}$ mice. While no differences in body weights were found, differential changes in body composition in response to fasting were observed, suggesting that each of these FABPs has a different impact on whole body energy metabolism (7). Hence, in the current study, we fed high-fat diets containing TG rich in long chain FA to generate an abundance of long chain FA and MG in the

intestinal lumen, hypothesizing that more striking phenotypic changes in IFABP^{-/-} and LFABP^{-/-} mice would be revealed, in order to help elucidate unique functions of these related proteins. Remarkably, highly divergent whole body phenotypes were found.

The LFABP^{-/-} mice displayed increases in body weight and body fat mass relative to WT when fed high-fat diets. The mice used in these studies were derived from the LFABP null mouse which was generated by Martin et al., using the C57BL/6N background strain, and first described in 2003 (180). The mice had been backcrossed 6 generations onto the C57BL/6N strain and were subsequently backcrossed another 6 generations onto the C57BL/6J strain upon arrival to our laboratory, as previously described (7). In agreement with the present findings, Martin and coworkers found that male and female LFABP^{-/-} mice were prone to obesity when fed high LCFA diets, with increases in body weight and FM relative to WT mice; this body weight phenotype has been repeated several times (183–185). Interestingly, the body weight data are in contrast to findings by Newberry et al., who generated a separate LFABP^{-/-} mouse on a mixed C57BL6 and SV129 background, then backcrossed to the C57BL/6J wild type strain (179, 187, 196). In those studies, female LFABP^{-/-} mice fed diets containing high levels of medium chain saturated FA (40 kcal% fat as hydrogenated coconut oil) had lower BW relative to WT mice (187, 196). Both lines showed apparent decreases in hepatic FA β-oxidation, and lower levels of hepatic TG (152, 179, 206, 207). We find reduced intestinal FA oxidation in the LFABP^{-/-} mice as well, both on chow (7) and high fat diets, supporting a tissue-independent function for LFABP in FA oxidation. It is likely that these effects on oxidation are not caused by diminished oxidative capacity, but rather by defective FA trafficking.

Despite consistent effects of LFABP$^{-/-}$ ablation on FA oxidation and liver TG, the increased body weights and total body fat observed in the present studies and those of Schroeder and coworkers (180, 183, 185), is different than the reduced body weights seen in the Missouri LFABP$^{-/-}$ mice (179, 187, 196). The differences may in part be related to sex, as female mice tend to be more resistant to obesity during high-fat feeding relative to males (208, 209), and have higher levels of LFABP protein in the liver (124). Further, the diets may play a role in the outcome differences between studies. The present high-fat diets and those of the Texas studies contain sources of LCFA, used to model the more common lipids in the human diet. The long chain 2-MGs and FAs released by pancreatic lipase in the intestinal lumen enter the enterocyte where they are then used to generate TG which is incorporated into chylomicrons that enter the lymphatic system and then the general circulation. MCFA, used in the Missouri studies, are more soluble in the hydrophilic cytosol and do not bind to FABPs (124, 135). MCFA are metabolized differently that LCFA in that they are not included in chylomicrons, but rather directly enter the liver via the portal vein and therefore do not first enter the general circulation (65). In addition, it has been shown that diets containing MCFA are not as obesogenic as those containing LCFA (66–68). Therefore, metabolism of the FA may differ and may provide some clues for the differences in results. Nevertheless, the Missouri group reported that a Western diet (40 kcal% milk fat with 0.21% cholesterol) also resulted in decreased weight gain compared to WT, although differences in males were not as large as in females (181). A number of other differences could contribute to the divergence in body weight phenotype, including residual background gene differences, the gene targeting constructs employed, the potential for residual small fragments of the LFABP (210), or perhaps environmental effects of the facilities in which each mouse line is housed, as has been recently shown to impact susceptibility to diet-induced obesity in two separately housed but isogenic mouse strains (211).

In dramatic contrast to the results in LFABP$^{-/-}$ mice, under identical conditions, the IFABP$^{-/-}$ mice fed a HFS diet displayed 30% less weight gain compared to WT mice, which was accompanied by a reduction in food intake. No changes in fecal fat were found, thus lipid malabsorption did not account for the lower weight gains observed. The IFABP$^{-/-}$ mice had a trend toward lower feed efficiency, i.e. less weight gain per calorie consumed, on both HF diets, however the results did not reach statistical significance. In further contrast to the LFABP null mice, IFABP ablation resulted in a very lean phenotype, with significantly lower FM and greater lean mass. The IFABP$^{-/-}$ mice also displayed consistently higher losses of fat mass during fasting.

As noted above, the body weight phenotype found in the present studies, using a substrain of IFABP$^{-/-}$ mice that were nonetheless bred by intercrossing, differs from that observed in the original line (23, 24). Indeed, in earlier studies we found that the effects of IFABP deletion in the original IFABP$^{-/-}$ line appear to be sensitive to sex, age, and diet (190, 191, 212). Similarly, while we found that chow-fed IFABP$^{-/-}$ mice from the substrain showed no change in body weight through 20 weeks of age (7), these same mice in the present study, also examined through 20 weeks of age and fed HFS for 12 weeks, showed significantly lower body weight gain than WT mice. Moreover, female IFABP$^{-/-}$ mice fed a high-fat chow diet with added cocoa butter and 1.25% cholesterol also had lower body weights than WT, however by contrast the male mice were heavier (24). On a high safflower oil diet that was fed for 2 weeks, older (30-40 week) male and female IFABP$^{-/-}$ mice both gained more weight than WT mice, while on a high beef tallow diet, the males were found to have slightly (9%) higher body weights, with female IFABP$^{-/-}$ mice of the same age and on the same diet showing no body weight change (191). In addition to body weight differences, the relative absence of gene expression changes found by qPCR analysis of mucosal samples for male IFABP$^{-/-}$ mice in this study, is in contrast with results of a

microarray analysis of intestinal RNA of male IFABP$^{-/-}$ mice from the original line, which showed

significant differences compared to WT males, including increased expression of genes involved

in fatty acid metabolism (213).

It will be of great interest to determine the underlying reasons behind the discrepant phenotype

exhibited by the two IFABP$^{-/-}$ lines from a common founder, and future studies will address this

issue. Irrespective of the origin(s) of the body weight gain results under different conditions, the

present direct comparison of IFABP and LFABP null mice under identical conditions of age, sex,

and diet, highlights the dramatically different outcomes for body weights and body composition,

strongly supporting distinct roles of the two FABPs in the regulation of whole body energy

metabolism.

The IFABP$^{-/-}$ and LFABP$^{-/-}$ also mice displayed differences in fuel utilization, which appear to be

driven by lipid stores. The very lean IFABP mice, with low body fat, have a higher RER indicative

of increased carbohydrate oxidation, while the obese LFABP$^{-/-}$ mice display a lower RER

indicative of increased fat utilization. When adjusted for lean mass, the LFABP$^{-/-}$ mice displayed

higher energy expenditure on the high-unsaturated fat diet and were surprisingly more active,

despite their much higher body weights and adiposity. Interestingly, feeding a high-saturated

fat diet did not promote changes in plasma glucose or insulin levels in the LFABP$^{-/-}$ mice, despite

their being markedly obese. The IFABP$^{-/-}$ mice, by contrast, had lower plasma glucose levels and

a higher adiponectin index, reflecting increased insulin sensitivity and fat-free mass. In both

genotypes, plasma leptin values varied as expected with adipose tissue mass, thus LFABP$^{-/-}$ mice

fed HFS or HFU had elevated plasma leptin levels, and IFABP$^{-/-}$ mice had markedly lower

circulating leptin levels than the LFABP null mice (214–216).

Since LFABP is involved in chylomicron assembly (31, 54), and because we and others have recently shown that obesity and high fat feeding result in substantially reduced rates of TG secretion from the intestine (60, 217), we expected to see a lower TG secretion rate from the LFABP$^{-/-}$ intestine during an oral fat tolerance test (181). However, as previously found for chow-fed LFABP$^{-/-}$ (7), blood TG values were not different from WT in the high-fat fed LFABP$^{-/-}$ mice. Thus the LFABP null mice, even in the face of marked obesity, display normal intestinal TG secretion. The IFABP$^{-/-}$ mice, in contrast, exhibited an increase in secretion of TG relative to WT during HFS feeding.   As IFABP appears not to be involved in chylomicron formation (54), the increased TG secretion likely correlates with the more rapid intestinal secretion observed in lean mice (60, 217).

The site of FA and MG entry into the enterocyte (apical versus basolateral) determines their metabolic fate, with lipids from the bloodstream primarily incorporated into PL or oxidized, in contrast to dietary FA and MG which are primarily esterified in TG (62, 63). The mechanisms underlying this 'metabolic compartmentation' are unknown. Here we found that chronic feeding of a high fat diet promotes a decrease in bloodstream FA incorporation into TG relative to PL in both the IFABP and LFABP null mice, effects that were largely absent in chow-fed mice (9) and in the present low fat diet-fed mice. Thus, high fat feeding exacerbates the effects of IFABP and LFABP ablation on FA trafficking, particularly for FA entering the enterocyte from the bloodstream. By contrast, this potentiating effect of high fat feeding on FA metabolism was not found for MG metabolism. In particular, the decreased incorporation of diet-derived MG into TG relative to PL observed in chow-fed mice (9) was also found in the present studies for both low fat and high fat-fed mice. Thus, LFABP is involved in trafficking of diet-derived MG under all dietary conditions examined, consistent with it being the MG binding and transport protein in

cytosol (138). Analysis of ILBP ablated mice demonstrated a defect in mucosal to serosal transport of taurocholic acid in everted gut sacs, and supports the idea that FABPs are involved in the cellular transport of their respective ligands (133).

We also found that LFABP ablation results in a reduction in mucosal oxidation of the administered radiolabeled oleate in both LFD and HFS-fed LFABP$^{-/-}$mice, in keeping with our previous results in chow-fed mice (7). Reduced hepatic oxidation of FA and ketones in LFABP$^{-/-}$ mice has also been reported (152, 179, 186, 210). Taken together, the results strongly support a role for LFABP in trafficking of FA substrates toward oxidative pathways. Decreased FA oxidation could, in part, give rise to the obese phenotype observed in the LFABP$^{-/-}$ mice herein.

Changes in food intake may also contribute to the body weight and fat changes in the LFABP$^{-/-}$ and IFABP$^{-/-}$ mice. While no changes in caloric consumption of the LFABP$^{-/-}$ mice were found on the LFD, as observed previously with chow feeding (7), an approximately 20% increase in caloric intake was observed with the HFS diet in particular, and an increased 'food efficiency' was found on both high fat diets. In the IFABP$^{-/-}$ mice decreased food intake and efficiency were found. Higher mucosal levels of the orexigenic endocannabinoids 2-AG and AEA on the HFS diet may be involved in the apparent increase in LFABP$^{-/-}$ appetite; higher levels of 2-linoleoylglycerol were also found, and this has been suggested to be a weak CB1 agonist (218). In contrast, 2-AG levels appeared lower in the mucosa of IFABP$^{-/-}$ mice.

Although endocannabinoid activity in the central nervous system is well known to impact appetitive behavior, recent evidence suggests that the gut endocannaibinoid system may also be important in the regulation of food intake, and that specific nutrients may regulate gut

endocannabinoid levels. (219, 220) For example, fasting increased and re-feeding decreased intestinal 2-AG and AEA levels, and also modulated cannabinoid receptor 1 expression in vagal afferents innervating the gastrointestinal tract (221). In genetically obese rats, intestinal 2-AG levels were shown to be markedly elevated, and the abovementioned postprandial reduction was diminished, relative to lean rats (222). Furthermore, it has been recently shown that ingestion of mono- and dienoic fatty acids, but not sucrose, protein, or saturated fatty acids, led to increased jejunal levels of 2-AG and AEA (96, 223). Thus, the observed alterations in mucosal 2-AG levels in the enterocyte FABP null mice may be involved in their altered food intake, and may also be related to altered fatty acid trafficking secondary to FABP absence.

Indeed, we recently showed that LFABP binds long chain monoacylglycerols, including the endocannabinoid 2-AG, and several FABPs have been reported to bind AEA (83, 84), thus alterations in endocannabinoid levels secondary to FABP ablation may be involved in the appetite and body weight phenotypes observed. However, since it is not thought that IFABP binds the endocannabinoids, the link between intestinal IFABP ablation and altered endocannabinoid status is not clear. Notably, we found no changes in levels of either MGL or FAAH in LFABP$^{-/-}$ or IFABP$^{-/-}$ compared to WT mucosa, thus the results support a ligand availability and/or transport defect rather than a transcriptionally mediated change in enzyme activity.   The genes encoding for FA and MG metabolic enzymes, both anabolic and catabolic, are also essentially unchanged relative to WT in response to high fat feeding, in the mucosa of either the LFABP$^{-/-}$ or IFABP$^{-/-}$ mouse, again indicating that the functions of both of these enterocyte proteins involves intracellular ligand transport and, likely, targeting.

It is interesting to note that the LFABP null mouse, while obese, is nevertheless surprisingly healthy—it is normoglycemic and normoinsulinemic, has reduced hepatic steatosis (187, 196), intestinal TG secretion rates similar to a lean mouse, and appears more active than the WT mouse. Indeed, preliminary studies suggest that LFABP$^{-/-}$ mice have a greater exercise tolerance than WT mice, in spite of their obese phenotype (see Appendix). The IFABP$^{-/-}$ mice in this study are also healthy, with greater FFM, higher intestinal lipid secretion rates, lower plasma glucose and cholesterol levels, and a higher adiponectin index. We observed small but significant differences in food intake, and preliminary experiments using singly housed older mice also suggest that lower caloric consumption might in fact be playing a role in the IFABP$^{-/-}$ phenotype (results not shown). Studies are also underway to examine fuel utilization in muscle and adipose tissue in order to further understand how the loss of IFABP in the intestine impacts whole body metabolism as well as fat and lean mass deposition. Overall, the present results suggest that simultaneous inhibition of the two enterocyte FABPs may prove useful for promoting a healthy phenotype and preventing high fat diet-associated metabolic changes. On the other hand, given the different body weight phenotype of the original IFABP$^{-/-}$ line, as well as the differences displayed by the two independently generated LFABP$^{-/-}$ lines, it is important to consider the remarkably multifactorial nature of obesity, with multiple genetic and environmental factors contributing to body weight outcome (224). Thus, it is perhaps not surprising that IFABP or LFABP ablation *per se* may not be a dominant determinant of body weight, or whole body energy metabolism. As well, while most obesity is associated with unhealthy comorbidities, an appreciation for the 'medically healthy but obese (MHO)' state is emerging (225); in this regard, it is noteworthy that for the LFABP null mice, a healthy metabolic phenotype is contemporaneous with markedly higher body weight and adiposity.

Ablation of LFABP or IFABP results in changes that appear to be greater at the systemic level than at the cellular level, with both knockout models displaying large alterations in whole body energy homeostasis. While high fat feeding did significantly exacerbate the changes in enterocyte FA metabolic fate found for low fat fed mice, and while MG metabolism was consistently impacted in the LFABP$^{-/-}$ mice, these effects remained relatively modest overall—no fat malabsorption was found, for example. By contrast, the deficiency in either IFABP or LFABP was seen to cause profound systemic effects. These results contribute to a growing appreciation of the important link between intestinal lipid metabolism and whole body energy balance. For instance, ablation of the intestinal TG synthesis enzymes DGAT1 or MGAT2 resulted in more substantial changes in whole body energy homeostasis, with both lines exhibiting a lean phenotype, than in cellular lipid metabolism (50, 103, 105). Further, we recently showed that intestine-specific overexpression of the hydrolytic enzyme MGL led to an obese phenotype, with relatively modest effects on intestinal lipid metabolism (108). As in the present studies, the mechanisms underlying all these changes are not completely understood, however together they point to the important linkage between intestinal lipid metabolic enzymes and whole body energy homeostasis. For the LFABP$^{-/-}$ mouse, the whole body phenotype undoubtedly results from a combination of liver-specific and intestine-specific effects. These associations with whole body energy homeostasis may not be caused by changes in levels of enzymatic pathways themselves, but more likely, via alterations in signaling pathways which regulate activity, food intake, and energy utilization (217).

In summary, the present studies demonstrate that IFABP and LFABP, despite being co-expressed and homologous proteins that bind long chain fatty acids, play unique roles in intestinal lipid processing, with each FABP distinctly involved in downstream signaling to the body. Ablation of

LFABP results in marked obesity on a high fat diet, yet the mice remain apparently healthy. Ablation of IFABP, in contrast, results in a lean phenotype with lower plasma glucose levels in certain circumstances. While the LFABP$^{-/-}$ phenotype likely arises from changes occurring in both tissues where the gene is normally expressed, the liver and the intestine, the IFABP$^{-/-}$ phenotype arises secondary to alterations in intestinal mucosa alone. Tissue-specific ablation of LFABP will help elucidate the origin of the body weight phenotype. As well, simultaneous ablation of both these FABPs in the enterocyte will further enable an understanding of the role of the FABPs in lipid absorption and intestinal secretion.

Chapter 3

Simultaneous Ablation of Liver and Intestinal-Fatty Acid Binding Proteins in Mice Does Not Reduce Lipid Uptake into the Intestine and Further Supports Unique Functions of the Enterocyte FABPs

Abstract

The intestinal enterocyte expresses two fatty acid-binding proteins (FABP): intestinal- (IFABP; FABP2) and liver FABP (LFABP; FABP1). It is known that these proteins bind long chain fatty acids (LCFA) with high affinity, but with some different ligand preferences and mechanisms of FA transport. However, their individual functions in intestinal lipid metabolism remain unclear. Previously, we showed that ablation each of these proteins results in divergent phenotypes in response to high-fat feeding, with LFABP$^{-/-}$ mice displaying an obese phenotype, while IFABP$^{-/-}$ mice remain lean relative to WT. Here, we generated an LFABP and IFABP double knockout mouse (DKO) to study the effects of simultaneous ablation of these proteins. Male WT, IFABP$^{-/-}$, LFABP$^{-/-}$ and DKO mice were fed a low-fat (LFD) or high saturated fat (HFS) diet for 12 weeks. We found that the phenotypes of DKO mice were integrated between LFABP$^{-/-}$ and IFABP$^{-/-}$ mice, with body weight and body compositions in between those found for the single knockouts. Interestingly, DKO mice are similar to IFABP$^{-/-}$ and primarily use carbohydrates for energy when fed HFS, which is opposite of the LFABP$^{-/-}$ mice which primarily oxidize lipids for energy. Surprisingly, DKO mice appear to have lower 24-hour spontaneous activity relative to WT, despite our previous observations of the obese LFABP$^{-/-}$ mice having greater activity. Above all, there were no differences between any of the groups for fecal lipids, revealing that these proteins are not required for the bulk uptake of FA into the intestine. Overall, simultaneous ablation of LFABP and IFABP does not show a clear dominant effect of either protein, suggesting that IFABP and LFABP have different functions in intestinal lipid metabolism, resulting in downstream alterations in systemic energy metabolism.

Introduction

The enterocyte of the small intestine is the major site of absorption of dietary lipids, with efficiency >95%. Triglycerides (TG) are the primary class of dietary lipids in the mammalian diet. Hydrolysis of dietary TG by lipases in the gastro-intestinal tract results in fatty acids (FA) and monoacyglycerols (MG) formed in the intestinal lumen (16). These hydrophobic molecules enter the absorptive enterocytes of the small intestine, but soluble carrier proteins are believed to be necessary for transport of lipids throughout the hydrophilic environment of the cytosol for various metabolic processes including oxidation, storage, transport into the circulation, and also to serve as ligands for transcription factors (45). Fatty acid binding proteins (FABP) are highly abundant intracellular proteins that are present in almost every tissue in the mammal and are known to have high affinity for binding to long chain fatty acids (>14C). The proteins in the family consist of >10 distinct small (~15 kD) cytosolic proteins which make up 2-5% of all cytosolic proteins, with some tissues containing more than one FABP (110, 111, 192). In the intestinal enterocyte, two FABPs are present: Liver FABP (LFABP; FABP1) and Intestinal FABP (IFABP; FABP2). As the name suggests, LFABP was initially discovered in the liver, but it is also highly expressed in the intestine. IFABP is solely expressed in the small intestine, but has similar high expression levels to LFABP in the mouse (122, 193).

While these proteins were identified about 40 years ago, the individual functions of IFABP and LFABP have not been identified, thus it remains unclear why the same cell type expresses two similar proteins. Indeed, in vitro studies have shown differences in binding affinities and transfer mechanisms, offering clues regarding the individual functions of these proteins. IFABP is typical of the FABP family in that it has a single high affinity binding site for FA, whereas LFABP

is unique in that it can bind two FA as well as other lipids including monoacylglycerides (MG)

(137, 138)   In vitro transfer studies have shown that LFABP transfers FA to membranes via an

aqueous diffusional mechanism, while IFABP interacts directly with membranes during the

transfer (119, 142, 166). LFABP binds unsaturated FA with greater affinity than IFABP (135, 136).

Hence, the differences in ligand binding affinity and transfer mechanism have led to the

hypothesis that these intracellular proteins may have different functions in lipid transport in the

enterocyte.

There are presently two strains of LFABP$^{-/-}$ mice, which were generated by Independent

laboratories. Remarkably, there have been differences in body weights reported in response to

high-fat feeding. Several reports from each lab have demonstrated that one line gains more

weight in response to a high-fat diet while the other remains lean, hence the secondary effects

of LFABP ablation remain unclear (181, 182, 185, 187).   In spite of these differences, there are

similarities in the hepatic effects of LFABP ablation such as a reduction in FA uptake and

secretion of VLDLs, as wells as impairment of FA oxidation (152, 179, 181, 182). Also, LFABP$^{-/-}$

mice have normal levels of fecal fat, indicating that these mice have normal levels of lipid

absorption into the intestinal enterocyte (7, 181).

IFABP$^{-/-}$ mice have also been generated (190). Male mice fed a high-fat diet with cholesterol

gained more weight and had elevated TG relative to WT, but females were not different. Males

also had elevated hepatic TG (191). Like LFABP$^{-/-}$ mice, IFABP$^{-/-}$ mice do not show any evidence

of lipid malabsorption (7, 190, 191).   It has also been shown that intestinal expression of LFABP

does not increase in the absence of IFABP, and vice-versa (7, 191), which provides further

evidence that these proteins have different functions.

We have recently made direct comparisons of mice null for LFABP and IFABP and observed the effects of ablation in the intestine and found that body weight differences were not apparent in IFABP$^{-/-}$ and LFABP$^{-/-}$ mice compared to WT when fed chow diets (7). However, as hypothesized, high-fat feeding resulted in robust phenotypic changes. Interesting, LFABP$^{-/-}$ became obese and hyperphagic when given a high-fat diet, while IFABP$^{-/-}$ mice remained lean, regardless of dietary amount or type (169). Indirect calorimetry measurements revealed that LFABP$^{-/-}$ mice had lower respiratory exchange ratios relative to WT mice, suggesting that they preferentially utilize lipids for energy. In stark contrast, IFABP$^{-/-}$ mice are opposite and have higher RERs, indicative of a preference for oxidation of carbohydrates for energy (169). LFABP$^{-/-}$ mice also had elevated endogenous endocannabinoid levels in the intestine, which may play a role in their increase in food intake. On both low and high-fat diets, LFABP$^{-/-}$ mice had reduced [^{3}H] monoolein incorporation into TG, relative to PL, which suggests that LFABP is involved with trafficking MGs towards synthesis of TG, rather than PL (7, 169). We also observed a reduction in intestinal oxidation of [^{14}C] FA in low and high-fat fed LFABP$^{-/-}$ mice, similar to what has been previously shown in livers (7, 149, 152).

It is unusual that two similar proteins would perform the same functions in a single cell type. Indeed, we observed that LFABP$^{-/-}$ and IFABP$^{-/-}$ mice display disparate phenotypes in response to high-fat feeding, suggesting that these proteins have distinct roles in the intestinal enterocyte. Interestingly, however, neither LFABP$^{-/-}$ or IFABP$^{-/-}$ mice showed evidence of lipid malabsorption on a high-fat diet (169, 181, 186). Therefore to further understand the unique and overlapping functions of these proteins in the intestine, we generated mice that do not express either LFABP or IFABP. Given that the intestine is intrinsic in uptake of dietary lipids, and both of these proteins are known to bind FA, we hypothesized that mice which did not express LFABP nor

IFABP in the intestine would have difficulty with uptake and processing of dietary lipids as efficiently as WT mice. We used a high-fat feeding regimen in order to challenge the intestinal enterocytes with an abundance of fatty acids in order to gain a better understanding of the functions of these proteins in lipid uptake and metabolism in the intestine.

Experimental Procedures

Animals and Diets

LFABP^{-/-} mice, originally generated by Binas and coworkers, were used in these studies (7, 169, 180). As described previously, the mice were additionally back-crossed with C57BL/6J mice from The Jackson Laboratory (Bar Harbor, ME) for six generations to create congenic LFABP mice (7). IFABP^{-/-} mice used in the present studies are a substrain bred by intercrossing of the original IFABP^{-/-} mice generated by Agellon and coworkers (169, 190), and are also on a C57BL/6J background. Wild type C57BL/6J mice bred in our animal facility were used as controls. LFABP and IFABP-double knockouts (DKO) were generated by breeding LFABP^{-/-} and IFABP^{-/-} mice of which offspring were identified by DNA genotyping and immunoblotting to verify simultaneous ablation of the proteins in the intestine and LFABP in the liver (Figures 3-1 and 3-2). The DKO mice were phenotypically normal and did not display any overt differences in breeding or litter sizes.

Mice were maintained on a 12-hour light/dark cycle, and allowed *ad libitum* access to standard rodent chow (Purina Laboratory Rodent Diet 5015). At 2 months of age, male LFABP^{-/-}, IFABP^{-/-}, DKO, and WT (C57BL/6J) mice were housed 2-3 per cage and fed one of the following diets for 12 weeks: a low fat diet (LFD) containing 10 kcal% fat or a 45 kcal% fat diet with high saturated fat (HFS). Product numbers are D10080401 and D10080402 respectively (Research Diets, Inc., New Brunswick, NJ) and the compositions have been published previously (169).

Body weights were measured weekly. The food pellets were weighed each week to determine weekly food intakes for each cage. Grams per week was divided by the number of animals per cage and then

divided by 7 days to determine the daily food intake; independent measures were taken as the number of cages. Daily caloric intake was determined using the caloric densities of 3.9 kcal/g for the LFD or 4.7 kcal/g for HFS (Research Diets, Inc.). At the end of the experiment, the mice were fasted for 16 hours and anesthetized with ketamine/xylazine/ace promazine (80:100:150mg/kg, intraperitoneally, respectively), prior to collection of blood and tissues. Rutgers University Animal Care and Use Committee approved all animal experiments.

Genotyping

Genotyping was performed as described previously (7). Briefly, a 0.5cm tail biopsy is incubated overnight at 37°C in lysis buffer (0.3M sodium acetate, 10mM Tris-HCl pH7.9, 1mM EDTA, 1% SDS, 0.2mg/mL proteinase K). The following morning, the crude tail lysate is cooled on ice and the precipitate is pelleted by centrifugation in a pre-cooled microfuge at maximum speed. 100 uL of the clear supernatant is heated for 15 minutes at 95°C to obtain a heat-inactivated cleared tail lysate.

LFABP genotyping was performed as described by Martin et al. (180). PCR was performed with primers to amplify 123 base pairs of exon 2 of the WT allele (5'-CAAGGGGGTGTCAGAAATCGTGC and 5'-CCAGTCATGGTCTCCAGTTCGCA), or primers to amplify 227 base pairs of a sequence specific to the knockout (neomycin resistance marker: 5'-AAGAGCTTGGCGGCGAATGGand 5'-TGGCCATTTGTGGCTGTGCTC), 10X PCR buffer (SIGMA-buffer for REDTaq), dNTPs, REDTaq-polymerase (Sigma-Aldrich), and the heat-inactivated cleared tail lysate in a final volume of 25 uL. For IFABP genotyping, PCR was performed with primers to amply 804 base pairs of the WT allele (5'-TGTACACCACCATGGTTTGC-3'), or 208 base pairs of the KO sequence (5'-TGTGGAATGTGTGTGCGAGG-3') as described by Vassileva et al (190). The primers were added

to SYBR Green SuperMix (Bio-Rad) for a 20 uL reaction. 10 uL of the PCR reaction product was

loaded directly onto a 2% agarose gel and separated electrophoretically. Representative gels

are shown in Figure 3-1.

Immunoblotting to Verify Absence of IFABP and LFABP

Western blotting was performed as described previously (7) to confirm ablation of IFABP and

LFABP in intestinal mucosa and of LFABP in the liver. Mucosa and liver were harvested as

described above and homogenized in 10 or 20 volumes, respectively, of PBS pH 7.4 with 0.5%

(v/v) protease inhibitors (Sigma 8340) with a Potter-Elvejhem homogenizer. Protein

concentration was determined by the Bradford assay (7, 200). 100 µg of total cell protein or 3 ug

of purified protein was loaded onto 12% polyacrylamide gels and separated by SDS-PAGE. The

proteins were transferred onto polyvinylidenedifluoride membranes using a semi-dry transfer

system (BioRad) for 1 hour at 20V. The membranes were incubated in a 5% nonfat dry milk or

2% gelatin blocking solution overnight at 4 °C and then probed with primary antibody for 1 hour

(7). After thorough washing, blots were then incubated with anti-rabbit, IgG-horseradish

peroxidase conjugate, for 1 hour and then developed by chemiluminescence (ECL reagent, GE

Healthcare, Piscataway, NJ). Representative blots are shown in Figure 3-2.

Body Composition

Fat mass and lean body mass measurements were taken by MRI (Echo Medical Systems, LLC.,

Houston, TX) 2-3 days prior to starting the feeding protocol and 2-3 days prior to sacrifice. The

instrument was calibrated each time according to the manufacturer's instructions. Two

measurements for fat and lean body mass were taken for each mouse and averaged.

Energy Expenditure and Activity

Energy expenditure and activity were assessed using the Oxymax system (Columbus Instruments, Columbus, OH). Mice were placed in an indirect calorimetry chamber for a total of 48 h, which includes a 24-h period for adaptation prior to measurements. The ratio of VO_2 (oxygen consumption) to VCO_2 (carbon dioxide production) release was used to determine the respiratory exchange ratio (RER) as an estimation of the respiratory quotient.   Energy expenditure was assessed using the gas exchange measurements as follows: (3.815 + 1.232 × RER) × VO_2 (197, 198). The number of IR-beam breaks in a plane was recorded as spontaneous activity.   The number of *X* axis IR beam breaks during the 24-h period (X Total), successive X-axis IR beam breaks (X ambulatory), and number of vertical IR beam breaks (Z total) were counted over the 24-h period measurements.

Food Intake and Meal Pattern Analysis

Food consumption was measured using a BioDAQ food intake monitoring system (Research Diets, Inc., New Brunswick, NJ) with 16 cages for maintaining animals. Eight-week-old male mice were individually housed in standard caging with continuous access to food. Mice were fed the high-fat diet (HFS) in the cages for 12 weeks. Measurements are shown for the last 8 weeks of high-fat feeding. Food intake measurements are taken once per second. When the mouse is eating, the weight of the food hopper is unsteady. This is the start of a "bout". The bout ends when the mouse stops eating and moves away from the food hopper. A "meal" Is made up of a series of bouts within a determined time period and meal amounts. If the food hopper is not disturbed for a period, then the meal has ended and is counted. We defined the inter-meal interval as 10 min and a minimum meal amount of 0.02 g, as previously described (226). The

BioDAQ software (version 2.3.07) allows for measurements of cumulative intake, meal grams, number of meals, and the percent of time in meals.

Preparation of Tissues and Plasma

At sacrifice, blood was drawn and glucose (Accu-chek, Hoffmann-La Roche) and TG levels (Cardiochek, Polymer Technology Systems, Inc.) were measured. Plasma was extracted after centrifugation for 6 min at 4000 rpm and stored at -80°C. Livers and inguinal, perirenal, and epididymal fat pads were removed and immediately placed on dry ice, and subsequently stored at -80°C for further analysis. The intestine from stomach to cecum was removed and measured lengthwise, rinsed with 60 mL ice-cold 0.1M NaCl, opened longitudinally and mucosa scraped with a glass microscope slide into tared tubes in dry ice. Mucosal samples were subsequently diluted with 10 X volume of PBS pH 7.4 per gram wet weight, and homogenized using 20 strokes with a Potter-Elvejhem homogenizer on ice. Protein concentration was determined (200), and lipid extraction performed on samples containing 1 mg protein/mL using the Folch procedure (62, 201). Lipids were extracted twice with 10 mL chloroform/methanol (2:1) and the aqueous phase non-lipid fractions discarded. The organic lipid layer was dried under a nitrogen stream and resuspended in chloroform/methanol (2:1) for further analysis.

Plasma Analyses

At time of sacrifice, plasma was collected and stored at -80°C for further analyses as noted above. ELISA kits were used to measure plasma leptin, adiponectin, and insulin (Millipore). Plasma total cholesterol, TG, and FA levels were also analyzed (Wako Diagnostics, Inc.). Adiponectin and leptin indices (202) were calculated as the plasma adiponectin or leptin levels

divided by the total fat mass determined by MRI. Homeostatic Model Assessment (HOMA-IR)

was determined using fasting glucose (mg/dl) X fasting insulin (μU/mL)/405 (203).

Oral Glucose Tolerance Tests

During week 11 of high-fat feeding, mice were fasted for 6 h. Time 0 blood was taken from

conscious mice via the tail vein using 10 μl of whole blood using an Accu-Chek instrument

(Roche Diagnostics, Inc. Basel, Switzerland). Immediately after the blood was taken for t=0, the

mice were then gavaged with 2 g/kg BW of glucose. Blood was taken at t = 30, 60, 90, and 120

min.

Oral Fat Tolerance Tests

After 3 months of high-fat feeding, mice were fasted for 24 h. Time 0 blood was taken from

conscious mice via the tail vein and then an intraperitoneal injection of Tyloxapol (500 mg/kg

BW) was administered to prevent lipoprotein TG uptake via inhibition of lipoprotein lipase.

After 30 min, an orogastric gavage of 300 μL of olive oil was given. Blood was taken at t = 60,

120, 180, and 240 min. Blood TG levels were measured using 15 μl of whole blood using a

Cardiochek instrument (Polymer Technology Systems, Inc. Zionsville, IN).

Fecal Lipid Content

Fecal lipids were measured to determine if there were any alterations in total lipid absorption in

the gene-ablated mice. Feces were collected from the cages between 4 and 10 weeks during the

12 week period and then dried overnight at 60°C and weighed. 0.5 g (dry weight) was dissolved

in water overnight and lipid extracted using the Folch method (201). The extracted lipids in 2:1

chloroform:methanol were placed in pre-weighed glass tubes and dried down completely under

a nitrogen stream. They were weighed again to determine recovered lipid. The weight of the extract was divided by original weight of the feces to determine percent of lipid in the feces.

Quantitative RT-PCR for mRNA Expression Analysis

The protocol for mRNA acquisition and analysis was adapted from Chon *et al.* (204). Briefly, tissues were homogenized in 4M guanidiniumthiocyanate,25mM sodium citrate, 0.1M β-mercaptoethanol using several strokes of a Polytron. Total RNA was further purified by phenol extraction and the RNeasy cleanup kit (Qiagen,Valencia, CA) along with DNase treatment to minimize genomic DNA contamination. Reverse transcription was performed using 1 µg of RNA, random primers, an RNase inhibitor, and reverse transcriptase (Promega Madison, WI) in a total volume of 25 µl. Primer sequences were obtained from Primer Bank (Harvard Medical School QPCR primer data base). The efficiency of PCR amplifications was analyzed for all primers to confirm similar amplification efficiency. Real time PCR reactions are performed in triplicate using an Applied Biosystems 7300instrument. Each reaction contained 80 ng cDNA, 250 nM of each primer, and 12.5 µl of SYBR Green Master Mix (AppliedBiosystems, Foster City, CA) in a total volume of 25 µl. Relative quantification of mRNA expression is calculated using the comparative Ct method normalized to β-actin.

Statistical Analysis

Data are presented as mean ± S.E.M. Statistical comparisons for body weights were made by two-way repeated measures ANOVA (genotype X time). For OFTT tests, comparisons were made by Student's t-test (IFABP^{-/-} or LFABP^{-/-} versus WT) for each time point. The effect of genotype within each diet was made by one-way ANOVA followed by Tukey's post-hoc test using JMP statistical software (version 10, SAS Institute).

Figure 3-1

A

227 bp (LFABP KO)

123 bp (WT)

-/- -/- +/+ +/+ +/- +/-

B

804 bp (WT)

208 bp (IFABP KO)

+/+   -/-   +/-
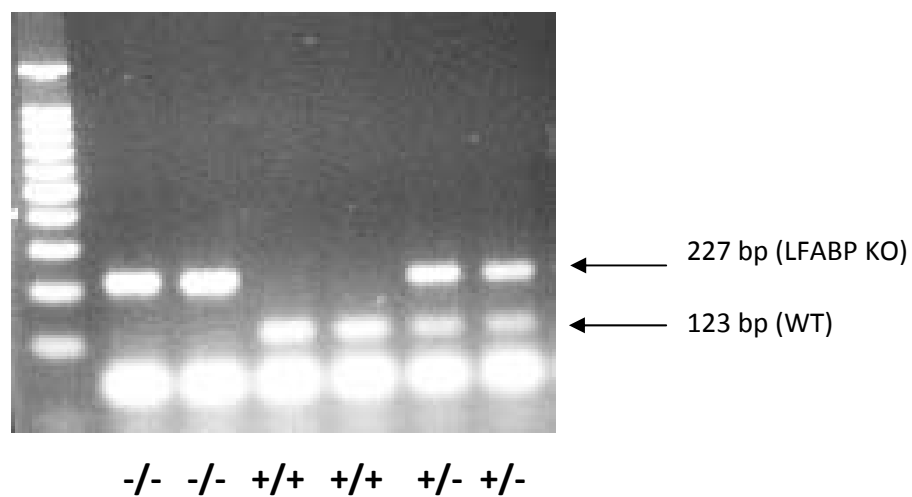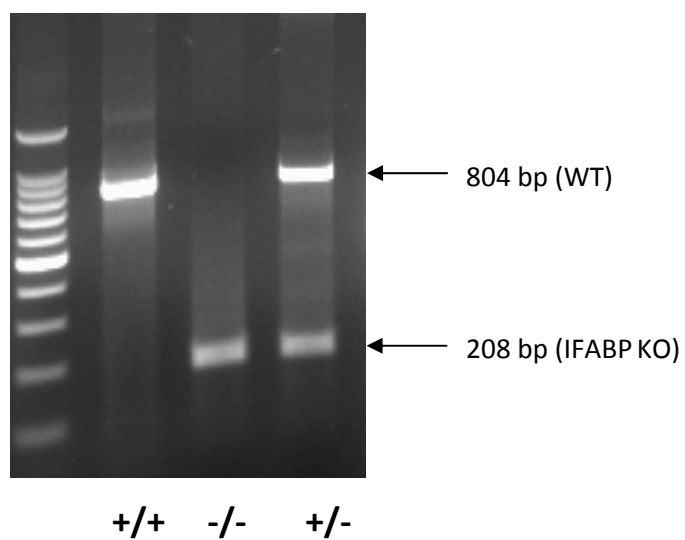
Figure 3-1. Verification of genotype by PCR. Representative images of the PCR products of heterozygous (+/-), homozygous (-/-), and wild-type (+/+) mice for verification of A. LFABP or B. IFABP.

Figure 3-2

LFABP (A) or IFABP (B) expression in intestine

LFABP (C) or IFABP (D) expression in liver
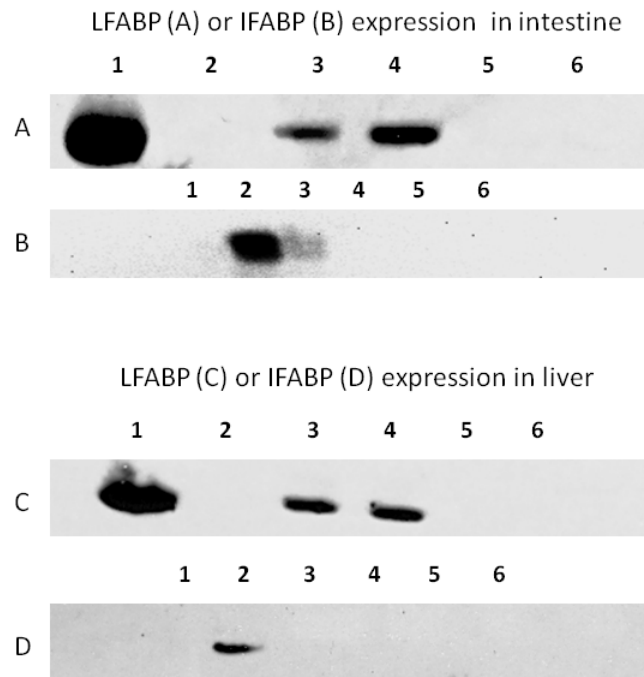
Figure 3-2. Verification of genotype by Immunoblotting. Representative images of Western blotting. A. Probing for LFABP in intestine: Lane 1, purified LFABP; Lane 2, purified IFABP; Lane 3, WT; Lane 4, IFABP$^{-/-}$; Lane 5, LFABP$^{-/-}$; Lane 6, DKO. B. Probing for IFABP in intestine: Lane 1, purified LFABP; Lane 2, purified IFABP; Lane 3, WT; Lane 4, IFABP$^{-/-}$; Lane 5 and Lane 6, DKO. C. Probing for LFABP in liver: Lane 1, purified LFABP; Lane 2, purified IFABP; Lane 3, WT; Lane 4, IFABP$^{-/-}$; Lane 5, LFABP$^{-/-}$; Lane 6, DKO. D. Probing for IFABP in liver: Lane 1, purified LFABP; Lane 2, purified IFABP; Lane 3, WT; Lane 4, IFABP$^{-/-}$; Lane 5, LFABP$^{-/-}$; Lane 6, DKO.

Results

Simultaneous Ablation of LFABP and IFABP Affects Body Weight and Body Composition

Body weights (BW) were measured for WT, IFABP^{-/-}, LFABP^{-/-}, and DKO mice fed a low-fat diet

(LFD) or high-saturated fat diet (HFS) for 12 weeks (Figure 3-3). IFABP^{-/-} mice fed the LFD had

similar BW relative to WT over the 12-week study (Figure 3-3A), however IFABP^{-/-} mice fed the

high-fat diet (HFS) had lower BW relative to WT (p<0.05) (Figure 3-3B). Along these lines, IFABP^{-/-}

mice gained a similar amount of weight to WT when fed the LFD, but net weight gain tended to

be lower after HFS diet feeding (p <0.09) (Figure 3-3C). Baseline fat mass (FM) was similar to WT,

but fat-free mass (FFM) was slightly lower (p<0.05) (Figure 3-3D, E). IFABP^{-/-} mice have similar

FM and FFM relative to WT when fed LFD, but have reduced FM and a higher FFM relative to WT

when fed HFS (p <0.05) (Figure 3-3D, E). The calorie efficiency of IFABP^{-/-} mice was not different

relative to WT (Figure 3-3F). As shown previously (169), there was no difference in fecal fat,

which is indicative of normal lipid absorption (Figure 3-3G).

 In contrast to results from IFABP^{-/-} mice, LFABP^{-/-} mice had increased BW relative to WT on LFD

and HFS after 12 weeks of feeding (p<0.05) (Figure 3-3A, B). Net weight gain of LFABP^{-/-} mice

was also increased (p<0.05) relative to WT when fed when fed LFD and HFS (Figure 3-3C), in

keeping with our previous results (169). The baseline body compositions of LFABP^{-/-} mice were

not different, however, LFABP^{-/-} mice had greater adiposity (p<0.05) compared to WT when fed

LFD and HFS (Figure 3-3 D, E). LFABP^{-/-} mice had greater food efficiency than WT (p<0.05) when

fed LFD and HFS (3-F). No differences were noted for fecal fat% of LFABP^{-/-} mice (Figure 3-5G), in

agreement with previous studies (7, 169, 186).

The DKO mice tended to have slightly higher body weights at baseline for LFD (p=0.013), and HFS (p=0.08) feeding (Figure 3-3), however 3 months of feeding resulted in similar BW to WT (Figure 3-3A, B). Baseline FM of DKO mice was higher than WT (p<0.05), however body compositions of DKO mice were similar to WT for the endpoint measurements (Figure 3-3D, E). DKO mice had similar calorie efficiency to WT mice (Figure 3-3F). It was also interesting that DKO mice showed no signs of malabsorption of dietary lipid in the absence of both LFABP and IFABP, suggesting that these proteins are not required for bulk uptake of dietary lipid into the intestine (Figure 3-5F).

LFABP$^{-/-}$ and IFABP$^{-/-}$ Mice Have Alterations in Food Intake

We measured meal patterns of mice fed HFS diet for 8 weeks beginning at 4 weeks during the 12 week feeding trial (Figure 3-4). IFABP$^{-/-}$ mice tended to eat less food throughout the study, but these trends did not reach statistical significance with n=4/group (Figure 3-4A, B). We had previously observed that IFABP$^{-/-}$ mice ate less food than WT mice (169). Here we show that they eat less food per day than WT mice, particularly at night, when the mice are active (p<0.05) (Figure 3-4B). Interestingly, they tend to eat more during the day versus WT (0.5 ± 0.1 g/d for WT vs 0.9 ± 0.1 g/d for IFABP$^{-/-}$ mice) (p = 0.07), suggesting a possible trend for altered circadian activity. Moreover, IFABP$^{-/-}$ mice eat fewer total meals each day (p<0.05) compared to WT mice (Figure 3-4D).

In contrast, LFABP$^{-/-}$ mice tended to have greater cumulative food intake of the high-fat diet relative to WT mice (Figure 3-4A, B). Interestingly, we found that these mice eat more food and consume more meals during the light period (p<0.05) (Figure 3-4C, D), resulting in an increase in time spent eating compared to WT mice (Figure 3-4E). These data suggest that they too, have

altered circadian rhythms. As for many other analyses, we found that food intake of DKO mice

was in between the IFABP$^{-/-}$ and LFABP$^{-/-}$ mice and, as such, were not different from WT.

Figure 3-3
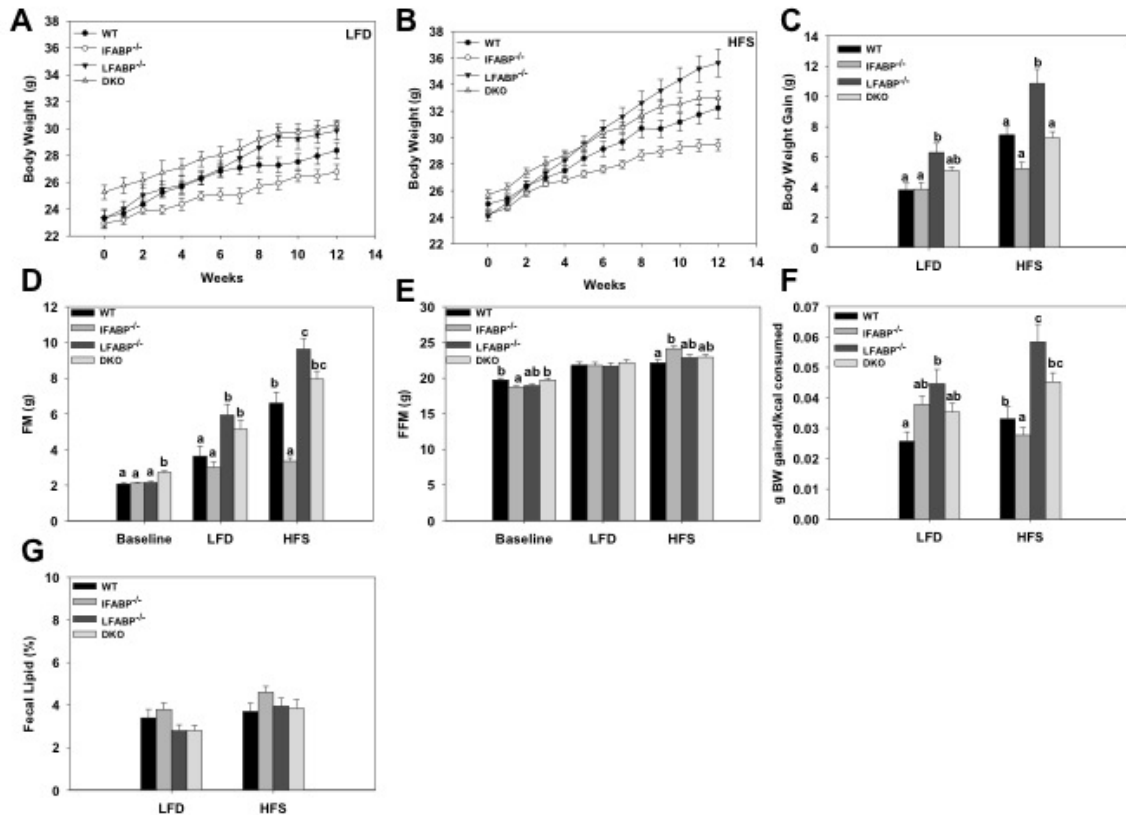
Figure 3-3. Body weight and composition for WT, IFABP^{-/-} and LFABP^{-/-}, and DKO mice after 12 weeks on a low-fat (LFD) or high saturated fat (HFS). A. Body weights on LFD (n=16-18). No differences were noted for the knockout mice on LFD relative to WT; B. Body weights on HFS (n=16-18). Body weights of LFABP^{-/-} were greater (p<0.05) than WT. IFABP^{-/-} mice had lower body weight relative to WT; C. Body weight gain (n=16-18); D. Fat mass (n=16-18); D. Fat-free mass (n=16-18); F. Food efficiency (g BW gained/kcal food intake) for mice fed LFD (n=5-7), HFS (n = 5-6). G. Fecal fat% for mice fed LFD (n=5-7), HFS (n = 5-6). For Figures A–B, data are mean ± SEM, analyzed using two way ANOVA using repeated measures with post-hoc Tukey's test (genotype x time). For Figures C-G, data are mean ± SEM, analyzed using one way ANOVA with a Tukey's post-hoc test. Results with different letters within diet treatment are significantly different (p<0.05).

Figure 3-4
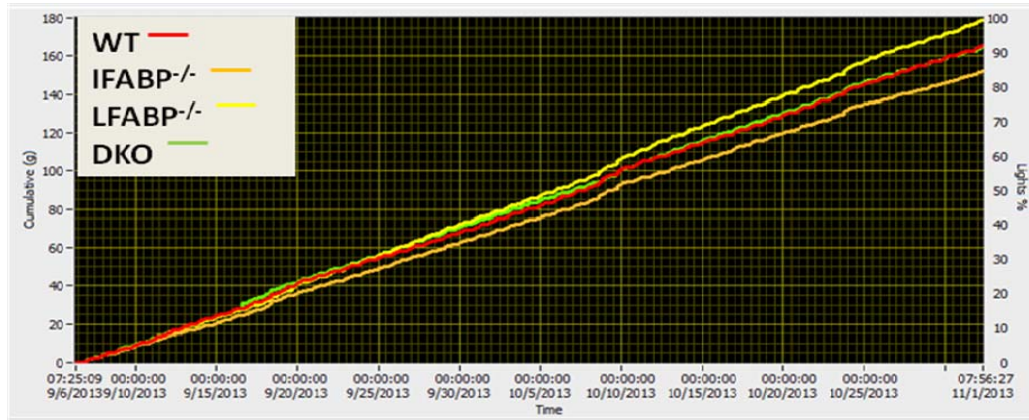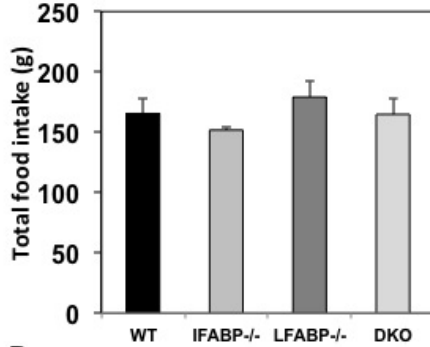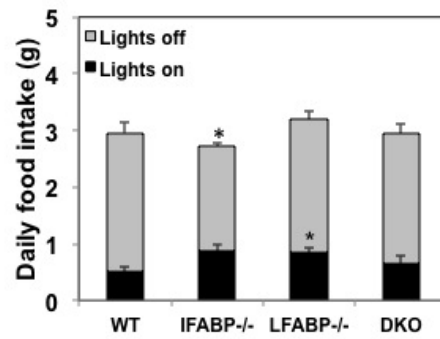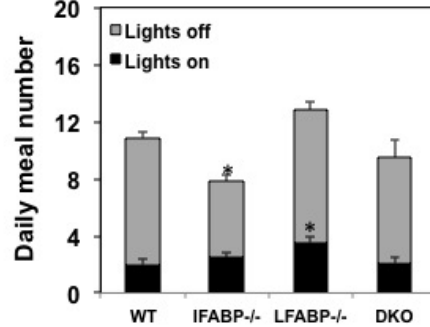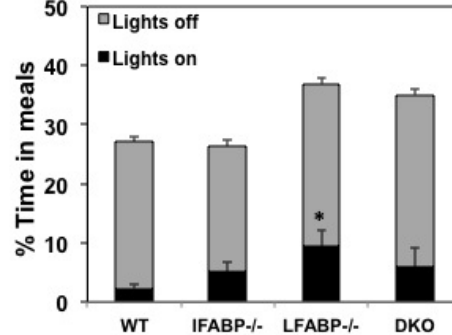
Figure 3-4. Meal pattern analysis for WT, IFABP^{-/-} and LFABP^{-/-}, and DKO mice fed high saturated fat (HFS) diet. A. Cumulative intake for 8 weeks (BioDAQ data viewer). B. Cumulative food intake. C. Daily food intake. D. Daily meal number. E. Percent time in meals. n= 4/group. Data are given as mean ± SEM, analyzed using Student's t-test *p<0.05 vs WT.

Ablation of IFABP and/or LFABP Results in Differences in Markers of Whole Body Energy

Metabolism

As previously found (169), fasting blood glucose levels of IFABP$^{-/-}$ mice were lower relative to WT

mice when fed HFS (p<0.05), but there were no changes in insulin, cholesterol, or NEFA (Table 3-

1).   Leptin and adiponectin levels were also lower in these mice when fed HFS (p < 0.05). Since

we found much lower FM in IFABP$^{-/-}$ mice, leptin and adiponectin indices were used to normalize

for adiposity. We found that leptin levels per g FM of IFABP$^{-/-}$ mice were lower than WT, but

adiponectin was not different. Total livers weights of IFABP$^{-/-}$ mice were similar to WT and were

also not different when normalized for BW. Not surprisingly, given their lower adiposity (Figure

3-5A), IFABP$^{-/-}$ fed the HFS diet had smaller epididymal, perirenal, and inguinal fat pads relative

to WT (p < 0.05)

LFABP$^{-/-}$ mice did not display differences in fasting blood glucose, insulin, cholesterol or

adiponectin levels on HFS relative to WT mice (Table 3-1), in keeping with previous findings

(169). Plasma NEFAs were higher in LFABP$^{-/-}$ mice when fed HFS only (p<0.05). LFABP$^{-/-}$ mice on

HFS had markedly higher leptin levels, which correspond to their increased adiposity compared

to WT (p < 0.05) (Figure 3-5). Leptin levels expressed per g FM were higher than WT, while

adiponectin levels were lower when normalized for FM. As suggested by MRI measurements of

fat mass (Figure 3-4A), LFABP$^{-/-}$ mice had larger epididymal, perirenal, and inguinal fat pads

when fed HFS (p<0.05). Liver weights of LFABP$^{-/-}$ mice were lower than WT mice when

expressed per g BW (p<0.05).

DKO mice had blood glucose, insulin, cholesterol, TG, leptin, and adiponectin concentrations

that were similar to WT mice fed LFD and HFS (Table 3-1). Plasma NEFAs were higher in DKO

mice when fed HFS (p<0.05). Like LFABP$^{-/-}$ mice, liver weights of DKO mice were lower than WT

mice when expressed per g BW (p<0.05). Epididymal and perirenal fat pads were similar in mass

to WT, but inguinal fat pads were larger (p<0.05). Overall, metabolic markers for DKO mice

were integrated between LFABP$^{-/-}$ and IFABP$^{-/-}$ mice, in that the phenotype was not more

strongly influenced by ablation of one protein over the other.

Table 3-1

	LFD				HFS			
	WT	IFABP$^{-/-}$	LFABP$^{-/-}$	DKO	WT	IFABP$^{-/-}$	LFABP$^{-/-}$	DKO
Glucose, mg/dL	131 ± 9	90 ± 6	137 ± 17	122 ± 14	184 ± 15[b]	104 ± 4[a]	218 ± 16[b]	178 ± 16[b]
Insulin, ng/mL	0.33 ± 0.10	0.35 ± 0.02	0.26 ± 0.02	0.36 ± 0.02	0.24 ± 0.02	0.17 ± 0.01	0.17 ± 0.01	0.24 ± 0.02
HOMA, IR	3.1 ± 0.6	2.0 ± 0.2	2.3 ± 0.4	2.7 ± 0.3	2.5 ± 0.1[b]	1.1 ± 0.1[a]	2.4 ± 0.3[b]	2.7 ± 0.4[b]
Total Cholesterol, mg/dL	77 ± 6	67 ± 3	65 ± 8	62 ± 5	102 ± 11	100 ± 5	112 ± 6	106 ± 3
TG, mg/dL	35 ± 5	22 ± 5	43 ± 4	33 ± 5	27 ± 4	55 ± 14	38 ± 14	47 ± 5
NEFA, mEq/L	0.23 ± 0.03[a]	0.26 ± 0.01[ab]	0.36 ± 0.03[b]	0.28 ± 0.03[ab]	0.25 ± 0.03[a]	0.35 ± 0.02[ab]	0.44 ± 0.05[b]	0.40 ± 0.03[b]
Leptin, ng/mL	1.5 ± 0.8	0.3 ± 0.1	2.6 ± 0.8	2.2 ± 0.6	3.7 ± 0.8[ab]	0.8 ± 0.3[a]	8.6 ± 1.5[c]	6.8 ± 1.3[bc]
Leptin Index	0.3 ± 0.1	0.1 ± 0.0	0.4 ± 0.1	0.5 ± 0.2	0.6 ± 0.1[b]	0.2 ± 0.1[a]	0.9 ± 0.1[b]	0.9 ± 0.1[b]
Adiponectin, ng/mL	10.0 ± 0.7	7.6 ± 0.6	10.9 ± 1.1	9.6 ± 1.2	8.8 ± 0.0[b]	4.6 ± 0.2[a]	7.1 ± 0.6[b]	6.9 ± 0.5[ab]
Adiponectin Index	3.3 ± 0.5	2.8 ± 0.3	2.0 ± 0.4	2.3 ± 0.5	1.8 ± 0.3[b]	1.6 ± 0.2[ab]	0.8 ± 0.1[a]	0.9 ± 0.1[a]
Intestine Length, cm	34 ± 1[ab]	32 ± 0[a]	34 ± 0[ab]	35 ± 1[b]	36 ± 1[ab]	35 ± 0[a]	37 ± 0[bc]	39 ± 0[c]
Liver Wt, g	0.85 ± 0.03	0.84 ± 0.02	0.93 ± 0.03	0.84 ± 0.02	0.93 ± 0.04	0.92 ± 0.03	0.96 ± 0.04	0.90 ± 0.03
Liver, g/g BW	0.034 ± 0.004[b]	0.034 ± 0.001[b]	0.034 ± 0.001[ab]	0.031 ± 0.001[a]	0.035 ± 0.001[b]	0.035 ± 0.001[b]	0.030 ± 0.001[a]	0.030 ± 0.000[a]
Epididymal Fat, g	0.37 ± 0.05[a]	0.26 ± 0.05[a]	0.68 ± 0.07[b]	0.61 ± 0.05[b]	0.78 ± 0.11[b]	0.29 ± 0.03[a]	0.98 ± 0.11[b]	0.85 ± 0.06[b]
Perirenal Fat, g	0.09 ± 0.02[a]	0.08 ±0.02[a]	0.19 ±0.02[b]	0.18 ± 0.02[b]	0.23 ± 0.04[b]	0.08 ± 0.01[a]	0.39 ± 0.04[c]	0.28 ± 0.03[bc]
Inguinal Fat, g	0.35 ± 0.08[ab]	0.22 ± 0.03[a]	0.56 ± 0.05[c]	0.42 ± 0.04[bc]	0.43 ± 0.06[b]	0.20 ± 0.03[a]	0.73 ± 0.07[c]	071 ±0.06[c]

Table 3-1. Plasma and tissue analyses for WT, IFABP$^{-/-}$, LFABP$^{-/-}$, or DKO mice after 12 weeks on a low-fat (LFD) or high saturated fat (HFS).

Data are mean ± SEM, analyzed using one-way ANOVA with Tukey's post-hoc test. Results with different letters within a dietary treatment are significantly different (p<0.05). n=6-9 for all groups.

Oral Glucose Tolerance Tests

We performed oral glucose tolerance tests (OGTT) on 6 hour fasted mice fed either LFD or HFS formulas (Figure 3-5). There were no differences in blood glucose concentrations for LFD-fed mice at any time point (Figure 3-5A).   However, we did observe that IFABP$^{-/-}$ mice have lower blood glucose levels at the 60, 90, and 120 minute timepoints ($p<0.05$) and have a smaller AUC ($p<0.05$), suggesting that these mice have improved glucose tolerance relative to the other groups when fed HFS (Figure 3-5B). Interestingly, despite their increased adiposity, high-fat fed LFABP$^{-/-}$ mice were not different from WT mice (Figure 3-5B). Glucose levels of DKO mice throughout the 2-hour time period were similar to LFABP$^{-/-}$ and WT mice (Figure 3-5A, B).

Figure 3-5

A

B
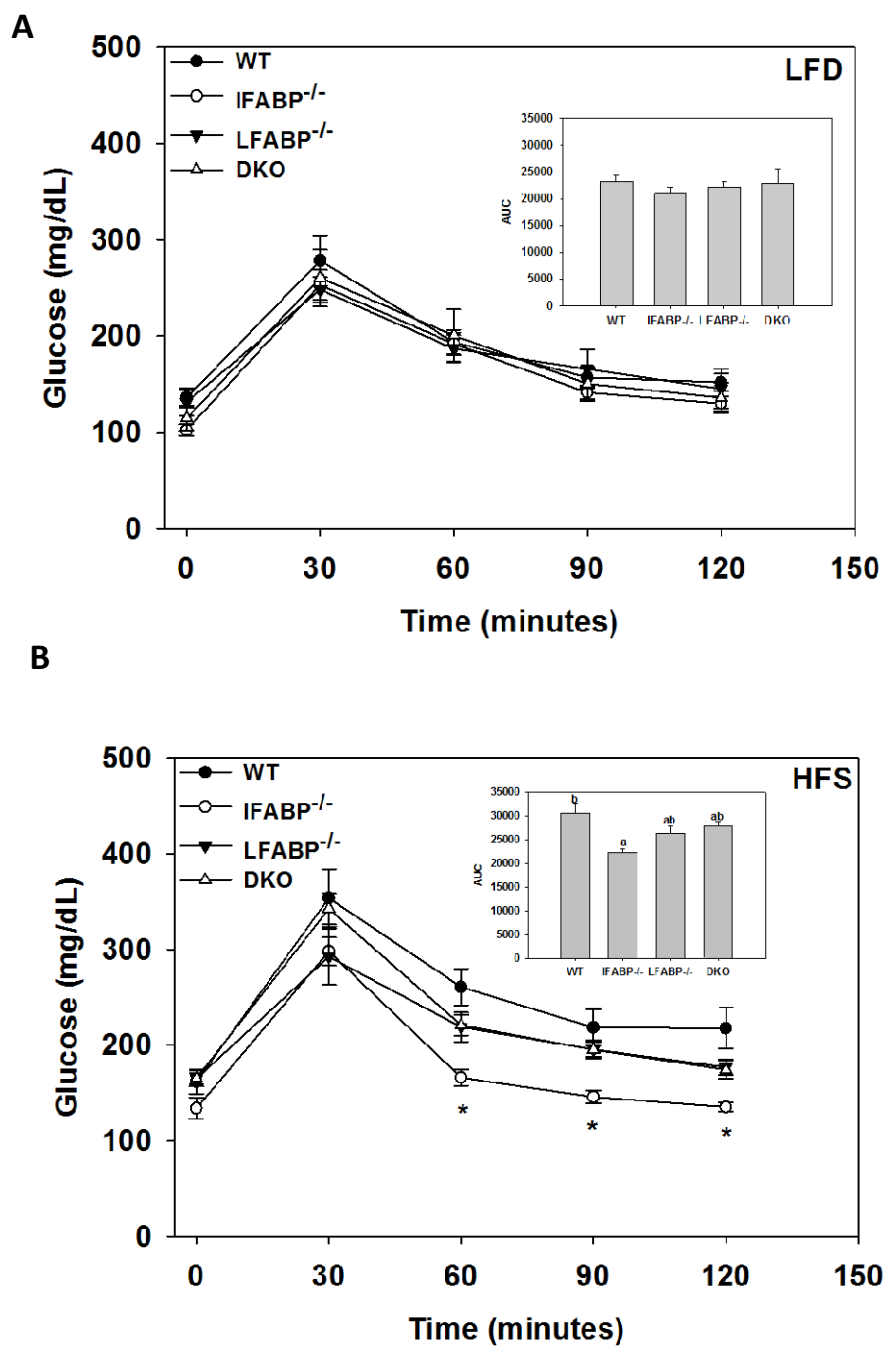
Figure 3-5. Oral glucose tolerance test for WT, IFABP^{-/-}, LFABP^{-/-}, and DKO mice of mice fed a low-fat (LFD) or high saturated fat (HFS) diet. A. LFD. B. HFS. Data are mean ± SEM, n= 6-9 for all groups *p<0.05 vs WT.

Ablation of IFABP and/or LFABP Results in Altered Metabolic Fuel Source Utilization and 24-h

Energy Expenditure

We had previously observed differences in metabolic fuel source utilization between IFABP^{-/-} and LFABP^{-/-} mice (169); hence we performed similar experiments in which we compared these diets to DKO mice fed LFD and HFS. We observed that IFABP^{-/-} mice fed LFD were not different for VO_2 consumption and VCO_2 expiration (Figure 3-6A, B).   However, IFABP^{-/-} mice had higher VO_2 and VCO_2 than WT when fed HFS (Figure 3-6A,B), similar to our previously reported results (169). Additionally, and similar to our previous results (169), the ratios of VCO_2/VO_2 for (respiratory exchange ratios; RER) for IFABP^{-/-} mice were higher than WT, suggesting that IFABP^{-/-} have a preference for oxidation of carbohydrates as a fuel source (p <0.05) (Fig. 3-6C). No differences were noted for energy expenditure of IFABP^{-/-} mice (Figure 3-6D).

LFABP^{-/-} mice, on the other hand, displayed lower VO_2, VCO_2, and RER on LFD and HFS compared to WT (p <0.05) (Fig. 3-6A, B, C). The latter measurements are similar to our previous results which indicate that these mice preferentially oxidize lipids for energy (169). Furthermore, there were no differences in energy expenditure for these mice relative to WT (Figure 3-6D).

The DKO mice seemed to follow LFABP^{-/-} mice with lower VO2 relative to WT when LFD and HFS (Figure 3-6A). They also had a lower VCO_2 when fed LFD relative to WT mice (Figure 3-6B). However, DKO mice fed HFS had high RERs, thus they followed the phenotype of IFABP^{-/-} mice for metabolic fuel preference (Figure 3-6C).   No differences were noted for energy expenditure for the DKO mice relative to WT and the single knockouts (Figure 3-6D).

Figure 3-6
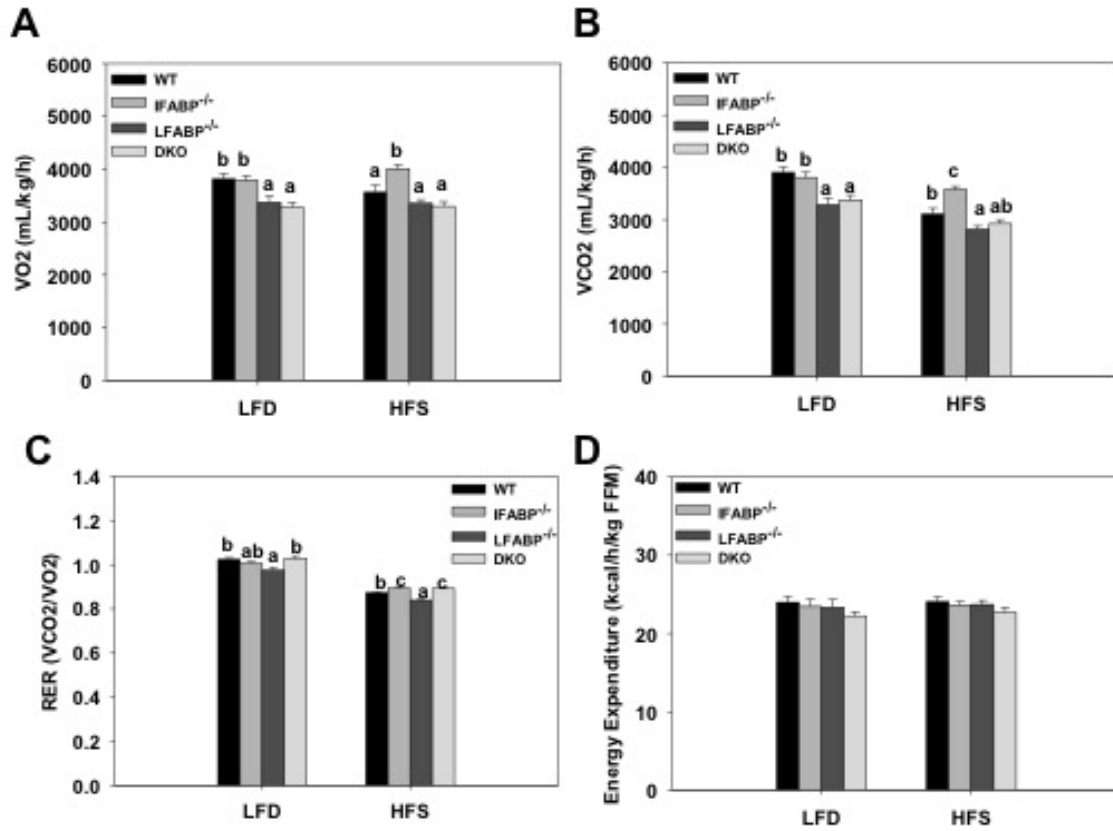
Figure 3-6. Indirect calorimetry for WT, IFABP^{-/-}, LFABP^{-/-}, or DKO mice fed a low-fat (LFD) or high-saturated fat (HFS) diet. A. VCO2 B. VO2 C. Respiratory Exchange Ratio. D. Energy expenditure. Data presented as mean ± SEM, analyzed using one-way ANOVA with Tukey's post-hoc test. n=16-18/group. Results with different letters within a dietary treatment are significantly different (p<0.05).

LFABP Ablation Results in Changes in Spontaneous Activity

We also measured activity of mice in the indirect calorimetry chambers and made comparisons for when the lights are off (when the mice are most active), and also when the lights are on (mice are least active) (Figure 3-7). We did not observe any changes in activity for IFABP$^{-/-}$ mice relative to WT.

In contrast, LFABP$^{-/-}$ mice had increased 24 hour X activity compared to WT mice after LFD and HFS feeding (p < 0.05) (Figure 3-7 A, B). They also had increased X activity relative to WT when the lights were off (and when the mice are most active).   LFABP$^{-/-}$ mice had higher total 24 hour X ambulatory activity than WT when fed HFS. Interestingly, when we looked at changes activity of the mice during the day and night periods, we found that LFABP$^{-/-}$ mice had higher ambulatory activity compared to WT both when the lights were on and when the lights were off (Figure 3-7 C, D). Moreover, Z activity was increased for LFABP$^{-/-}$ mice relative to WT when the lights were on (Figure 3-7 E, F).

In contrast to LFABP$^{-/-}$ and IFABP$^{-/-}$ mice, the DKO mice had lower spontaneous activity counts for all measurements (Figure 3-7A-F). DKO mice tended to have reduced activity relative to WT for all measurements, which reached statistical significance (p<0.05) for 24 hour X activity and X ambulatory activity during HFS feeding.

Figure 3-7
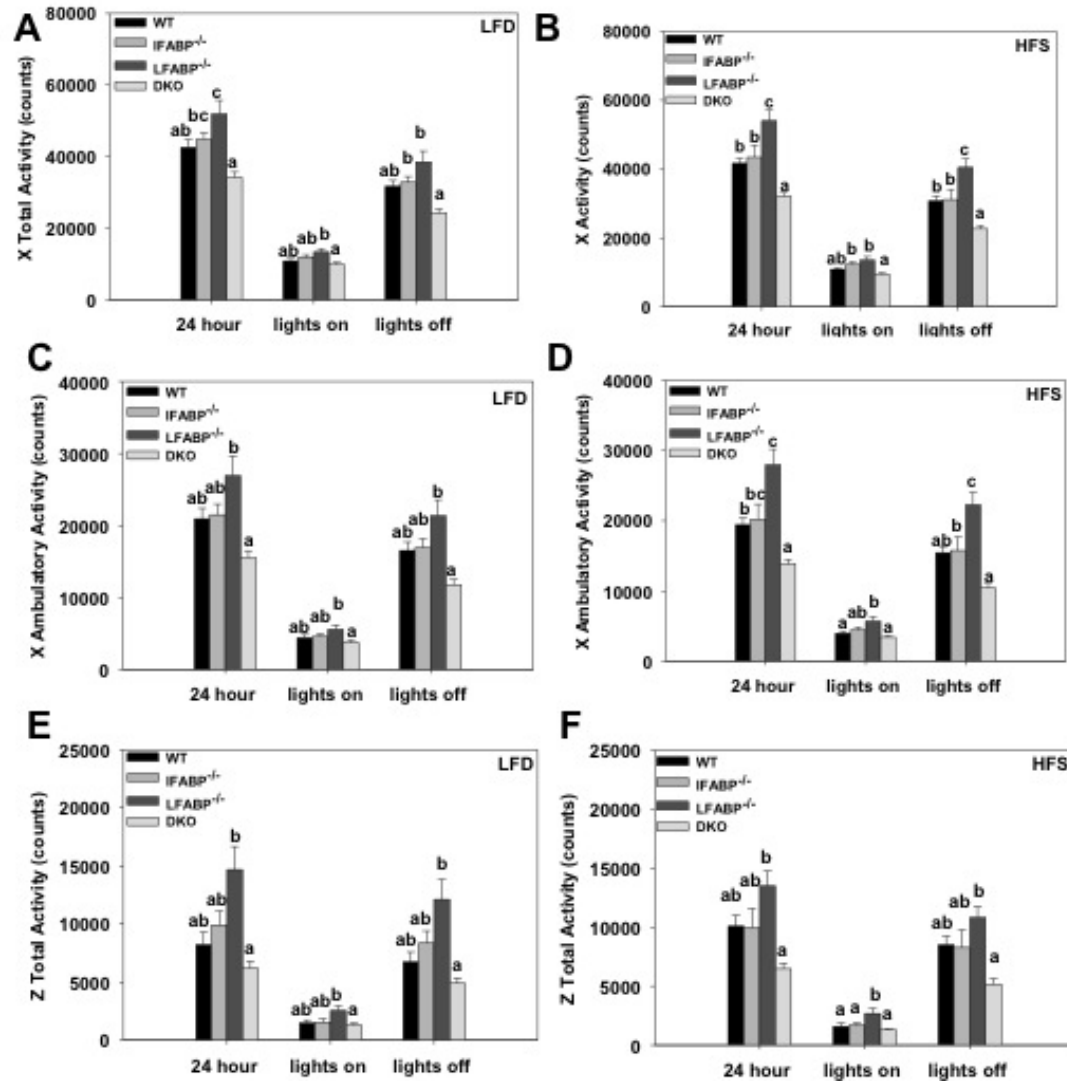
Figure 3-7. 24-hour activity of WT, IFABP$^{-/-}$, LFABP$^{-/-}$, or DKO fed (LFD) or a high saturated fat (HFS) diet. A. X Activity on LFD B. X Activity on HFS, C. X ambulatory activity on LFD. D. X ambulatory activity on HFS. E. Z total activity on LFD. F. Z total activity on HFS. Data are mean ± SEM, analyzed using one-way ANOVA with Tukey's post-hoc test. n=16-18/group. Results with different letters within a dietary treatment for the same time period are significantly different (p<0.05).

DKO Mice Do Not Exhibit Alterations in Chylomicron Secretion Rates

Oral fat tolerance tests were performed on 24 hour fasted mice; tyloxypol was administered to prevent clearance of circulating TG-rich lipoproteins (Figure 3-8). During LFD-feeding IFABP$^{-/-}$ mice had higher TG levels than WT at t = 2, 3, and 4 hours (Figure 3-8A). As shown previously (169), IFABP$^{-/-}$ mice also had higher blood TG levels when fed HFS at t= 3 h, and was significant vs WT at t=4 h (Figure 3-8B). Interestingly, despite the hypothesis that LFABP is involved with prechylomicron assembly (54), we did not observe differences in intestinal secretion rates for LFABP$^{-/-}$ or DKO mice.

Figure 3-8
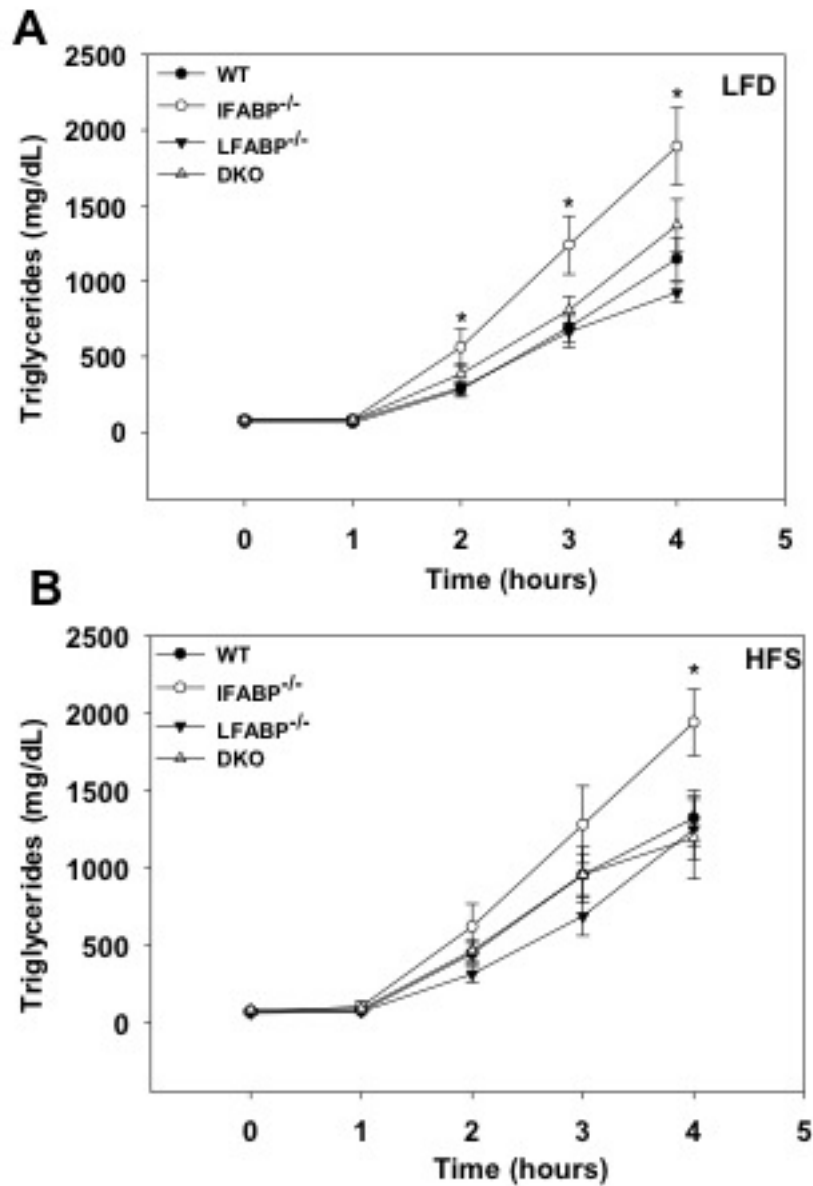
Figure 3-8. Oral fat tolerance tests following a 24 hour fast for WT, IFABP^{-/-}, LFABP^{-/-} mice, and DKO mice after 12 weeks on a low-fat (LFD) or high saturated fat (HFS) diet. Blood TG levels for A. LFD-fed mice (n=6-9); B. HFS-fed mice (n=8-12); Data are given as mean ± SEM, analyzed using Student's t-test *p<0.05 for IFABP^{-/-} vs WT at the same timepoint.

Effects of IFABP and LFABP Ablation on Expression of Intestinal Membrane and Intracellular Lipid

Binding Proteins

We measured expression of genes involved in lipid trafficking in the intestine (Figure 3-9). As

found previously, we did not find compensation for IFABP or LFABP in the absence of each

protein in the single knockout mice (7). There were no changes in expression of the Ileal lipid

binding protein (ILBP; FABP6), an FABP that is expressed in the distal regions of the intestine and

is known for having higher affinity for bile acids than FA (125, 128, 134). We also did not

observe changes in expression of CD36, a membrane FA transporter. However, we did find

increases in expression of Scavenger Receptor Type B1 (SRB1) in LFABP$^{-/-}$ and DKO mice fed LFD

(Figure 3-11A). It was also upregulated in LFABP$^{-/-}$ mice fed HFS (Figure 3-9B). This membrane

protein is known for transport of LDL into the cell.   Other FABPs that are not expressed in WT

intestines were measured, including FABP3 (heart FABP), FABP4 (adipose FABP), FABP5

(kerinocyte FABP). We found very high Ct levels that are only consistent with nonspecific

binding in all of the knockout mice, including the DKO, with similar levels observed in WT

samples (data not shown).   Thus, there does not appear to be compensatory upregulation of

expression of other FABPs, even in the DKO intestine.

Figure 3-9
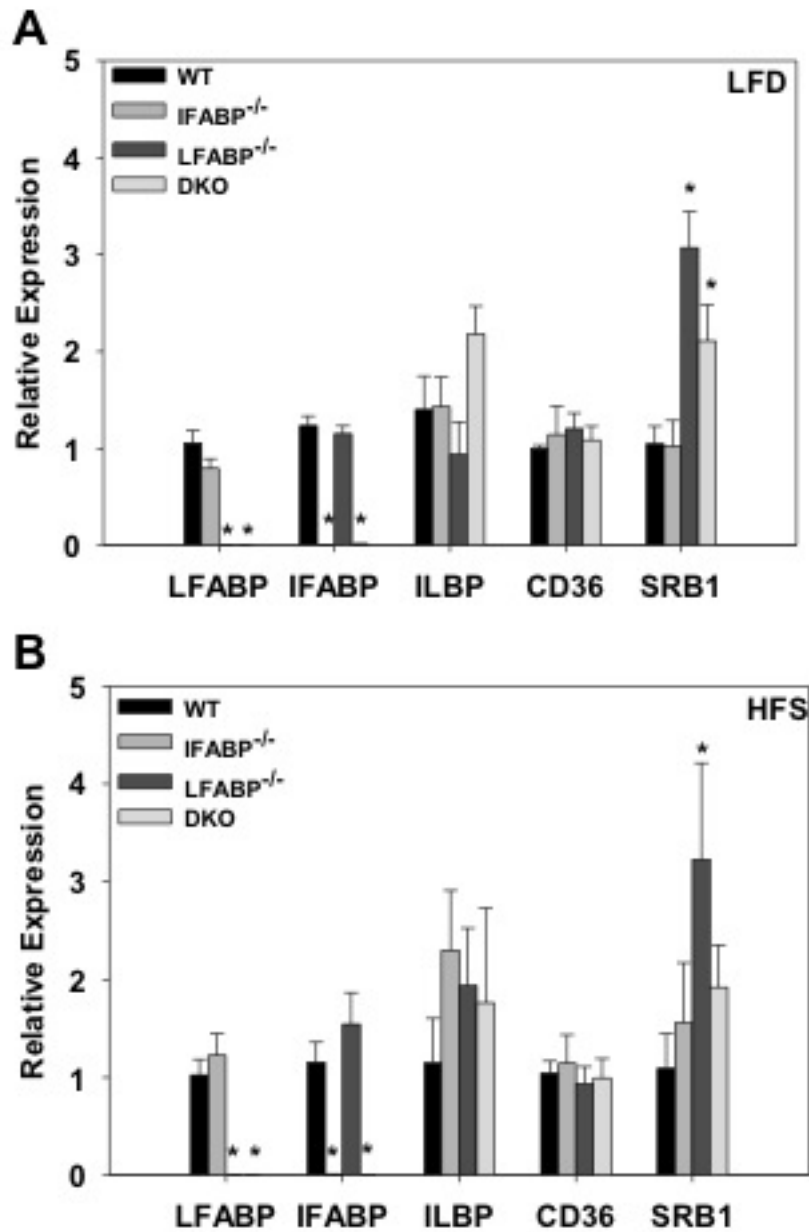
Figure 3-9. Relative quantification of mRNA expression of intestinal lipid transport genes for WT, IFABP^{-/-} and LFABP^{-/-} mice after 12 weeks on a low-fat (LFD) or high saturated fat (HFS) diet. A. LFD (n=8) B. HFS (n=8). Data are given as mean ± SEM, and are analyzed using Student's t-test. *p<0.05 vs same WT fed the same diet.

Discussion

The intestinal enterocyte serves the important functions of absorption, processing, and transport of dietary lipids from the lumen and into the body. Both IFABP and LFABP are highly expressed in this cell type and have high affinity for binding FA, but it still remains unclear why two similar proteins are coexpressed in the same cell type. Indeed, earlier reports have demonstrated differences in functionality between the proteins. In vitro studies have shown that IFABP has one single high affinity binding site for FA, whereas LFABP is unique in that it can bind two FA as well as other lipids including MG (137, 138).   IFABP has high affinity for binding FA, but LFABP seems to bind unsaturated FA with a greater affinity than IFABP (136). In vitro transfer studies have shown that LFABP trafficks FA to membranes by a diffusional mechanism, while IFABP transfers FA by a collisional mechanism (119, 142, 166).   Hence, these differences suggest that these proteins have distinct functions in the intestinal enterocyte.

In vivo studies have also revealed that ablation of these proteins results in different changes in the whole body phenotypes of mice (169, 182, 191, 196). Studies comparing both LFABP and IFABP-null mice have been conducted to further investigate the individual functions of these proteins.   There has been no evidence of compensatory upregulation of IFABP in intestinal mucosa in response to ablation of LFABP, and vice versa (7, 179) , and there have not been any FABPs which have been shown to be upregulated in the liver and intestine in response to ablation of IFABP or LFABP. We measured intestinal mRNA for ILBP, an FABP that has greater affinity for bile acids than FA (135), but nonetheless, could be potentially compensating for ablation of IFABP and LFABP. However, we did not find changes in expression.   Further, in light of findings that KFABP (keritinocyte FABP; FABP5), a protein that is not normally highly

expressed in adipose tissue, is upregulated when AFABP (adipose FABP; FABP4) is ablated (227, 228), we also measured intestinal mRNA levels of KFABP and of HFABP (heart FABP; FABP3), which is expressed more ubiquitously than other FABPs, and did not find any changes in expression.

Two independent laboratories have generated LFABP^{-/-} mice and there have been body weights differences reported for these mice. The line that was derived in Missouri has a lean phenotype in response to high-fat feeding (179, 187, 196). In contrast, a strain derived in Texas has an obese phenotype (183–185).   There have been differences in gender, diet, age, and length of the feeding periods that may have led to these differences.   Importantly, both strains of mice have shown impaired hepatic FA uptake and oxidation as well as VLDL secretion (152, 179, 181, 182). One strain of IFABP^{-/-} mice has also been generated previously (190).   Previous reports showed that male mice fed a 35 kcal% fat diet with coconut containing added cholesterol had increases in body weight accompanied by hepatic steatosis and hypertriglyceridemia, but females gained less weight and had similar hepatic lipid levels to WT (190, 191).   In another study, 30-40 week old IFABP^{-/-} male mice were fed 41 kcal% fat diets with beef tallow or safflower oil for 14 days and had higher body weights relative to WT (191).

We have previously published work using LFABP^{-/-} mice which were derived from the Texas strain and backcrossed an additional 6 generations onto the C57BL/6J strain upon arrival to our facility (7). Our IFABP^{-/-} mice are derived from the original strain without further backcrossing (7, 169). We did not observe any differences in body weight in response to chow feeding, but as shown here we have found that LFABP or IFABP ablation results in divergent phenotypes during high-fat feeding (7, 169).   LFABP^{-/-} mice are heavier and have greater adiposity relative to WT

mice, while IFABP^{-/-} mice are resistant to obesity (169). In the present studies, we observed the whole body phenotype response to high-fat feeding of mice with simultaneous ablation of both IFABP and LFABP, and compared to the single-null mice. We found that DKO mice display body weights and composition that are in between those of LFABP^{-/-} and IFABP^{-/-} mice during high-fat feeding, though this was not entirely unexpected given that the body weight phenotypes of LFABP and IFABP-null mice are opposite (169).   Interestingly, we did not see a dominant effect of the DKO phenotype from either protein, strongly supporting the hypothesis that the roles of these proteins in intestinal lipid metabolism are quite different.

Lipid uptake into the intestine is highly efficient, with greater than 95% being absorbed in a healthy adult (18). It was thought that the enterocyte FABPs play a role in lipid uptake into the intestine because they are expressed at levels of 2-5% of total cytosolic proteins, with the highest expression in the proximal intestine where lipid uptake is highest, and are also increased in response to large lipid loads during high-fat feeding (122, 154, 229, 230). However, LFABP^{-/-} and IFABP^{-/-} mice do not exhibit signs of lipid malabsoption as determined by fecal fat measurements, in agreement with data from other laboratories (7, 169, 186, 187, 190).   In the present study, we found that DKO mice also do not show signs of lipid malabsorption and gain weight similarly to WT in response to high-fat feeding. Hence, we conclude that these proteins do not, in fact, have a critical role in the net uptake of lipids into the intestine.   Interestingly, in vitro studies suggest otherwise. Uptake of radiolabeled FA into intestinal L cells is increased when LFABP is overexpressed relative to controls (194). Additionally, studies using primary hepatocytes of LFABP^{-/-} mice have shown that FA uptake into liver is reduced relative to WT (149, 179), and hepatic uptake of FA is reduced in LFABP^{-/-} mice relative to WT after 48 hours of fasting, suggesting impairment of trafficking into this tissue (179).

Lipids can enter the enterocyte via passive diffusion, though other transport proteins may be involved in uptake into the enterocyte because it is, in part, a saturable process (27). In this regard, it is possible that other proteins are functioning to transport FA in the dual absence LFABP and IFABP in the intestine. There are several candidates that may be more important for uptake of lipids into the enterocyte. FATP4 (Fatty Acid Transport Protein 4), FABPpm (Plasma membrane FABP), and CD36 are enterocyte membrane proteins which are known to have affinity for binding FA and are also thought to have a role in their uptake (28, 29). However, it is not very clear as to which of these proteins is the most important for net uptake of lipid into the intestine. CD36 is located on the brushborder membranes of enterocytes in the proximal region of the small intestine and has a high affinity for binding to FA (30). The CD36$^{-/-}$ mice only showed signs of malabsorption of FA when given very long chain (>20 carbon) fatty acids, but not (12-20 carbon) LCFA (32–34). Moreover, ablation of CD36 in mice did not result in changes in net absorption of lipids, although absorption shifted towards the distal region of the intestine (34). In the present experiments, we did not find changes in CD36 expression in the intestine in our null mice, therefore this protein does not compensate for ablation of IFABP and/or LFABP. Fatty acid transport protein 4 (FATP4) is also a membrane protein, found on the brush border of the enterocytes as well as the endoplasmic reticulum, and is known to have a high affinity for binding to FA. However, it was shown that FATP4-null mice have normal lipid uptake efficiency, (35). FABPpm is another membrane protein that is thought to have a role in lipid intake in that it binds FA. Fasting and endurance training promotes expression of this protein, thus FABPpm may play a role in delivering FA into the enterocytes (37–39). Along these lines, it is important to also note that LFABP and IFABP are expressed in the proximal intestine, thus it is possible that net absorption of dietary lipid does not change due to compensatory absorption in the distal intestine, as noted above in studies of CD36$^{-/-}$ mice (34). We are presently conducting

experiments to investigate this possibility. Additionally, while we did not find changes in ILBP, HFABP, KFABP, or AFABP, expression of other proteins in the enterocyte that can bind FA such as the acyl-CoA binding proteins, and cellular retinoid binding proteins will also be measured to determine whether any changes in transcriptional regulation occur in response to ablation of LFABP and IFABP.

Thus, here we have found that LFABP and IFABP are not required for efficient uptake of dietary lipid into the intestine. Given that these proteins are so highly abundant, they must have other roles in intestinal lipid metabolism. In particular, the intestine is responsible for absorption of high levels of dietary of FA. Therefore, these proteins may be important for binding the high levels of FA, thereby regulating the levels of unbound free fatty acid concentrations in the cytosol. The regulation of free fatty acid levels is critical because high cellular concentrations are cytotoxic (43, 231). Consequently, it has been hypothesized that FABPs are responsible for binding excess FA thereby maintaining levels of unbound for important cellular processes (210). Furthermore, expression of enterocyte FABPs is upregulated in response to high-fat feeding, thus providing additional evidence that these proteins may be important for maintaining cellular FA concentrations (154, 229).

 Differences in fuel utilization also exist in that LFABP$^{-/-}$ mice fed high-fat diets had lowered respiratory exchange ratios (RER) than WT mice suggesting that these mice preferentially oxidize fat as an energy source. In stark contrast, high-fat fed IFABP$^{-/-}$ mice had higher RERs, indicating that these mice are primarily utilizing carbohydrates as an energy source. We also observed that DKO mice have alterations in respiratory exchange ratios, with higher RER in response to high-fat feeding, relative to WT. Thus, they are more similar to IFABP$^{-/-}$ mice, with a preference

for carbohydrate oxidation. We speculate that because the IFABP^{-/-} mice have reduced adiposity,

less FA is available; therefore these mice have a preference for carbohydrate oxidation relative

to WT mice. In contrast, LFABP^{-/-} mice have greater amounts of lipids available from adipose

tissue for oxidation, and have lower RERs relative to WT. On one hand, it is surprising that

LFABP^{-/-} mice may be oxidizing more fat, due to evidence that this protein interacts with PPARα

and traffics FA towards this important regulator of genes involved with lipid oxidation (148,

149). However, it has been hypothesized that the obese phenotype of LFABP^{-/-} mice may result

from decreased lipid uptake in the liver and promoting more storage of FA into other tissues,

particularly adipose and muscle (210). Recent unpublished findings in our laboratory (see

Appendix) have revealed that the LFABP^{-/-} mice have increased endurance relative to WT during

a treadmill test and therefore we hypothesize that there is higher fat oxidation occurring in the

muscle allowing for greater stamina during activity, and additional analysis of muscle tissue is

presently underway. In light of the endurance phenotype, we were surprised to observe

apparently lower spontaneous activity in DKO mice, a phenotypic difference from both LFABP^{-/-}

and IFABP^{-/-} mice, which had increased or similar activity to WT, respectively. The changes in

activity observed in DKO will need to be further investigated to see if these mice have altered

stamina during an exercise test.

We have previously shown that LFABP^{-/-} mice consume more calories while IFABP^{-/-} mice

consume fewer calories during high saturated fat diet feeding (169). Thus, we were interested

to conduct more in-depth meal pattern analysis of these mice. We found that IFABP^{-/-} mice are

consuming less food and fewer meals relative to WT mice, which correlates with their resistance

to diet-induced obesity. In contrast, we found a trend for increased food intake of LFABP^{-/-} mice

(p<0.08) relative to WT mice. Interestingly, these mice seem to eat more food than WT when

the lights are on. Mice are nocturnal and are more active during the dark cycle; hence, these

data suggest that these mice may have alterations in circadian activity.   Indeed, WT mice fed

high-fat diets do have altered eating patterns and shift their food intake to when the lights are

on, (232), thus this may contribute to their increase in adiposity. Additionally, several

transcription factors involved with regulation of circadian genes have been identified in intestine

(ie Clock, Bmal, Per, and Cry), and moreover, expression of genes for proteins involved with

intestinal lipid metabolism have diurnal variation including MTP, ApoA1V, MGAT2, DGAT, and

also PPARα (232–235).   Indeed, expression of IFABP and LFABP is diurnal in the liver and

intestine (232, 233, 236). Additional studies will investigate alterations in expression of clock

genes in the enterocyte, which may help elucidate the mechanisms underlying the apparent

changes in circadian rhythms observed in these mice.

It is possible that the differences in food intake observed in LFABP$^{-/-}$ and IFABP$^{-/-}$ mice may be

attributed to changes in endocannabinoid levels. Other FABPs have been shown to bind to

anandamide (arachinodoylethanolamide; AEA) (83, 84), an N-acylethanolamine (NAE) that binds

to the cannabinoid 1 receptor (CB$_1$) which promotes food intake (82). Indeed, we have found

that LFABP$^{-/-}$ mice have elevated levels of AEA in the intestine which correlates with their

hyperphagia (169). In addition, we also observed increased intestinal levels of 2-

arachidonoylglycerol (2-AG), an MG, that also promotes food intake by activation of the CB$_1$

receptor (220, 222). Therefore, it is possible that LFABP has an important function as a lipid

sensor for regulation of food intake, potentially by regulating the levels of endocannabinoids in

the enterocyte.

We performed glucose tolerance tests to investigate alterations in glucose metabolism in the

mice.   In our previous and present work, we have shown that IFABP$^{-/-}$ mice remain lean in

response to high-fat feeding with lower adiposity relative to WT (169); hence it is not surprising

that these mice are able to clear glucose into the tissues more quickly, relative to WT mice.

Surprisingly, we did not find any changes in LFABP$^{-/-}$ mice relative to WT during high-fat feeding,

despite these mice having increased adiposity.   DKO mice seemed to follow LFABP$^{-/-}$ mice, with

very similar area under the curve.   In addition, fasting glucose and insulin measurements of DKO

mice were not different than WT, suggesting they maintain glucose homeostasis during high-fat

feeding.   This is in keeping with their similar body weight and fat mass relative to WT.

We have not observed any changes in fasting TG levels between any these groups during LFD or

HFS feeding.   To investigate TG secretion out of the intestine, we also performed oral fat

tolerance tests using tyloxypol to inhibit lipoprotein lipase, which results in attenuation of TG

clearance into tissues. As observed previously, IFABP$^{-/-}$mice exhibited an increase in secretion of

TG relative to WT (169).   It is known that IFABP is not involved in chylomicron assembly (54),

therefore we hypothesize that these mice have increased secretion of TG because of their lean

phenotype, as we have previously shown that obese mice have reduced TG secretion out of the

intestine relative to lean mice (60, 217).   In contrast, LFABP is thought to be involved with

formation of chylomicrons (31, 54), and given that these mice are obese, we expected to see

slower TG secretion out of the intestine. However, we found that they have similar secretion

rates to WT when fed chow or a high-fat diet (7, 169). Furthermore, DKO mice do not exhibit

any changes in TG secretion out of the intestine and are similar to WT and LFABP$^{-/-}$ mice. These

results suggest that trafficking of TG out of the intestine is not impaired; however it is possible

that absence of LFABP disrupts FA trafficking in the enterocyte and therefore may impact the

size and/or composition of the chylomicron particles. For instance, CD36 is an enterocyte protein involved with chylomicron formation and deficiency of this protein results in secretion of smaller chylomicron remnants into the lymph (31, 32, 237)

In summary, the present studies demonstrate that simultaneous ablation of IFABP and LFABP largely results in an integration of the single knockout phenotypes, indicating that one protein is not dominant over the other. Ablation of LFABP results in a healthy obese phenotype relative to WT, IFABP$^{-/-}$ mice remain healthy and lean, and the DKO mice have body weights and body compositions that are in between. LFABP$^{-/-}$ mice fed a high-fat diet preferentially oxidize lipids for energy, while IFABP$^{-/-}$ and DKO mice seem to preferentially oxidize carbohydrates during high-fat feeding. The reason for this remains unclear, therefore studies of these mice during exercise may provide for further clues as to the functions of these proteins in whole body energy homeostasis. Above all, we found that neither IFABP nor LFABP is critically required for FA uptake into the intestine therefore other mechanisms may be involved to maintain efficient lipid uptake. Future work will involve studying the tissue-specific effects of LFABP ablation in the intestine and liver, where this protein is highly expressed. The use of tissue specific knockouts will help identify the contributions of ablation of this protein in each of these tissues to the whole body phenotype.

Chapter 4

General Conclusions and Future Directions

Intestinal Absorption of Dietary Lipids is a Highly Efficient Process

The intestine has the essential role of lipid uptake and secretion to peripheral organs. This is known to be a very efficient process with greater than 95% absorption in healthy adults (18). This efficiency is likely attributed to evolutionary adaptations for the body to adapt to situations of food scarcity. Unfortunately, in the current age, there is an overabundance of food in Westernized countries that has resulted in higher prevalence of obesity and related metabolic diseases. In particular, alterations in neutral lipid metabolism can result in hypertriglyceridemia, which is major risk factor for cardiovascular disease (4, 6). Hence, it is important to investigate the processes involved with uptake of lipids into the intestine, how they are processed in the enterocytes, as well as trafficking out of the cell and into the general circulation.

Dietary lipids can enter the enterocyte via a diffusional mechanism, but it is also believed that membrane proteins play a role in uptake (27, 238). However, studies of candidate transmembrane proteins that have been shown to bind FA, (FABPpm, CD36, and FATP4) have not yet shown a definitive role of FA uptake into the intestine (28, 47). It has been hypothesized that IFABP and LFABP are involved with uptake of FA into the intestine, but this does not seem to be the case, as mice which are null for either protein do not display any indications of malabsorption based on fecal fat analyses. Here, we have also shown that mice, which do not express either protein, absorb high levels of dietary lipids with normal efficiency, suggesting that neither of these proteins is involved with bulk FA uptake. Because LFABP and IFABP are expressed in the proximal region of the intestine, it is possible that lipid absorption is being shifted to the distal region of the intestine. Therefore, further studies will be done to investigate this possibility. Indeed, there have been reports of alterations in intestinal uptake

resulting from ablation of proteins involved with intestinal lipid metabolism. For example, CD36^{-/-} and MGAT2^{-/-} mice exhibited a shift in lipid absorption from the proximal to the distal region of the intestine which resulted in no change in net uptake (34, 50).

Potential Roles of LFABP and IFABP as Sensors of Intestinal FA and MG Status

If IFABP and LFABP are not required for bulk lipid uptake into the intestine, then what are their functions?   LFABP and IFABP must be important for other roles in lipid metabolism in the intestine given that they are both present at levels of 2-5% of all cytosolic proteins (45, 124).   It is possible that instead of being involved with bulk uptake of FA and MGs into the intestine, these proteins are involved with regulation of FA and MGs levels inside the cell by acting as lipid sensors. In vitro studies have shown that LFABP and IFABP have high affinities for binding FA (136, 138).   Therefore, these proteins may be involved with maintaining free fatty acid concentrations. Additionally, LFABP and IFABP are also thought to be involved with trafficking FAs for various functions. In particular, LFABP may be responsible for delivering FAs for chylomicron biogenesis and transcription factors by direct protein-protein interactions. Additionally, LFABP and IFABP may be involved in important signaling transduction pathways by regulation of lipid endocannabinoid levels, which are involved with regulation of food intake.

One important role of the FABPs may be for sequestration of unbound FA in the cytosol, thereby regulating the level of unbound fatty acids. The intestinal enterocyte has a profusion of free fatty acids being delivered to this tissue from the diet, and it is known that high levels of free fatty acids in all cells are cytotoxic (43, 231). Therefore, it has been proposed that these proteins serve a protective function to the cell by binding excess FA (210). It is possible that the

FABPs keep a stable pool of FA and MGs, allowing for steady availability for regulation of gene expression, TG and PL synthesis, chylomicron biogenesis, rather than catabolism of TG. FAs also must be activated by acyl CoA synthetase to fatty acyl CoAs. To that effect, LFABP has been shown to also bind FA acyl CoAs (239), providing further evidence of a role in maintaining cellular concentrations. Moreover, enterocyte FABP expression is also upregulated during high-fat feeding, presumably to compensate for a greater amount of FA delivered to the enterocyte (154, 229). Thus, these proteins likely play a role in trafficking the large quantity of FA in the cytosol, from the intestinal lumen during the fed state, perhaps to prevent excess accumulation of unbound FA in the cytosol and to establish a certain unbound FA concentration.

IFABP and LFABP may also play roles in nutrient sensing in the intestine in response to feeding status. In particular, there have been data which have offered clues about LFABP and IFABP and their respective roles of trafficking FAs within the intestinal enterocyte in response to FA and MG. Previous work using an intestinal explant system showed that both IFABP and LFABP are localized on the apical side of the enterocytes of fasted rats, but were located throughout the cytoplasm in the fed state (120), suggesting that localization of these proteins is influenced by the availability of FA. It is known that FAs enter the enterocyte brush border membrane side of the enterocyte, and bloodstream-derived FAs are delivered to the cell via the basolateral side of the enterocyte. It is believed that there is compartmentation of FA into two different pools, which is dependent on the site of entry into the cell (61). This idea is based on observations that dietary FAs enter the apical side of the enterocyte and are formed into TGs and then packaged into chylomicrons for secretion into the lymph, while FA from the circulation are oxidized or incorporated into PL (61–64). Here, we have shown that more FAs from the bloodstream are formed into PL during ablation of LFABP and IFABP relative to WT, suggesting that these

proteins are involved with trafficking bloodstream derived FA towards TG synthesis pathways (7, 169).

In addition to FAs, MGs are also delivered in large quantities from the lumen of the small intestine and into the enterocyte. Our laboratory has previously shown that LFABP is a cytosolic protein that binds MG (138).   Our present results show that LFABP$^{-/-}$ mice given an oral gavage of radiolabelled MG have a decrease in the TG/PL ratio in the intestinal mucosa relative to WT, suggesting that LFABP is involved with targeting dietary MG towards TG synthesis and away from PL synthesis pathways (7, 169). Thus, LFABP has a role in trafficking the large amount of dietary MGs that arrive into the intestinal enterocyte from dietary TG hydrolysis.

It is also known that LFABP interacts with several proteins including apoB48 and CD36 to generate prechylomicron transport vesicles (PCTVs) from the ER for assembly into chylomicrons in the Golgi apparatus, which are then secreted out of the enterocyte (31, 54). However, we did not observe any differences in TG output for LFABP$^{-/-}$ mice into the circulation during an oral fat tolerance test. Indeed, it is possible that the chylomicron composition may be altered in case of LFABP ablation. For example, the amount of TG may be reduced due to less efficient trafficking of FA in the enterocyte for TG synthesis and subsequent chylomicron assembly. Also, IFABP is not directly involved with chylomicron assembly (54), but it is possible that its absence would influence the amount of unbound fatty acids available for chylomicron assembly, and therefore the size, and perhaps the composition, of the chylomicron particles. For example, it has been shown that CD36-null mice have decreased chylomicron size with altered lipid and lipoprotein compositions (32). Hence, compositional analysis of chylomicrons may reveal changes resulting from LFABP and/or IFABP ablation.

In addition to protein interactions for formation of PCTVs, LFABP has also been shown to
interact with transcription factors (148, 240, 241).   Indeed, it has been proposed that LFABP has
an important role in trafficking FA to PPARα, an important regulator of lipid oxidation that is
present in both the intestine and liver (57, 148, 149, 241, 242). PPARs, like FABPs, are located in
the cytoplasm of the cell and are activated by ligands which cause the PPARs to localize in the
nucleus where they bind to peroxisome proliferator activated receptor response elements
(PPREs) as a heterodimer with Retinoid X receptor (RXR), resulting in initiation of expression of
PPAR-regulated target genes (144, 243).   In the present studies, we have also found that LFABP$^{-/-}$ mice have a reduction in intestinal oxidation of FA relative to WT, hence LFABP also seems to
be involved with targeting FA towards oxidative pathways (7, 169). We and others have also
observed this defect resulting from LFABP ablation in the liver and intestine (7, 149, 152, 169).
Recent studies have shown that ablation of LFABP results in attenuation of PPARα localization in
the nucleus, thereby inhibiting its functionality (148, 149).   Additionally, it seems that LFABP
also regulates its own expression as it has does contain a PPRE in its promoter region (143).
LFABP expression is also increased in the presence of high levels of FA during high-fat feeding
(154, 229). Therefore, LFABP may be acting as a nutrient sensor in response to high levels of FA
and plays a role in trafficking FA towards oxidative pathways by protein-protein interactions
with PPARα.

Indeed, PPARα activation also occurs due to binding of oleoylethanolamide (OEA). This N-
acylethanolamine is secreted by the intestine in response to feeding and is known to have an
inhibitory effect on food intake (87, 244). Hence, it is likely that an important function of LFABP
may be trafficking FAs, OEA, and other lipid agonists to PPARα.   Along these lines, other FABPs
have been shown to bind to anandamide (arachinodoylethanolamide; AEA) (83, 84), an agonist

for the cannabinoid 1 receptor (CB$_1$) which promotes food intake (82). While LFABP has not yet

been shown to bind AEA, we speculate that this protein is involved with trafficking AEA because

LFABP$^{-/-}$ mice have elevated levels in the intestine (169). Additionally, we have demonstrated

that LFABP$^{-/-}$ mice display hyperphagia when fed a high-fat diet (169). Thus, LFABP may play a

role in trafficking AEA to CB$_1$ receptors. Furthermore, we have provided evidence that LFABP

ablation results in increased intestinal levels of 2-AG (169), an endocannabinoid that is also an

MG, that promotes food intake by activation of the CB$_1$ receptor (220, 222). Therefore, LFABP

may play a role in the important intestinal function of lipid sensing in the regulation of food

intake.

Ablation of IFABP or LFABP Results in Changes in Systemic Energy Metabolism

Previous studies using mice that are null for important genes involved with intestinal lipid

metabolism such as CD36, DGAT, MGAT, and PPARα have revealed that these changes influence

whole body energy homeostasis (50, 87, 88, 105, 106). As well, our results have also

demonstrated that ablation of IFABP or LFABP results in changes in whole body energy

metabolism. These results provide further evidence of a link between intestinal metabolism and

whole body energy homeostasis. In particular, IFABP$^{-/-}$ mice have a lean phenotype in response

to high-fat feeding, while LFABP$^{-/-}$ mice are obese. We also found that LFABP$^{-/-}$ preferentially

oxidize lipids, while IFABP$^{-/-}$ are opposite and primarily utilize carbohydrates for energy while at

rest. These changes occurred without any alterations in energy expenditure (169). We have

also observed alterations in food intake in our high-fat fed IFABP$^{-/-}$ and LFABP$^{-/-}$ mice. Indeed,

we observed that LFABP$^{-/-}$ mice had increased food intake relative to WT (169), likely related to

the increases in 2-arachidonoyl glycerol (2-AG) and anandamide (AEA) in the mucosa, as both of

these endocannabinoids are known to promote food intake (82, 98). We also observed that these mice primarily increase their food intake during the light cycle (Chapter 3), which is typically when the animals are at rest. In contrast, IFABP$^{-/-}$ mice have lower daily food intake relative to WT, but their circadian rhythms are altered in that they shift their more of these meals to the light phase. Interestingly, it is known that proteins involved with lipid metabolism, including LFABP, IFABP, and PPARα have diurnal expression patterns (123, 233, 245). Hence, it would be of interest to measure mRNA of transcription factors involved with circadian rhythms in our high-fat fed LFABP- and IFABP-null mice to determine if there are changes in expression relative to WT mice.

It is important to note that LFABP is simultaneously expressed in the liver and also in the intestine, therefore it is important to consider the individual functions of this protein in both of these tissues and the tissue-specific contributions to the whole body phenotype of LFABP$^{-/-}$ mice. To date, only whole body knockouts of LFABP have been studied (7, 179, 180). Effects of whole body LFABP ablation has resulted in changes in body weight and composition, fuel utilization, and lipid oxidation, but the tissue-specific effects on these systemic changes are not known (7, 152, 181).   Hence, future work will focus on generation of LFABP$^{-/-}$ mice, in which ablation of this protein is specific to the liver or intestine in an effort to understand the functions of the proteins in these tissues and their contributions to the phenotype of the whole body knockout.

Ablation of FABPs Results in Overt Changes in Whole Body Phenotype: Lessons from Other FABP-null mice

We have observed that LFABP^{-/-} and IFABP^{-/-} mice seem to have healthy phenotypes during high-fat feeding. These proteins are part of a larger family of intracellular binding proteins that are present in various tissues. Studies of AFABP (adipose FABP; FABP4) and KFABP (keratinocyte FABP; FABP5) null mice have some parallels to what we have observed in the LFABP^{-/-} mouse. The AFABP protein is an abundant cytosolic protein that is mainly expressed in adipose and also in macrophages, and mice null for AFABP did not display an overt phenotype when fed a low-fat diet (246). However, high-fat feeding resulted in obesity in null mice, but with improved glucose tolerance and normoinsulinemia (246). Indeed, studies of inhibitors of AFABP have shown similar effects (247). AFABP has been implicated as being involved with the early stages of the development of atherosclerosis, in which macrophages are altered to form foam cells that accumulate along the vasculature, eventually forming atherosclerotic lesions (248). AFABP ablation also results in resistance to atherosclerosis as shown when AFABP is knocked out in ApoE-null mice, a strain that develops atherosclerosis (249). In another study, bone marrow from ApoE/AFABP-null mice or ApoE-null mice was transplanted into ApoE-null mice so that AFABP was only expressed in macrophages (250). Interestingly, the mice that received the bone marrow without AFABP had smaller lesion sizes and reductions in inflammatory markers, suggesting that AFABP present in macrophages, rather than adipose, plays a role in the development of atherosclerosis (250).

It is known that KFABP is expressed in adipose, but at very low levels, hence, it was surprising that ablation of AFABP results in marked upregulation of KFABP in adipose tissue (227). In contrast, AFABP is not upregulated in response to ablation of KFABP (251). Mice that are null for both KFABP and AFABP were resistant to obesity during high-fat feeding with improved glucose tolerance, insulin sensitivity, and resistance to hepatic steatosis (228). Interestingly, it

was also found that these mice had increased fat oxidation in muscle tissue resulting from elevation in expression of AMP-activated protein kinase (AMPK). Moreover, when AFABP and KFABP were simultaneously ablated in *ob/ob* mice lacking leptin, the AMPK response was attenuated, suggesting that leptin is responsible for activation of AMPK (252). AFABP and KFABP have also been shown to interact with PPAR-γ and PPAR-β, respectively, suggesting that these proteins are important for delivery of their ligands in adipose and macrophages (253).

Overall, the phenotype of AFABP/KFABP-null mice, like LFABP- and IFABP-nulls, results in a healthier phenotype than WT mice. In particular, AFABP/KFABP-null mice have increased lipid oxidation occurring in muscle tissues, resulting from an increase in AMPK expression. Hence, future work will involve measurements of this important in metabolic regulator in muscle. Additionally, like LFABP, AFABP and KFABP seem to play a role with regulation of gene expression by interactions with nuclear transcription factors. Moreover, inhibitors of AFABP have been studied as potential therapeutic agents for human disease (247), as can be suggested for IFABP and LFABP, based on our current findings.

LFABP and IFABP Ablation Results in Healthy Phenotypes

In the present studies, we have demonstrated that ablation of IFABP or LFABP results in a healthy phenotype. IFABP^{-/-} mice are lean and glucose tolerant during a high-fat feeding. LFABP^{-/-} mice are obese, but remain normoglycemic, quite active, and also have increased stamina during exercise. Additionally, others have demonstrated that LFABP ablation prevents hepatic steatosis (184, 186, 187).

In addition, previous reports have shown that ablation of each these proteins does not result in reduction of lipid uptake into the intestine (7, 181, 186), and we have now shown that simultaneous ablation of these proteins does not impact lipid uptake. This is a desirable effect for clinical applications because steatorrhea is associated with gastrointestinal discomfort and is viewed as an unfavorable side effect, as observed by administration of lipase inhibitors such as orlistat (254, 255).   Therefore, these results suggest that inhibition of these proteins may lead to promising therapeutic interventions. Indeed, there are populations that have single base pair gene polymorphisms resulting in single amino acid changes of IFABP and LFABP (161, 170). Individuals with a polymorphism of IFABP, in which threonine is substituted for alanine at amino acid 54, have a higher prevalence of insulin resistance and high plasma triglycerides (170–174). Additionally, a polymorphism of LFABP has been identified in which alanine is substituted for threonine at position 94 (T94A), has been correlated with increased blood TG and FFA levels (158, 161). Hence, it is possible that pharmaceutical inhibition or IFABP or LFABP may provide for treatment options for these individuals in order to maintain normal lipid homeostasis.

In summary, we have uncovered very distinct phenotypes resulting from IFABP and/or LFABP ablation during high-fat feeding.   Mice null for either protein display a healthier metabolic phenotype relative to normal controls. These results will be valuable to develop further studies to fully elucidate the functions of these proteins in intestinal lipid metabolism and how they can impact the health of humans. It is possible that this work will increase interest in development of inhibitors for these proteins that may lead to therapeutic interventions for metabolic disease.

Appendix

Untrained LFABP$^{-/-}$ Mice Have Increased Stamina During a Treadmill Endurance Test

Abstract

Intestinal enterocytes form the brush border membrane of the small intestine, across which dietary lipid absorption takes place. Enterocytes express two fatty acid-binding proteins (FABP), intestinal FABP (IFABP; FABP2) and liver FABP (LFABP; FABP1) in the cytosol, and it is not currently understood why two similar proteins are simultaneously expressed in such high abundance. High fat feeding studies showed divergent phenotypes in null mice; LFABP^{-/-} mice become obese and preferentially oxidize lipid for energy, while IFABP^{-/-} mice are lean and utilize carbohydrates relative to WT mice. Markers of whole body metabolism showed that not only IFABP^{-/-} mice were metabolically healthy, but also LFABP^{-/-} mice were healthy, despite their increased adiposity. In particular, high-fat fed LFABP^{-/-} mice had increased spontaneous activity relative to WT mice, as measured by beam break technology, thus we hypothesized that these mice might have an improved response to exercise relative to WT. In the present studies, we found that untrained high-fat fed LFABP^{-/-} mice have increased stamina on a treadmill, with greater distance and time relative to WT and IFABP^{-/-} mice. This difference was not due to increased lipid oxidation because LFABP^{-/-} mice did not have different respiratory exchange ratios from WT during exercise. However, LFABP^{-/-} mice have lower energy expenditure per gram of body mass, suggesting that they are more metabolically efficient for equal workloads. Hence, we have observed that the LFABP^{-/-} mice, despite displaying an obese phenotype, have greater endurance during exercise compared to WT, further suggesting that these mice represent a model of the obese, but metabolically healthy phenotype.

Introduction

The fatty acid binding protein (FABP) family is a class of small (14-15) kD cytosolic proteins that are known to bind fatty acids (FA) and other lipids. In the intestine, 3 FABPs are present, 2 are expressed in the proximal intestine, while the other is expressed more distally and preferentially binds bile acids over FAs (134). Given that the intestine is responsible for uptake and assimilation of the large amount of dietary FA into the body, it is hypothesized that enterocyte FABPs play an important role in trafficking lipids in the intestinal enterocyte (111).

We have recently shown that LFABP and IFABP-null mice have divergent phenotypes in response to high-fat feeding, demonstrating that these proteins have distinct roles in intestinal lipid metabolism (7). We have previously reported that LFABP$^{-/-}$ mice became obese and hyperphagic when given a high-fat diet, while IFABP$^{-/-}$ mice remained lean (169). Indirect calorimetry measurements revealed that IFABP$^{-/-}$ mice had higher respiratory exchange ratios (RER) relative to WT mice, suggesting that they preferentially utilize carbohydrates for energy. In stark contrast, LFABP$^{-/-}$ mice display an opposite phenotype and have lower RERs, indicative of a preference for lipid oxidation for energy. Interestingly, in spite of being obese, we observed that LFABP$^{-/-}$ mice have an increase in spontaneous activity relative to WT.   We hypothesized that LFABP$^{-/-}$ mice have a healthy obese phenotype and may have greater endurance during exercise, given that human athletes have better endurance when lipids are used as the primary fuel source (256).   Therefore, in the present studies, we subjected untrained WT, IFABP$^{-/-}$ and LFABP$^{-/-}$ mice to a treadmill test to determine if the LFABP$^{-/-}$ mice would have increased endurance in response to an exercise bout.

Experimental Procedures

Animals and Diets

LFABP^{-/-} mice, previously generated by Binas and coworkers, were used in these studies (7, 169, 180). As described previously, the mice were additionally back-crossed with C57BL/6J mice from The Jackson Laboratory (Bar Harbor, ME) for six generations to create congenic LFABP mice (7). IFABP^{-/-} mice used in the present studies have been bred by intercrossing of the original IFABP^{-/-} mice (190), and are also on a C57BL/6J background. Wild type (WT) C57BL/6J mice bred in our animal facility were used as controls.

Until 2 months of age, male mice were given *ad libitum* access to standard rodent chow (Purina Laboratory Rodent Diet 5015) and were maintained on a 12-hour light/dark cycle. LFABP [-/-], IFABP^{-/-}, and WT (C57BL/6J) mice were started on the semipurified diets at 8 weeks of age. The mice were housed 2-3 per cage and fed either a low fat diet (LFD) containing 10 kcal% fat or a 45 kcal% fat diet with high saturated fat (HFS). Product numbers are D10080401 and D10080402 respectively (Research Diets, Inc., New Brunswick, NJ) and the compositions have been published previously (169).

Endurance Test

After 12 weeks of high-fat feeding mice were placed on a treadmill with 6 individual lanes to run multiple mice concurrently (Columbus Instruments, Columbus OH). At the bottom of the treadmill is a shock grid, which was set to 1 Hz in order for the mice to stay on the treadmill. One day prior to the test, the mice were run for 5 min at 5 m/min with a 0 degree incline in order to acclimate them to the treadmill. Mice were tested in groups with the same two trained spotters for each test.   On the day of

the test, the mice were run on the treadmill set to a constant 25-degree incline throughout the

experiment. The speed of the treadmill was adjusted as presented in Table 1 (257). The mice were run

until they were declared to have reached exhaustion by the trained spotters. Exhaustion was defined

as when the mice remained on the shock grid for 5 seconds. The time was taken when the mice

finished the test and the distance was calculated based on the elapsed time and speed (Table 1).

Indirect Calorimetry During Exercise

Mice were fed LFD or HFS diets for 12 weeks. Each mouse was run individually on a similar treadmill as

described above, except that it was positioned inside an indirect calorimetry chamber (Columbus

Instruments, Columbus OH). The shock grid was set to 1 Hz, as described above. One day prior to the

test, mice were acclimated to the treadmill, as described above. On the day of the test, food was taken

away at 7am to ensure that the mice were in the same metabolic state. The test started at 9 am and 4-

5 mice run were run per day. The genotypes were rotated each test day to ensure that there was not

an effect of fasting time. The treadmill was set to a constant 25-degree incline throughout the

experiment. At the start of the test, the mouse was placed in the chamber, allowing rest for 2 minutes

in the stationary treadmill. After the resting phase of the experiment, the treadmill was set to 5 m/min

for 5 minutes. Then, speed was increased to 10 m/min for 10 minutes, at which gas exchange and

energy expenditure measurements were taken. This speed was chosen to ensure that all mice could

complete the test, based on results from the endurance test. VO_2 and VCO_2 (VCO_2/VCO_2) were used

to determine the respiratory exchange ratio (RER) as an estimation of the Respiratory Quotient.

Energy expenditure was assessed using the gas exchange measurements as follows: $(3.815 +$

$1.232 \times RER) \times VO_2$ (197, 198).

Table 1

Time (min)	Speed (m/min)
0-5	6
5-7	9
7-9	12
9-11	15
11-13	18
13-15	21
15-17	24
17-19	27
19-21	30
21-23	33
23-25	36
25-27	39
27-29	42
29-31	45
31-33	48

Table 1. Protocol for speed adjustment of treadmill during endurance test. The distance run by the

mice on the treadmill (Columbus Instruments) was calculated based on the time of exhaustion.

Results

Untrained LFABP$^{-/-}$ Mice Have Increased Endurance

We did not observe any differences for LFD-fed mice, but we were surprised to find that high-fat

fed LFABP$^{-/-}$ mice had a significant increase in length of time and distance run until exhaustion

relative to WT mice (Figure 1).   There were no differences for IFABP$^{-/-}$ compared to WT. This

was also somewhat unexpected, given that these mice have less adiposity relative to WT.

Different Fuel Utilization for LFABP$^{-/-}$ and IFABP$^{-/-}$ Mice During Exercise Compared to Rest

For mice were fed the LFD, we did not observe any differences between groups during the

exercise bout for VO_2, VCO_2, respiratory exchange ratio, or energy expenditure (Figure 2).

However, high-fat fed LFABP$^{-/-}$ mice had lower VCO_2 and VO_2 relative to WT mice when fed HFS,

as found previously in resting mice (169). In contrast to mice at rest, the high-fat fed LFABP$^{-/-}$

did not have lower RERs relative to WT mice during exercise. Furthermore, IFABP$^{-/-}$ mice had

lower RERs relative to WT mice during exercise, which was surprising given that these mice have

higher resting RER values (169).

We also measured energy expenditure (EE) per kilogram of BW to normalize for workload and

found that LFABP$^{-/-}$ mice had lower EE (Figure 2), suggesting that for the same workload

(movement of body weight uphill against gravity), these mice are more energy efficient, thereby

providing for greater stamina during an exercise test. No change was found for the IFABP$^{-/-}$ mice.

Figure 1

A

B

Figure 1. Endurance testing of WT, IFABP$^{-/-}$, and LFABP$^{-/-}$ mice fed a low-fat diet (LFD) or high-saturated fat diet (HFS). Measurements of A. time for LFD (n=9-10) or HFS (n=8-10) and B. distance for LFD (n=9-10) or HFS (n=8-10).
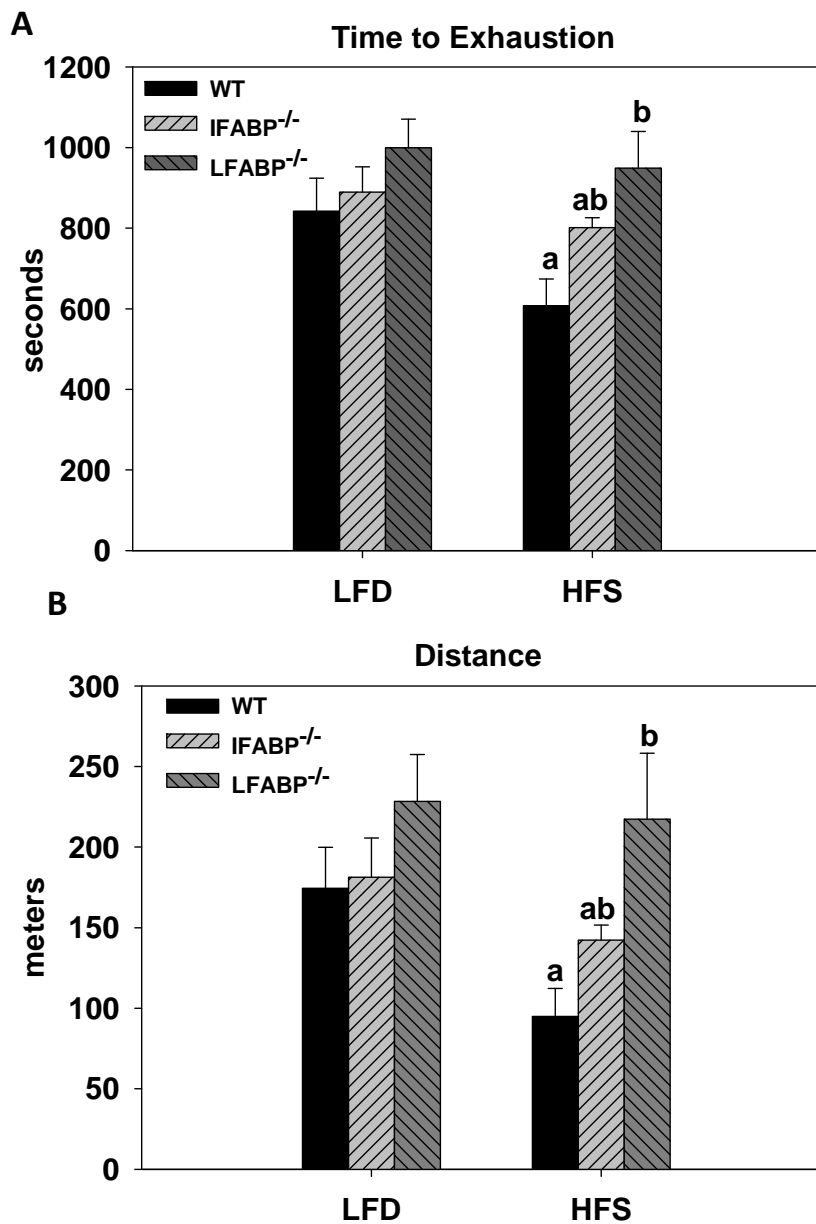
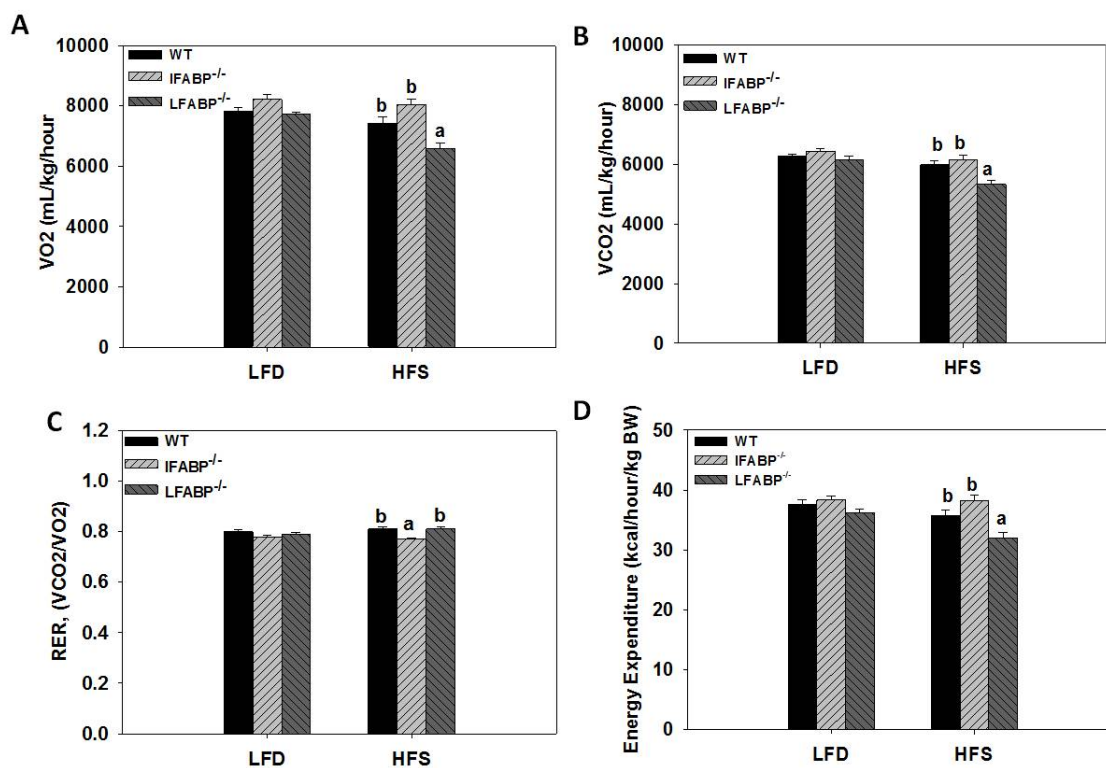**Figure 2**

Figure 2. Indirect calorimetry data of WT, IFABP^{-/-}, and LFABP^{-/-} mice fed a low-fat diet (LFD) or high-saturated fat diet (HFS). Measurements of mice fed LFD (n=9-11) or HFS (9-14). A. VO2. B. VCO2. C. RER. D. Energy expenditure

Discussion

The intestinal enterocyte has the important function of nutrient uptake into the body. LFABP and IFABP are highly expressed in this cell type, and are thought to play a role in uptake and assimilation of lipids, but their individual functions are presently not known. We have previously shown that high-fat feeding promotes very different phenotypes in IFABP and LFABP null mice. In particular, IFABP$^{-/-}$ mice are metabolically healthy and have a lean phenotype in response to high-fat feeding with improved glucose tolerance and similar TG and FFA levels in the blood (169). No changes in activity were found relative to WT (169). Also, LFABP$^{-/-}$ mice have greater adiposity in response to high-fat feeding, but are otherwise metabolically normal with no differences in blood glucose or TGs relative to WT, and also, these mice also have a lower respiratory exchange ratio at rest, suggesting that they have a preference for fat oxidation for energy production rather than carbohydrates (169). Moreover, we found that the LFABP$^{-/-}$ mice have greater spontaneous activity relative to WT. Overall, despite their increased adiposity, it is apparent that ablation LFABP results in a metabolically healthy obese phenotype.

It has been well established that obesity is typically associated with metabolic disease, but there has been increasing interest in metabolically healthy obese (MHO) individuals that do not exhibit markers of metabolic abnormalities (225). Like MHO humans, LFABP$^{-/-}$ mice seem to be metabolically healthy, with no aberrations in whole body glucose or lipid metabolism. Furthermore, they are also very active, with consistently higher activity counts. Indeed, in the present experiments, we found that the high-fat fed LFABP$^{-/-}$ mice have greater endurance during a treadmill test than WT and IFABP$^{-/-}$ mice, further supporting the "healthy obese" phenotype. Remarkably, the LFABP$^{-/-}$ mice ran twice the distance of WT mice. We hypothesized

that this was due to increased oxidation of lipids over carbohydrate for energy, as the

preferential use of fat for energy during exercise has been shown in endurance athletes (256).

Furthermore, MHO humans have also been shown to have increased lipid utilization during

exercise (258). Indirect calorimetry measurements in LFABP$^{-/-}$ mice, however, revealed that the

RER was not lower than WT during an exercise bout, as we had hypothesized. In addition, our

present observations were in agreement with our previous studies in that the resting energy

expenditure (EE) of LFABP$^{-/-}$ mice is not different than WT per gram of lean mass (169). To

ascertain differences in energy expenditure for the same amount of workload, we calculated the

EE/kg BW. Indeed, we found that LFABP$^{-/-}$ mice have lower energy expenditure per kilogram of

body weight during exercise, suggesting that when given the same amount of workload, the

LFABP$^{-/-}$ mice do not expend as much energy, and are therefore more efficient, allowing for

greater endurance.

It is possible that we did not observe changes in substrate oxidation during the exercise test due

to limitations in our experimental design. We performed the test in which the mice were run at

a set speed for a predetermined amount of time to determine the RER during exercise. This

exercise test was chosen over a VO2 max test because we were interested in observing

differences in substrate oxidation during exercise by taking the ratios of VCO_2/VO_2 to measure

RER. During a VO2 max test, the subjects are run on a treadmill inside an indirect calorimetry

unit with increasing speed over time until exhaustion.   During high intensity exercise,

bicarbonate is utilized as a buffer for increased lactic acid production to prevent metabolic

acidosis, which leads to non-metabolic CO2 production (dissociation of carbonic acid to CO_2 and

water) (259); hence we did not use this experimental paradigm because this would add a

confounding factor for the RER measurements.

Previously, we took measurements of sedentary mice placed in indirect calorimetry chambers with ad libitum access to food. We found that the IFABP^{-/-} mice had higher RERs while the LFABP^{-/-} mice were opposite relative to WT (169). It is possible that we did not see similar results during the exercise test due to feeding status. In the present experiments, the mice were fasted when the lights came on for at least 2 hours to ensure that the animals were in a similar metabolic state at the start of the exercise test. In contrast, the resting data in our previous experiments (169) were taken while the animals had access to food, which can affect the RER. We have previously observed that IFABP^{-/-} mice have a greater loss of fat mass following a fast (7, 169). Hence, it is possible that the low RER observed of IFABP^{-/-} during the exercise bout compared to the resting state was due to the effect of the fasting state.

LFABP is an intracellular lipid binding protein that is expressed in the liver, intestine, and to a lesser extent in the kidney, but importantly, not in muscle tissues (111). Therefore, it is not clear why LFABP^{-/-} mice have a preference for whole body oxidation of lipid relative to WT mice. In particular, it has been previously shown that these mice have a defect in oxidation in their tissues of expression, which has been attributed to an inefficiency in lipid trafficking (7, 152, 179, 185). Newberry et al demonstrated that LFABP^{-/-} mice are unable to efficiently traffic FA to the liver during fasting (179). Additional studies of high-fat mice have shown that these mice have smaller liver weight per g of body weight and are resistant to hepatic steatosis, suggesting that lipid uptake into these tissues is inhibited (186, 196). Indeed, these mice do not show signs of malabsorption of lipids, and the obese phenotype observed in LFABP-null mice suggests that the FAs are stored as TG in adipose tissue (169, 210).

The consistent increases in spontaneous activity of LFABP$^{-/-}$ mice are associated with what is known as spontaneous physical activity (SPA) (260). Therefore, this raises another possibility to explain their increased stamina, that because the animals are constantly active, they are more metabolically healthy because they are essentially chronically exercise trained. For instance, in an aging study, it was observed that mice with greater SPA had greater endurance and strength relative to sedentary animals (261).

Our previous studies showed that leptin is elevated in the circulation of high-fat fed LFABP$^{-/-}$ mice (Table 2-5), therefore it is possible that a regulators of muscle lipid metabolism such as AMPK are being activated in response to high levels of this adipokine, promoting greater lipid oxidation in this tissue (262). Interestingly, studies of KFABP/AFABP-null mice have demonstrated that ablation of these proteins results in a healthy phenotype with an increase in muscle lipid oxidation, due to an increase in expression of AMPK in muscle, despite the fact that these proteins are not expressed in this tissue (228).

In addition to studying regulators of lipid oxidation in muscle, further studies will involve analysis of mitochondrial proliferation in these mice; an increase in this organelle would allow for greater lipid oxidation and overall fuel use and endurance (263, 264). The LFABP$^{-/-}$ and IFABP$^{-/-}$ mice will be compared to the LFABP/IFABP-double knockout mice that display a phenotype, which, for the most part is in between both the IFABP and LFABP-null mice, except for a surprising decrease in spontaneous activity (Chapter 3). Therefore, it will be of interest to perform endurance tests to determine the effects of endurance in mice with ablation of both proteins.

In summary, we have observed that LFABP$^{-/-}$ mice have greater endurance during an exercise test, but it was not due to increased lipid oxidation relative to WT mice. Therefore, these observations may be caused by the increases in spontaneous activity observed in these mice, and/or possibly due to upregulation of oxidative genes and/or capacity in muscle. The present results support our earlier studies indicating that LFABP$^{-/-}$ mice have a metabolically healthy obese phenotype.

Acknowledgement of Previous Publications

The results of some of these studies have also been published previously. Sources for reference and background information are numbered throughout the text and listed in the bibliography at the end of this dissertation. Angela Gajda is the writer of all dissertation sections. Other individuals were involved in the research in the previously published work and have been identified here.

Previously published work

Gajda, A. M., Zhou, Y. X., Agellon, L. B., Fried, S. K., Kodukula, S., Fortson, W. M., Patel, K., and Storch, J. (2013) Direct Comparison of Mice Null for Liver- or Intestinal Fatty Acid Binding Proteins Reveals Highly Divergent Phenotypic Responses to High-Fat Feeding. *J. Biol. Chem.* **288**, 30330–30344.

Chapter 2 was previously published in the Journal of Biological Chemistry in 2013. Angela Gajda performed the research and writing with assistance from Yin Xiu Zhou (technician), Sarala Kodukula (technician), Walter Fortson (undergraduate), Khamoshi Patel (undergraduate), and Judith Storch. Reprinting of this article for the dissertation is permitted by the Journal of Biological Chemistry, which maintains ownership of the article content.

Literature Cited

1. Phan, C. T., and Tso, P. (2001) Intestinal lipid absorption and transport. *Front. Biosci.* **6**, D299–319

2. Moe, P. W. (1994) Future directions for energy requirements and food energy values. *J. Nutr.* **124**, 1738S–1742S

3. Center for Health Statistics, N. (2012) *Health, United States, 2012: With Special Feature on Emergency Care*, Hyattsville, MD

4. Mottillo, S., Filion, K. B., Genest, J., Joseph, L., Pilote, L., Poirier, P., Rinfret, S., Schiffrin, E. L., and Eisenberg, M. J. (2010) The metabolic syndrome and cardiovascular risk a systematic review and meta-analysis. *J. Am. Coll. Cardiol.* **56**, 1113–32

5. Isomaa, B., Almgren, P., Tuomi, T., Forsén, B., Lahti, K., Nissén, M., Taskinen, M. R., and Groop, L. (2001) Cardiovascular morbidity and mortality associated with the metabolic syndrome. *Diabetes Care* **24**, 683–9

6. Lakka, H.-M., Laaksonen, D. E., Lakka, T. a, Niskanen, L. K., Kumpusalo, E., Tuomilehto, J., and Salonen, J. T. (2002) The metabolic syndrome and total and cardiovascular disease mortality in middle-aged men. *JAMA* **288**, 2709–16

7. Lagakos, W. S., Gajda, A. M., Agellon, L., Binas, B., Choi, V., Mandap, B., Russnak, T., Zhou, Y. X., and Storch, J. (2011) Different functions of intestinal and liver-type fatty acid-binding proteins in intestine and in whole body energy homeostasis. *Am. J. Physiol. Gastrointest. Liver Physiol.* **300**, G803–14

8. Kennedy, E. T., Bowman, S. A., and Powell, R. (1999) Dietary-fat intake in the US population. *J. Am. Coll. Nutr.* **18**, 207–12

9. Ervin, R. B., Wright, J. D., Wang, C.-Y., and Kennedy-Stephenson, J. (2004) Dietary intake of fats and fatty acids for the United States population: 1999-2000. *Adv. Data*, 1–6

10. Howard, B. V, Van Horn, L., Hsia, J., Manson, J. E., Stefanick, M. L., Wassertheil-Smoller, S., Kuller, L. H., LaCroix, A. Z., Langer, R. D., Lasser, N. L., Lewis, C. E., Limacher, M. C., Margolis, K. L., Mysiw, W. J., Ockene, J. K., Parker, L. M., Perri, M. G., Phillips, L., Prentice, R. L., Robbins, J., Rossouw, J. E., Sarto, G. E., Schatz, I. J., Snetselaar, L. G., Stevens, V. J., Tinker, L. F., Trevisan, M., Vitolins, M. Z., Anderson, G. L., Assaf, A. R., Bassford, T., Beresford, S. A. A., Black, H. R., Brunner, R. L., Brzyski, R. G., Caan, B., Chlebowski, R. T., Gass, M., Granek, I., Greenland, P., Hays, J., Heber, D., Heiss, G., Hendrix, S. L., Hubbell, F. A., Johnson, K. C., and Kotchen, J. M. (2006) Low-fat dietary pattern and risk of cardiovascular disease: the Women's Health Initiative Randomized Controlled Dietary Modification Trial. *JAMA* **295**, 655–66

11. Katan, M. B., Zock, P. L., and Mensink, R. P. (1995) Dietary oils, serum lipoproteins, and coronary heart disease. *Am. J. Clin. Nutr.* **61**, 1368S–1373S

12. Kushi, L. H., Lenart, E. B., and Willett, W. C. (1995) Health implications of Mediterranean diets in light of contemporary knowledge. 2. Meat, wine, fats, and oils. *Am. J. Clin. Nutr.* **61**, 1416S–1427S

13. Burr, G., and Burr, M. (1929) A new deficiency disease produced by the rigid exclusion of fat from the diet. *J. Biol. Chem.* **82**, 345–367

14. Burr, G., Burr, M., and Miller, E. (1932) On the fatty acids essential in nutrition. III. *J. Biol. Chem.* **97**, 1–9

15. Dulloo, A. G., Mensi, N., Seydoux, J., and Girardier, L. (1995) Differential effects of high-fat diets varying in fatty acid composition on the efficiency of lean and fat tissue deposition during weight recovery after low food intake• 1. *Metabolism* **44**, 273–279

16. Tso, Patrick, Crissinger, K. (2006) in *Biochemical, Physiological, Molecular Aspects of Human Nutrition* (Stipanuk, M. H., ed.) Second, pp. 151–167, Elsevier, St. Louis, MO

17. Chiang, J. Y. L. (2013) Bile acid metabolism and signaling. *Compr. Physiol.* **3**, 1191–212

18. Caspary, W. F. (1992) Physiology and pathophysiology of intestinal absorption. *Am. J. Clin. Nutr.* **55**, 299S–308S

19. Tso, P., and Balint, J. A. (1986) Formation and transport of chylomicrons by enterocytes to the lymphatics. *Am. J. Physiol.* **250**, G715–26

20. Radtke, F., and Clevers, H. (2005) Self-renewal and cancer of the gut: two sides of a coin. *Science* **307**, 1904–9

21. Specian, R. D., and Oliver, M. G. (1991) Functional biology of intestinal goblet cells. *Am. J. Physiol.* **260**, C183–93

22. CREAMER, B., Shorter, R. G., and Bamforth, J. (1961) The turnover and shedding of epithelial cells. I. The turnover in the gastro-intestinal tract. *Gut* **2**, 110–8

23. Green, P. H., and Glickman, R. M. (1981) Intestinal lipoprotein metabolism. *J. Lipid Res.* **22**, 1153–73

24. Porter, E. M., Bevins, C. L., Ghosh, D., and Ganz, T. (2002) Cellular and Molecular Life Sciences The multifaceted Paneth cell. **59**, 156–170

25. Cabou, C., and Burcelin, R. (2011) GLP-1, the gut-brain, and brain-periphery axes. *Rev. Diabet. Stud.* **8**, 418–31

26. Pan, X., and Hussain, M. M. (2012) Gut triglyceride production. *Biochim. Biophys. Acta* **1821**, 727–35

27.   Murota, K., and Storch, J. (2005) Uptake of Micellar Long-Chain Fatty Acid and sn-2-Monoacylglycerol into Human Intestinal Caco-2 Cells Exhibits Characteristics of Protein-Mediated Transport. *J. Nutr.* **135**, 1626–1630

28.   Abumrad, N. A., and Davidson, N. O. (2012) Role of the gut in lipid homeostasis. *Physiol. Rev.* **92**, 1061–85

29.   Niot, I., Poirier, H., Tran, T. T. T., and Besnard, P. (2009) Intestinal absorption of long-chain fatty acids: Evidence and uncertainties. *Prog. Lipid Res.* **48**, 101–115

30.   Silverstein, R. L., and Febbraio, M. (2009) CD36, a scavenger receptor involved in immunity, metabolism, angiogenesis, and behavior. *Sci. Signal.* **2**, re3

31.   Siddiqi, S., Saleem, U., Abumrad, N. A., Davidson, N. O., Storch, J., Siddiqi, S. A., and Mansbach, C. M. (2010) A novel multiprotein complex is required to generate the prechylomicron transport vesicle from intestinal ER. *J. Lipid Res.* **51**, 1918–28

32.   Nauli, A. M., Nassir, F., Zheng, S., Yang, Q., Lo, C.-M., Vonlehmden, S. B., Lee, D., Jandacek, R. J., Abumrad, N. A., and Tso, P. (2006) CD36 is important for chylomicron formation and secretion and may mediate cholesterol uptake in the proximal intestine. *Gastroenterology* **131**, 1197–207

33.   Drover, V. a, Nguyen, D. V, Bastie, C. C., Darlington, Y. F., Abumrad, N. a, Pessin, J. E., London, E., Sahoo, D., and Phillips, M. C. (2008) CD36 mediates both cellular uptake of very long chain fatty acids and their intestinal absorption in mice. *J. Biol. Chem.* **283**, 13108–15

34.   Nassir, F., Wilson, B., Han, X., Gross, R. W., and Abumrad, N. a (2007) CD36 is important for fatty acid and cholesterol uptake by the proximal but not distal intestine. *J. Biol. Chem.* **282**, 19493–501

35.   Shim, J., Moulson, C. L., Newberry, E. P., Lin, M.-H., Xie, Y., Kennedy, S. M., Miner, J. H., and Davidson, N. O. (2009) Fatty acid transport protein 4 is dispensable for intestinal lipid absorption in mice. *J. Lipid Res.* **50**, 491–500

36.   Stahl, A., Hirsch, D. J., Gimeno, R. E., Punreddy, S., Ge, P., Watson, N., Patel, S., Kotler, M., Raimondi, A., Tartaglia, L. A., and Lodish, H. F. (1999) Identification of the major intestinal fatty acid transport protein. *Mol. Cell* **4**, 299–308

37.   Turcotte, L. P., Srivastava, A. K., and Chiasson, J. L. (1997) Fasting increases plasma membrane fatty acid-binding protein (FABP(PM)) in red skeletal muscle. *Mol. Cell. Biochem.* **166**, 153–8

38.   Kiens, B., Kristiansen, S., Jensen, P., Richter, E. A., and Turcotte, L. P. (1997) Membrane associated fatty acid binding protein (FABPpm) in human skeletal muscle is increased by endurance training. *Biochem. Biophys. Res. Commun.* **231**, 463–5

39.   Abumrad, N., Coburn, C., and Ibrahimi, a (1999) Membrane proteins implicated in long-chain fatty acid uptake by mammalian cells: CD36, FATP and FABPm. *Biochim. Biophys. Acta* **1441**, 4–13

40.   Ho, S., and Storch, J. (2001) Common mechanisms of monoacylglycerol and fatty acid uptake by human intestinal Caco-2 cells. *Am. J. Physiol.* **281**, C1106–C1117

41.   Murota, K., Matsui, N., Kawada, T., Takahashi, N., and Fushuki, T. (2001) Inhibitory effect of monoacylglycerol on fatty acid uptake into rat intestinal epithelial cells. *Biosci. Biotechnol. Biochem.* **65**, 1441–3

42.   Rockenfeller, P., Ring, J., Muschett, V., Beranek, A., Büttner, S., Carmona-Gutierrez, D., Eisenberg, T., Khoury, C., Rechberger, G., Kohlwein, S. D., Kroemer, G., and Madeo, F. (2010) Fatty acids trigger mitochondrion-dependent necrosis. *Cell Cycle* **9**, 2908–2914

43.   Listenberger, L. L., Ory, D. S., and Schaffer, J. E. (2001) Palmitate-induced apoptosis can occur through a ceramide-independent pathway. *J. Biol. Chem.* **276**, 14890–5

44.   Mashek, D. G., Li, L. O., and Coleman, R. A. (2006) Rat long-chain acyl-CoA synthetase mRNA, protein, and activity vary in tissue distribution and in response to diet. *J. Lipid Res.* **47**, 2004–10

45.   Furuhashi, M., and Hotamisligil, G. S. (2008) Fatty acid-binding proteins: role in metabolic diseases and potential as drug targets. *Nat. Rev. Drug Discov.* **7**, 489–503

46.   Cao, J., Hawkins, E., Brozinick, J., Liu, X., Zhang, H., Burn, P., and Shi, Y. (2004) A predominant role of acyl-CoA:monoacylglycerol acyltransferase-2 in dietary fat absorption implicated by tissue distribution, subcellular localization, and up-regulation by high fat diet. *J. Biol. Chem.* **279**, 18878–86

47.   Niot, I., Poirier, H., Tran, T. T. T., and Besnard, P. (2009) Intestinal absorption of long-chain fatty acids: Evidence and uncertainties. *Prog. Lipid Res.* **48**, 101–115

48.   Trotter, P. J., and Storch, J. (1991) Fatty acid uptake and metabolism in a human intestinal cell line (Caco-2): comparison of apical and basolateral incubation. *J. Lipid Res.* **32**, 293–304

49.   Kayden, H. J., Senior, J. R., and Mattson, F. H. (1967) The monoglyceride pathway of fat absorption in man. *J. Clin. Invest.* **46**, 1695–703

50.   Yen, C.-L. E., Cheong, M.-L., Grueter, C., Zhou, P., Moriwaki, J., Wong, J. S., Hubbard, B., Marmor, S., and Farese, R. V (2009) Deficiency of the intestinal enzyme acyl CoA:monoacylglycerol acyltransferase-2 protects mice from metabolic disorders induced by high-fat feeding. *Nat. Med.* **15**, 442–6

51. Takeuchi, K., and Reue, K. (2009) Biochemistry, physiology, and genetics of GPAT, AGPAT, and lipin enzymes in triglyceride synthesis. *Am. J. Physiol. Endocrinol. Metab.* **296**, E1195–209

52. Kennedy, E. P. (1958) The biosynthesis of phospholipids. *Am. J. Clin. Nutr.* **6**, 216–20

53. Hussain, M. M. (2000) A proposed model for the assembly of chylomicrons. *Atherosclerosis* **148**, 1–15

54. Neeli, I., Siddiqi, S. a, Siddiqi, S., Mahan, J., Lagakos, W. S., Binas, B., Gheyi, T., Storch, J., and Mansbach, C. M. (2007) Liver fatty acid-binding protein initiates budding of pre-chylomicron transport vesicles from intestinal endoplasmic reticulum. *J. Biol. Chem.* **282**, 17974–84

55. O'Driscoll, C. M. (2002) Lipid-based formulations for intestinal lymphatic delivery. *Eur. J. Pharm. Sci.* **15**, 405–15

56. Monsalve, F. A., Pyarasani, R. D., Delgado-Lopez, F., and Moore-Carrasco, R. (2013) Peroxisome proliferator-activated receptor targets for the treatment of metabolic diseases. *Mediators Inflamm.* **2013**, 549627

57. Braissant, O., Foufelle, F., Scotto, C., Dauça, M., and Wahli, W. (1996) Differential expression of peroxisome proliferator-activated receptors (PPARs): tissue distribution of PPAR-alpha, -beta, and -gamma in the adult rat. *Endocrinology* **137**, 354–66

58. Zhu, J., Lee, B., Buhman, K. K., and Cheng, J.-X. (2009) A dynamic, cytoplasmic triacylglycerol pool in enterocytes revealed by ex vivo and in vivo coherent anti-Stokes Raman scattering imaging. *J. Lipid Res.* **50**, 1080–9

59. Obrowsky, S., Chandak, P. G., Patankar, J. V, Povoden, S., Schlager, S., Kershaw, E. E., Bogner-Strauss, J. G., Hoefler, G., Levak-Frank, S., and Kratky, D. (2013) Adipose triglyceride lipase is a TG hydrolase of the small intestine and regulates intestinal PPARα signaling. *J. Lipid Res.* **54**, 425–35

60. Uchida, A., Whitsitt, M. C., Eustaquio, T., Slipchenko, M. N., Leary, J. F., Cheng, J.-X., and Buhman, K. K. (2012) Reduced triglyceride secretion in response to an acute dietary fat challenge in obese compared to lean mice. *Front. Physiol.* **3**, 26

61. Mansbach, C. M., and Dowell, R. F. (1982) Uptake and metabolism of circulating fatty acids by rat intestine. *Am. J. Physiol.* **263**, G927–33.

62. Storch, J., Zhou, Y. X., and Lagakos, W. S. (2008) Metabolism of apical versus basolateral sn-2-monoacylglycerol and fatty acids in rodent small intestine. *J. Lipid Res.* **49**, 1762–9

63. Gangl, A., and Ockner, R. K. (1975) Intestinal metabolism of plasma free fatty acids. Intracellular compartmentation and mechanisms of control. *J. Clin. Invest.* **55**, 803–13

64. Luchoomun, J., and Hussain, M. M. (1999) Assembly and secretion of chylomicrons by differentiated Caco-2 cells. Nascent triglycerides and preformed phospholipids are preferentially used for lipoprotein assembly. *J. Biol. Chem.* **274**, 19565–72

65. Bach, A. C., Ingenbleek, Y., and Frey, A. (1996) The usefulness of dietary medium-chain triglycerides in body weight control: fact or fancy? *J. Lipid Res.* **37**, 708–26

66. Omar, B., Pacini, G., and Ahrén, B. (2012) Differential development of glucose intolerance and pancreatic islet adaptation in multiple diet induced obesity models. *Nutrients* **4**, 1367–81

67. Buettner, R., Parhofer, K. G., Woenckhaus, M., Wrede, C. E., Kunz-Schughart, L. A., Schölmerich, J., and Bollheimer, L. C. (2006) Defining high-fat-diet rat models: metabolic and molecular effects of different fat types. *J. Mol. Endocrinol.* **36**, 485–501

68. Papamandjaris, A. A., MacDougall, D. E., and Jones, P. J. (1998) Medium chain fatty acid metabolism and energy expenditure: obesity treatment implications. *Life Sci.* **62**, 1203–15

69. Porter, C. J. H., Trevaskis, N. L., and Charman, W. N. (2007) Lipids and lipid-based formulations: optimizing the oral delivery of lipophilic drugs. *Nat. Rev. Drug Discov.* **6**, 231–48

70. Piomelli, D. (2013) A fatty gut feeling. *Trends Endocrinol. Metab.* **24**, 332–41

71. Janssen, P., Rotondo, a, Mulé, F., and Tack, J. (2013) Review article: a comparison of glucagon-like peptides 1 and 2. *Aliment. Pharmacol. Ther.* **37**, 18–36

72. Aponte, G. W. (2002) PYY-mediated fatty acid induced intestinal differentiation. *Peptides* **23**, 367–76

73. Halldén, G., and Aponte, G. W. (1997) Evidence for a role of the gut hormone PYY in the regulation of intestinal fatty acid-binding protein transcripts in differentiated subpopulations of intestinal epithelial cell hybrids. *J. Biol. Chem.* **272**, 12591–600

74. Troke, R. C., Tan, T. M., and Bloom, S. R. (2014) The future role of gut hormones in the treatment of obesity. *Ther. Adv. Chronic Dis.* **5**, 4–14

75. Bello, N. T., and Moran, T. H. (2007) What happens in the vagus,...? *Am. J. Physiol. Regul. Integr. Comp. Physiol.* **292**, R2122–3

76. Smith, G. P., Jerome, C., and Norgren, R. (1985) Afferent axons in abdominal vagus mediate satiety effect of cholecystokinin in rats. *Am. J. Physiol.* **249**, R638–41

77. Greenberg, D., and Smith, G. P. (1996) The controls of fat intake. *Psychosom. Med.* **58**, 559–69

78. Hayes, M. R., and Covasa, M. (2005) CCK and 5-HT act synergistically to suppress food intake through simultaneous activation of CCK-1 and 5-HT3 receptors. *Peptides* **26**, 2322–30

79. Feinle-Bisset, C., Patterson, M., Ghatei, M. A., Bloom, S. R., and Horowitz, M. (2005) Fat digestion is required for suppression of ghrelin and stimulation of peptide YY and pancreatic polypeptide secretion by intraduodenal lipid. *Am. J. Physiol. Endocrinol. Metab.* **289**, E948–53

80. Gillum, M. P., Zhang, D., Zhang, X.-M., Erion, D. M., Jamison, R. a, Choi, C., Dong, J., Shanabrough, M., Duenas, H. R., Frederick, D. W., Hsiao, J. J., Horvath, T. L., Lo, C. M., Tso, P., Cline, G. W., and Shulman, G. I. (2008) N-acylphosphatidylethanolamine, a gut-derived circulating factor induced by fat ingestion, inhibits food intake. *Cell* **135**, 813–24

81. Piomelli, D. (2013) More surprises lying ahead. The endocannabinoids keep us guessing. *Neuropharmacology*, 1–7

82. Devane, W. A., Hanus, L., Breuer, A., Pertwee, R. G., Stevenson, L. A., Griffin, G., Gibson, D., Mandelbaum, A., Etinger, A., and Mechoulam, R. (1992) Isolation and structure of a brain constituent that binds to the cannabinoid receptor. *Science* **258**, 1946–9

83. Kaczocha, M., Glaser, S. T., and Deutsch, D. G. (2009) Identification of intracellular carriers for the endocannabinoid anandamide. *Proc. Natl. Acad. Sci. U. S. A.* **106**, 6375–80

84. Kaczocha, M., Vivieca, S., Sun, J., Glaser, S. T., and Deutsch, D. G. (2012) Fatty acid-binding proteins transport N-acylethanolamines to nuclear receptors and are targets of endocannabinoid transport inhibitors. *J. Biol. Chem.* **287**, 3415–24

85. Schwartz, G. J., Fu, J., Astarita, G., Li, X., Gaetani, S., Campolongo, P., Cuomo, V., and Piomelli, D. (2008) The lipid messenger OEA links dietary fat intake to satiety. *Cell Metab.* **8**, 281–8

86. Rodríguez de Fonseca, F., Navarro, M., Gómez, R., Escuredo, L., Nava, F., Fu, J., Murillo-Rodríguez, E., Giuffrida, a, LoVerme, J., Gaetani, S., Kathuria, S., Gall, C., and Piomelli, D. (2001) An anorexic lipid mediator regulated by feeding. *Nature* **414**, 209–12

87. Fu, J., Gaetani, S., Oveisi, F., Lo Verme, J., Serrano, A., Rodríguez De Fonseca, F., Rosengarth, A., Luecke, H., Di Giacomo, B., Tarzia, G., and Piomelli, D. (2003) Oleylethanolamide regulates feeding and body weight through activation of the nuclear receptor PPAR-alpha. *Nature* **425**, 90–3

88. Guijarro, A., Fu, J., Astarita, G., and Piomelli, D. (2010) CD36 gene deletion decreases oleoylethanolamide levels in small intestine of free-feeding mice. *Pharmacol. Res.* **61**, 27–33

89. LoVerme, J., La Rana, G., Russo, R., Calignano, A., and Piomelli, D. (2005) The search for the palmitoylethanolamide receptor. *Life Sci.* **77**, 1685–98

90. Verme, J. Lo, Fu, J., Astarita, G., Rana, G. La, Russo, R., Calignano, A., Piomelli, D., and Verme, L. (2005) The nuclear receptor peroxisome proliferator-activated receptor-alpha mediates the anti-inflammatory actions of palmitoylethanolamide. *Mol. Pharmacol.* **67**, 15–19

91. Skaper, S. D., Facci, L., Fusco, M., Federica, M., Zusso, M., Costa, B., and Giusti, P. (2013) Palmitoylethanolamide , a naturally occurring disease-modifying agent in neuropathic pain.

92. Deutsch, D. G., Ueda, N., and Yamamoto, S. (2002) The fatty acid amide hydrolase (FAAH). *Prostaglandins. Leukot. Essent. Fatty Acids* **66**, 201–10

93. Touriño, C., Oveisi, F., Lockney, J., Piomelli, D., and Maldonado, R. (2010) FAAH deficiency promotes energy storage and enhances the motivation for food. *Int. J. Obes. (Lond).* **34**, 557–68

94. Caprioli, A., Coccurello, R., Rapino, C., Serio, S. Di, Tommaso, M. Di, Vertechy, M., Vacca, V., Battista, N., Pavone, F., and Maccarrone, M. (2012) The Novel Reversible Fatty Acid Amide Hydrolase Inhibitor ST4070 Increases Endocannabinoid Brain Levels and Counteracts Neuropathic Pain in Different Animal Models. **342**, 188–195

95. Keith, J. M., Jones, W. M., Pierce, J. M., Seierstad, M., Palmer, J. a, Webb, M., Karbarz, M. J., Scott, B. P., Wilson, S. J., Luo, L., Wennerholm, M. L., Chang, L., Brown, S. M., Rizzolio, M., Rynberg, R., Chaplan, S. R., and Breitenbucher, J. G. (2014) Heteroarylureas with spirocyclic diamine cores as inhibitors of fatty acid amide hydrolase. *Bioorg. Med. Chem. Lett.* **24**, 737–41

96. DiPatrizio, N. V, Astarita, G., Schwartz, G., Li, X., and Piomelli, D. (2011) Endocannabinoid signal in the gut controls dietary fat intake. *Proc. Natl. Acad. Sci. U. S. A.* **108**, 12904–8

97. Stella, N., Schweitzer, P., and Piomelli, D. (1997) A second endogenous cannabinoid that modulates long-term potentiation. *Nature* **388**, 773–8

98. Sugiura, T., Kodaka, T., Nakane, S., Miyashita, T., Kondo, S., Suhara, Y., Takayama, H., Waku, K., Seki, C., Baba, N., and Ishima, Y. (1999) Evidence that the cannabinoid CB1 receptor is a 2-arachidonoylglycerol receptor. Structure-activity relationship of 2-arachidonoylglycerol, ether-linked analogues, and related compounds. *J. Biol. Chem.* **274**, 2794–801

99. Fowler, C. J. (2012) Monoacylglycerol lipase - a target for drug development? *Br. J. Pharmacol.* **166**, 1568–85

100. Shi, Y., and Cheng, D. (2009) Beyond triglyceride synthesis: the dynamic functional roles of MGAT and DGAT enzymes in energy metabolism. *Am. J. Physiol. Endocrinol. Metab.* **297**, E10–8

101. Cases, S., Stone, S. J., Zhou, P., Yen, E., Tow, B., Lardizabal, K. D., Voelker, T., and Farese, R. V (2001) Cloning of DGAT2, a second mammalian diacylglycerol acyltransferase, and related family members. *J. Biol. Chem.* **276**, 38870–6

102. Cases, S., Smith, S. J., Zheng, Y. W., Myers, H. M., Lear, S. R., Sande, E., Novak, S., Collins, C., Welch, C. B., Lusis, a J., Erickson, S. K., and Farese, R. V (1998) Identification of a gene encoding an acyl CoA:diacylglycerol acyltransferase, a key enzyme in triacylglycerol synthesis. *Proc. Natl. Acad. Sci. U. S. A.* **95**, 13018–23

103. Chen, H. C., Ladha, Z., Smith, S. J., and Farese, R. V (2003) Analysis of energy expenditure at different ambient temperatures in mice lacking DGAT1. *Am. J. Physiol. Endocrinol. Metab.* **284**, E213–8

104. Buhman, K. K., Smith, S. J., Stone, S. J., Repa, J. J., Wong, J. S., Knapp, F. F., Burri, B. J., Hamilton, R. L., Abumrad, N. a, and Farese, R. V (2002) DGAT1 is not essential for intestinal triacylglycerol absorption or chylomicron synthesis. *J. Biol. Chem.* **277**, 25474–9

105. Smith, S. J., Cases, S., Jensen, D. R., Chen, H. C., Sande, E., Tow, B., Sanan, D. A., Raber, J., Eckel, R. H., and Farese, R. V (2000) Obesity resistance and multiple mechanisms of triglyceride synthesis in mice lacking Dgat. *Nat. Genet.* **25**, 87–90

106. Stone, S. J., Myers, H. M., Watkins, S. M., Brown, B. E., Feingold, K. R., Elias, P. M., and Farese, R. V (2004) Lipopenia and skin barrier abnormalities in DGAT2-deficient mice. *J. Biol. Chem.* **279**, 11767–76

107. Taschler, U., Radner, F. P. W., Heier, C., Schreiber, R., Schweiger, M., Schoiswohl, G., Preiss-Landl, K., Jaeger, D., Reiter, B., Koefeler, H. C., Wojciechowski, J., Theussl, C., Penninger, J. M., Lass, A., Haemmerle, G., Zechner, R., and Zimmermann, R. (2011) Monoglyceride lipase deficiency in mice impairs lipolysis and attenuates diet-induced insulin resistance. *J. Biol. Chem.* **286**, 17467–77

108. Chon, S.-H., Douglass, J. D., Zhou, Y. X., Malik, N., Dixon, J. L., Brinker, A., Quadro, L., and Storch, J. (2012) Over-expression of monoacylglycerol lipase (MGL) in small intestine alters endocannabinoid levels and whole body energy balance, resulting in obesity. *PLoS One* **7**, e43962

109. Ockner, R. K., and Manning, J. A. (1974) Fatty acid-binding protein in small intestine. Identification, isolation, and evidence for its role in cellular fatty acid transport. *J. Clin. Invest.* **54**, 326–38

110. Mishkin, S., Stein, L., Gatmaitan, Z., and Arias, I. M. (1972) The binding of fatty acids to cytoplasmic proteins: binding to Z protein in liver and other tissues of the rat. *Biochem. Biophys. Res. Commun.* **47**, 997–1003

111. Storch, J., and Corsico, B. (2008) The emerging functions and mechanisms of mammalian fatty acid-binding proteins. *Annu. Rev. Nutr.* **28**, 73–95

112. Smathers, R. L., and Petersen, D. R. (2011) The human fatty acid-binding protein family: evolutionary divergences and functions. *Hum. Genomics* **5**, 170–91

113. Hertzel, A. V, and Bernlohr, D. A. (2000) The mammalian fatty acid-binding protein multigene family: molecular and genetic insights into function. *Trends Endocrinol. Metab.* **11**, 175–80

114. Haunerland, N. H., and Spener, F. (2004) Fatty acid-binding proteins--insights from genetic manipulations. *Prog. Lipid Res.* **43**, 328–49

115. Coe, N. R., and Bernlohr, D. A. (1998) Physiological properties and functions of intracellular fatty acid-binding proteins. *Biochim. Biophys. Acta* **1391**, 287–306

116. Chmurzyńska, A. (2006) The multigene family of fatty acid-binding proteins (FABPs): function, structure and polymorphism. *J. Appl. Genet.* **47**, 39–48

117. Storch, J., and Thumser, A. E. (2010) Tissue-specific functions in the fatty acid-binding protein family. *J. Biol. Chem.* **285**, 32679–83

118. Córsico, B., Liou, H. L., and Storch, J. (2004) The alpha-helical domain of liver fatty acid binding protein is responsible for the diffusion-mediated transfer of fatty acids to phospholipid membranes. *Biochemistry* **43**, 3600–7

119. Corsico, B., Cistola, D. P., Frieden, C., and Storch, J. (1998) The helical domain of intestinal fatty acid binding protein is critical for collisional transfer of fatty acids to phospholipid membranes. *Proc. Natl. Acad. Sci. U. S. A.* **95**, 12174–8

120. Alpers, D. H., Bass, N. M., Engle, M. J., and DeSchryver-Kecskemeti, K. (2000) Intestinal fatty acid binding protein may favor differential apical fatty acid binding in the intestine. *Biochim. Biophys. Acta* **1483**, 352–62

121. Guilmeau, S., Niot, I., Laigneau, J. P., Devaud, H., Petit, V., Brousse, N., Bouvier, R., Ferkdadji, L., Besmond, C., Aggerbeck, L. P., Bado, a, and Samson-Bouma, M. E. (2007) Decreased expression of Intestinal I- and L-FABP levels in rare human genetic lipid malabsorption syndromes. *Histochem. Cell Biol.* **128**, 115–23

122. Levy, E., Ménard, D., Delvin, E., Montoudis, A., Beaulieu, J.-F., Mailhot, G., Dubé, N., Sinnett, D., Seidman, E., and Bendayan, M. (2009) Localization, function and regulation of the two intestinal fatty acid-binding protein types. *Histochem. Cell Biol.* **132**, 351–67

123. Pelsers, M. M. A. L., Namiot, Z., Kisielewski, W., Namiot, A., Januszkiewicz, M., Hermens, W. T., and Glatz, J. F. C. (2003) Intestinal-type and liver-type fatty acid-binding protein in the intestine. Tissue distribution and clinical utility. *Clin. Biochem.* **36**, 529–35

124. Bass, N. M., Manning, J. A., Ockner, R. K., Gordon, J. I., Seetharam, S., and Alpers, D. H. (1985) Regulation of the biosynthesis of two distinct fatty acid-binding proteins in rat

liver and intestine. Influences of sex difference and of clofibrate. *J. Biol. Chem.* **260**, 1432–6

125. Sacchettini, J. C., Hauft, S. M., Van Camp, S. L., Cistola, D. P., and Gordon, J. I. (1990) Developmental and structural studies of an intracellular lipid binding protein expressed in the ileal epithelium. *J. Biol. Chem.* **265**, 19199–207

126. Fujita, M., Fujii, H., Kanda, T., Sato, E., Hatakeyama, K., and Ono, T. (1995) Molecular cloning, expression, and characterization of a human intestinal 15-kDa protein. *Eur. J. Biochem.* **233**, 406–13

127. Labonté, E. D., Li, Q., Kay, C. M., and Agellon, L. B. (2003) The relative ligand binding preference of the murine ileal lipid binding protein. *Protein Expr. Purif.* **28**, 25–33

128. Gong, Y. Z., Everett, E. T., Schwartz, D. A., Norris, J. S., and Wilson, F. A. (1994) Molecular cloning, tissue distribution, and expression of a 14-kDa bile acid-binding protein from rat ileal cytosol. *Proc. Natl. Acad. Sci. U. S. A.* **91**, 4741–5

129. Zimmerman, A. W., van Moerkerk, H. T., and Veerkamp, J. H. (2001) Ligand specificity and conformational stability of human fatty acid-binding proteins. *Int. J. Biochem. Cell Biol.* **33**, 865–76

130. Ono, T. (2005) Studies of the FABP family: a retrospective. *Mol. Cell. Biochem.* **277**, 1–6

131. Grober, J. (1999) Identification of a bile acid-responsive element in the human ileal bile acid-binding protein gene. Involvement of the Farnesoid X receptor/9-cis-retinoic acid receptor heterodimer. *J. Biol. Chem.* **274**, 29749–29754

132. Hwang, S. T., Urizar, N. L., Moore, D. D., and Henning, S. J. (2002) Bile acids regulate the ontogenic expression of ileal bile acid binding protein in the rat via the farnesoid X receptor. *Gastroenterology* **122**, 1483–1492

133. Praslickova, D., Torchia, E. C., Sugiyama, M. G., Magrane, E. J., Zwicker, B. L., Kolodzieyski, L., and Agellon, L. B. (2012) The ileal lipid binding protein is required for efficient absorption and transport of bile acids in the distal portion of the murine small intestine. *PLoS One* **7**, e50810

134. Agellon, L. B., Toth, M. J., and Thomson, A. B. R. (2002) Intracellular lipid binding proteins of the small intestine. *Mol. Cell. Biochem.* **239**, 79–82

135. Richieri, G. V, Ogata, R. T., Zimmerman, A. W., Veerkamp, J. H., and Kleinfeld, A. M. (2000) Fatty acid binding proteins from different tissues show distinct patterns of fatty acid interactions. *Biochemistry* **39**, 7197–204

136. Richieri, G. V, Ogata, R. T., and Kleinfeld, a M. (1994) Equilibrium constants for the binding of fatty acids with fatty acid-binding proteins from adipocyte, intestine, heart, and liver measured with the fluorescent probe ADIFAB. *J. Biol. Chem.* **269**, 23918–30

137. Wolfrum, C., Borchers, T., Sacchettini, J., and Spener, F. (2000) Binding of fatty acids and peroxisome proliferators to orthologous fatty acid binding proteins from human, murine, and bovine liver. *Biochemistry* **39**, 14363

138. Lagakos, W. S., Guan, X., Ho, S.-Y., Sawicki, L. R., Corsico, B., Kodukula, S., Murota, K., Stark, R. E., and Storch, J. (2013) Liver Fatty Acid-binding Protein Binds Monoacylglycerol in Vitro and in Mouse Liver Cytosol. *J. Biol. Chem.* **288**, 19805–15

139. Storch, J. (1993) Diversity of fatty acid-binding protein structure and function: studies with fluorescent ligands. *Mol. Cell. Biochem.* **123**, 45–53

140. Burrier, R. E., and Brecher, P. (1986) Binding of lysophosphatidylcholine to the rat liver fatty acid binding protein. *Biochim. Biophys. Acta* **879**, 229–39

141. Storch, J., Veerkamp, J. H., and Hsu, K.-T. (2002) Similar mechanisms of fatty acid transfer from human anal rodent fatty acid-binding proteins to membranes: liver, intestine, heart muscle, and adipose tissue FABPs. *Mol. Cell. Biochem.* **239**, 25–33

142. Hsu, K. T., and Storch, J. (1996) Fatty acid transfer from liver and intestinal fatty acid-binding proteins to membranes occurs by different mechanisms. *J. Biol. Chem.* **271**, 13317–23

143. Issemann, I., Prince, R., Tugwood, J., and Green, S. (1992) A role for fatty acids and liver fatty acid binding protein in peroxisome proliferation? *Biochem. Soc. Trans.* **20**, 824–7

144. Nakamura, M. T., Yudell, B. E., and Loor, J. J. (2014) Regulation of energy metabolism by long-chain fatty acids. *Prog. Lipid Res.* **53**, 124–44

145. Mallordy, A., Poirier, H., Besnard, P., Niot, I., and Carlier, H. (1995) Evidence for transcriptional induction of the liver fatty-acid-binding-protein gene by bezafibrate in the small intestine. *Eur. J. Biochem.* **227**, 801–7

146. Mallordy, A., Besnard, P., and Carlier, H. (1993) Research of an in vitro model to study the expression of fatty acid-binding proteins in the small intestine. *Mol. Cell. Biochem.* **123**, 85–92

147. Besnard, P., Mallordy, a, and Carlier, H. (1993) Transcriptional induction of the fatty acid binding protein gene in mouse liver by bezafibrate. *FEBS Lett.* **327**, 219–23

148. Hostetler, H. A., McIntosh, A. L., Atshaves, B. P., Storey, S. M., Payne, H. R., Kier, A. B., and Schroeder, F. (2009) L-FABP directly interacts with PPARalpha in cultured primary hepatocytes. *J. Lipid Res.* **50**, 1663–75

149. McIntosh, A. L., Atshaves, B. P., Hostetler, H. a, Huang, H., Davis, J., Lyuksyutova, O. I., Landrock, D., Kier, A. B., and Schroeder, F. (2009) Liver type fatty acid binding protein (L-FABP) gene ablation reduces nuclear ligand distribution and peroxisome proliferator-

activated receptor-alpha activity in cultured primary hepatocytes. *Arch. Biochem. Biophys.* **485**, 160–73

150. McIntosh, A. L., Petrescu, A. D., Hostetler, H. A., Kier, A. B., and Schroeder, F. (2013) Liver-type fatty acid binding protein interacts with hepatocyte nuclear factor 4α. *FEBS Lett.* **587**, 3787–91

151. Babeu, J.-P., and Boudreau, F. (2014) Hepatocyte nuclear factor 4-alpha involvement in liver and intestinal inflammatory networks. *World J. Gastroenterol.* **20**, 22–30

152. Erol, E., Kumar, L. S., Cline, G. W., Shulman, G. I., Kelly, D. P., and Binas, B. (2004) Liver fatty acid-binding protein is required for high rates of hepatic fatty acid oxidation but not for the action of PPAR-alpha in fasting mice. *FASEB J.* **18**, 347–9

153. Poirier, H., Niot, I., Degrace, P., Monnot, M. C., Bernard, A., Besnard, P., and Monnot, C. (1997) Fatty acid regulation of fatty acid-binding protein expression in the small intestine . *Am. J. Physiol. - Gastrointest. Liver Physiol.* **273** , G289–G295

154. Malewiak, M., Bass, N., Griglio, S., and Ockner, R. K. (1988) Influence of genetic obesity and of fat-feeding on hepatic FABP concentration and activity. *Int. J. Obes.* **12**, 543–546

155. Petit, V., Arnould, L., Martin, P., Monnot, M.-C., Pineau, T., Besnard, P., and Niot, I. (2007) Chronic high-fat diet affects intestinal fat absorption and postprandial triglyceride levels in the mouse. *J. Lipid Res.* **48**, 278–87

156. Ockner, R. K., Burnett, D. A., Lysenko, N., and Manning, J. A. (1979) Sex differences in long chain fatty acid utilization and fatty acid binding protein concentration in rat liver. *J. Clin. Invest.* **64**, 172–81

157. Robitaille, J., Brouillette, C., Lemieux, S., Pérusse, L., Gaudet, D., and Vohl, M. C. (2004) Plasma concentrations of apolipoprotein B are modulated by a gene--diet interaction effect between the LFABP T94A polymorphism and dietary fat intake in French-Canadian men. *Mol. Genet. Metab.* **82**, 296–303

158. Brouillette, C., Bossé, Y., Pérusse, L., Gaudet, D., and Vohl, M.-C. (2004) Effect of liver fatty acid binding protein (FABP) T94A missense mutation on plasma lipoprotein responsiveness to treatment with fenofibrate. *J. Hum. Genet.* **49**, 424–32

159. Fisher, E., Weikert, C., Klapper, M., Lindner, I., Möhlig, M., Spranger, J., Boeing, H., Schrezenmeir, J., and Döring, F. (2007) L-FABP T94A is associated with fasting triglycerides and LDL-cholesterol in women. *Mol. Genet. Metab.* **91**, 278–84

160. Mansego, M. L., Martínez, F., Martínez-Larrad, M. T., Zabena, C., Rojo, G., Morcillo, S., Soriguer, F., Martín-Escudero, J. C., Serrano-Ríos, M., Redon, J., and Chaves, F. J. (2012) Common variants of the liver fatty acid binding protein gene influence the risk of type 2 diabetes and insulin resistance in Spanish population. *PLoS One* **7**, e31853

161. Fisher, E., Weikert, C., Klapper, M., Lindner, I., Möhlig, M., Spranger, J., Boeing, H., Schrezenmeir, J., and Döring, F. (2007) L-FABP T94A is associated with fasting triglycerides and LDL-cholesterol in women. *Mol. Genet. Metab.* **91**, 278–84

162. Gao, N., Qu, X., Yan, J., Huang, Q., Yuan, H.-Y., and Ouyang, D.-S. (2010) L-FABP T94A decreased fatty acid uptake and altered hepatic triglyceride and cholesterol accumulation in Chang liver cells stably transfected with L-FABP. *Mol. Cell. Biochem.* **345**, 207–14

163. Martin, G. G., McIntosh, A. L., Huang, H., Gupta, S., Atshaves, B. P., Landrock, K., Landrock, D., Kier, A. B., and Schroeder, F. (2013) Human liver fatty acid binding protein (L-FABP) T94A variant alters structure, stability, and interaction with fibrates. *Biochemistry*

164. He, Y., Yang, X., Wang, H., Estephan, R., Francis, F., Kodukula, S., Storch, J., and Stark, R. E. (2007) Solution-state molecular structure of apo and oleate-liganded liver fatty acid-binding protein. *Biochemistry* **46**, 12543–56

165. Lowe, J. B., Sacchettini, J. C., Laposata, M., McQuillan, J. J., and Gordon, J. I. (1987) Expression of rat intestinal fatty acid-binding protein in Escherichia coli. Purification and comparison of ligand binding characteristics with that of Escherichia coli-derived rat liver fatty acid-binding protein. *J. Biol. Chem.* **262**, 5931–7

166. Falomir-Lockhart, L. J., Franchini, G. R., Guerbi, M. X., Storch, J., and Córsico, B. (2011) Interaction of enterocyte FABPs with phospholipid membranes: clues for specific physiological roles. *Biochim. Biophys. Acta* **1811**, 452–9

167. Franchini, G. R., Storch, J., and Corsico, B. (2008) The integrity of the alpha-helical domain of intestinal fatty acid binding protein is essential for the collision-mediated transfer of fatty acids to phospholipid membranes. *Biochim. Biophys. Acta* **1781**, 192–9

168. De Gerónimo, E., Rodriguez Sawicki, L., Bottasso Arias, N., Franchini, G. R., Zamarreño, F., Costabel, M. D., Córsico, B., and Falomir Lockhart, L. J. (2013) IFABP portal region insertion during membrane interaction depends on phospholipid composition. *Biochim. Biophys. Acta* **1841**, 141–150

169. Gajda, A. M., Zhou, Y. X., Agellon, L. B., Fried, S. K., Kodukula, S., Fortson, W. M., Patel, K., and Storch, J. (2013) Direct Comparison of Mice Null for Liver- or Intestinal Fatty Acid Binding Proteins Reveals Highly Divergent Phenotypic Responses to High-Fat Feeding. *J. Biol. Chem.* **288**, 30330–30344

170. Baier, L. J., Sacchettini, J. C., Knowler, W. C., Eads, J., Paolisso, G., Tataranni, P. a, Mochizuki, H., Bennett, P. H., Bogardus, C., and Prochazka, M. (1995) An amino acid substitution in the human intestinal fatty acid binding protein is associated with increased fatty acid binding, increased fat oxidation, and insulin resistance. *J. Clin. Invest.* **95**, 1281–7

171. Pratley, R. E., Baier, L., Pan, D. A., Salbe, A. D., Storlien, L., Ravussin, E., and Bogardus, C. (2000) Effects of an Ala54Thr polymorphism in the intestinal fatty acid-binding protein on responses to dietary fat in humans. *J. Lipid Res.* **41**, 2002–8

172. Georgopoulos, A., Aras, O., and Tsai, M. Y. (2000) Codon-54 polymorphism of the fatty acid-binding protein 2 gene is associated with elevation of fasting and postprandial triglyceride in type 2 diabetes. *J. Clin. Endocrinol. Metab.* **85**, 3155–60

173. Agren, J. J., Valve, R., Vidgren, H., Laakso, M., and Uusitupa, M. (1998) Postprandial lipemic response is modified by the polymorphism at codon 54 of the fatty acid-binding protein 2 gene. *Arterioscler. Thromb. Vasc. Biol.* **18**, 1606–10

174. Yamada, K., Yuan, X., Ishiyama, S., Koyama, K., Ichikawa, F., Koyanagi, a, Koyama, W., and Nonaka, K. (1997) Association between Ala54Thr substitution of the fatty acid-binding protein 2 gene with insulin resistance and intra-abdominal fat thickness in Japanese men. *Diabetologia* **40**, 706–10

175. Baier, L. J., Bogardus, C., and Sacchettini, J. C. (1996) A polymorphism in the human intestinal fatty acid binding protein alters fatty acid transport across Caco-2 cells. *J. Biol. Chem.* **271**, 10892–6

176. Levy, E., Ménard, D., Delvin, E., Stan, S., Mitchell, G., Lambert, M., Ziv, E., Feoli-Fonseca, J. C., and Seidman, E. (2001) The polymorphism at codon 54 of the FABP2 gene increases fat absorption in human intestinal explants. *J. Biol. Chem.* **276**, 39679–84

177. Storch, J., and McDermott, L. (2009) Structural and functional analysis of fatty acid-binding proteins. *J. Lipid Res.* **50**, S126

178. Prows, D., Murphy, E., and Schroeder, F. (1995) Intestinal and liver fatty acid binding proteins differentially affect fatty acid uptake and esterification in L-cells. *Lipids* **30**, 907–910

179. Newberry, E. P., Xie, Y., Kennedy, S., Han, X., Buhman, K. K., Luo, J., Gross, R. W., and Davidson, N. O. (2003) Decreased hepatic triglyceride accumulation and altered fatty acid uptake in mice with deletion of the liver fatty acid-binding protein gene. *J. Biol. Chem.* **278**, 51664–72

180. Martin, G. G., Danneberg, H., Kumar, L. S., Atshaves, B. P., Erol, E., Bader, M., Schroeder, F., and Binas, B. (2003) Decreased liver fatty acid binding capacity and altered liver lipid distribution in mice lacking the liver fatty acid-binding protein gene. *J. Biol. Chem.* **278**, 21429–38

181. Newberry, E. P., Xie, Y., Kennedy, S. M., Luo, J., and Davidson, N. O. (2006) Protection against Western diet-induced obesity and hepatic steatosis in liver fatty acid-binding protein knockout mice. *Hepatology* **44**, 1191–205

182. Atshaves, B. P., McIntosh, A. L., Storey, S. M., Landrock, K. K., Kier, A. B., and Schroeder, F. (2010) High dietary fat exacerbates weight gain and obesity in female liver fatty acid binding protein gene-ablated mice. *Lipids* **45**, 97–110

183. Martin, G. G., Atshaves, B. P., McIntosh, A. L., Mackie, J. T., Kier, A. B., and Schroeder, F. (2008) Liver fatty acid-binding protein gene-ablated female mice exhibit increased age-dependent obesity. *J. Nutr.* **138**, 1859–65

184. Martin, G. G., Atshaves, B. P., McIntosh, A. L., Payne, H. R., Mackie, J. T., Kier, A. B., and Schroeder, F. (2009) Liver fatty acid binding protein gene ablation enhances age-dependent weight gain in male mice. *Mol. Cell. Biochem.* **324**, 101–15

185. McIntosh, A. L., Atshaves, B. P., Landrock, D., Landrock, K. K., Martin, G. G., Storey, S. M., Kier, A. B., and Schroeder, F. (2013) Liver fatty acid binding protein gene-ablation exacerbates weight gain in high-fat fed female mice. *Lipids* **48**, 435–48

186. Newberry, E. P., Kennedy, S. M., Xie, Y., Luo, J., and Davidson, N. O. (2009) Diet-induced alterations in intestinal and extrahepatic lipid metabolism in liver fatty acid binding protein knockout mice. *Mol. Cell. Biochem.* **326**, 79–86

187. Newberry, E. P., Kennedy, S. M., Xie, Y., Sternard, B. T., Luo, J., and Davidson, N. O. (2008) Diet-induced obesity and hepatic steatosis in L-Fabp / mice is abrogated with SF, but not PUFA, feeding and attenuated after cholesterol supplementation. *Am. J. Physiol. Gastrointest. Liver Physiol.* **294**, G307–14

188. Newberry, E. P., and Davidson, N. O. (2009) Liver Fatty Acid Binding Protein (L-FABP) as a Target for the Prevention of High Fat Diet Induced Obesity and Hepatic Steatosis. *Immunol. Endocr. Metab. Agents - Med. Chem. (Formerly Curr. Med. Chem. - Immunol. Endocr. Metab. Agents)* **9**, 30–37

189. Chen, A., Tang, Y., Davis, V., Hsu, F.-F., Kennedy, S. M., Song, H., Turk, J., Brunt, E. M., Newberry, E. P., and Davidson, N. O. (2013) Liver fatty acid binding protein (L-Fabp) modulates murine stellate cell activation and diet-induced nonalcoholic fatty liver disease. *Hepatology* **57**, 2202–12

190. Vassileva, G., Huwyler, L., Poirier, K., Agellon, L. B., and Toth, M. J. (2000) The intestinal fatty acid binding protein is not essential for dietary fat absorption in mice. *FASEB J.* **14**, 2040–6

191. Agellon, L. B., Drozdowski, L., Li, L., Iordache, C., Luong, L., Clandinin, M. T., Uwiera, R. R. E., Toth, M. J., and Thomson, A. B. R. (2007) Loss of intestinal fatty acid binding protein increases the susceptibility of male mice to high fat diet-induced fatty liver. *Biochim. Biophys. Acta* **1771**, 1283–8

192. Ockner, R. K., Manning, J. A., Poppenhausen, R. B., and Ho, W. K. (1972) A binding protein for fatty acids in cytosol of intestinal mucosa, liver, myocardium, and other tissues. *Science (80-.).* **177**, 56–8

193. Gordon, J. I., Elshourbagy, N., Lowe, J. B., Liao, W. S., Alpers, D. H., and Taylor, J. M. (1985) Tissue specific expression and developmental regulation of two genes coding for rat fatty acid binding proteins. *J. Biol. Chem.* **260**, 1995–8

194. Murphy, E. J., Prows, D. R., Jefferson, J. R., and Schroeder, F. (1996) Liver fatty acid-binding protein expression in transfected fibroblasts stimulates fatty acid uptake and metabolism. *Biochim. Biophys. Acta (BBA)-Lipids Lipid Metab.* **1301**, 191–198

195. Newberry, E. P., Kennedy, S. M., Xie, Y., Luo, J., Stanley, S. E., Semenkovich, C. F., Crooke, R. M., Graham, M. J., and Davidson, N. O. (2008) Altered hepatic triglyceride content after partial hepatectomy without impaired liver regeneration in multiple murine genetic models. *Hepatology* **48**, 1097–105

196. Newberry, E. P., Kennedy, S. M., Xie, Y., Luo, J., Crooke, R. M., Graham, M. J., Fu, J., Piomelli, D., and Davidson, N. O. (2012) Decreased body weight and hepatic steatosis with altered fatty acid ethanolamide metabolism in aged L-Fabp -/- mice. *J. Lipid Res.* **53**, 744–54

197. Lusk, G. (1928) *The elements of science of nutrition.*, 4th Ed., Saunders, Philadelphia

198. McLean, J., and Tobin, C. (1987) *Animal and human calorimetry*, Cambridge Univ Press, New York

199. Tschöp, M. H., Speakman, J. R., Arch, J. R. S., Auwerx, J., Brüning, J. C., Chan, L., Eckel, R. H., Farese, R. V, Galgani, J. E., Hambly, C., Herman, M. A., Horvath, T. L., Kahn, B. B., Kozma, S. C., Maratos-Flier, E., Müller, T. D., Münzberg, H., Pfluger, P. T., Plum, L., Reitman, M. L., Rahmouni, K., Shulman, G. I., Thomas, G., Kahn, C. R., and Ravussin, E. (2012) A guide to analysis of mouse energy metabolism. *Nat. Methods* **9**, 57–63

200. Bradford, M. M. (1976) A rapid and sensitive method for the quantitation of microgram quantities of protein utilizing the principle of protein-dye binding. *Anal. Biochem.* **72**, 248–54

201. Folch, J., Lees, M., and Sloane-Stanley, G. (1957) A simple method for the isolation and purification of total lipides from animal tissues. *J. Biol. Chem.* **226**, 497–509

202. Nishiumi, S., Bessyo, H., Kubo, M., Aoki, Y., Tanaka, A., Yoshida, K., and Ashida, H. (2010) Green and black tea suppress hyperglycemia and insulin resistance by retaining the expression of glucose transporter 4 in muscle of high-fat diet-fed C57BL/6J mice. *J. Agric. Food Chem.* **58**, 12916–23

203. Matthews, D. R., Hosker, J. P., Rudenski, A. S., Naylor, B. A., Treacher, D. F., and Turner, R. C. (1985) Homeostasis model assessment: insulin resistance and beta-cell function from fasting plasma glucose and insulin concentrations in man. *Diabetologia* **28**, 412–9

204. Chon, S.-H., Zhou, Y. X., Dixon, J. L., and Storch, J. (2007) Intestinal monoacylglycerol metabolism: developmental and nutritional regulation of monoacylglycerol lipase and monoacylglycerol acyltransferase. *J. Biol. Chem.* **282**, 33346–57

205. Storch, J., and Herr, F. M. (2001) in *Nutrient-Gene Interactions in Health and Disease* (Moustaid-Moussa, N., and Berdanier, C. D., eds.) pp. 101–130, CRC Press, Boca Raton

206. Atshaves, B. P., McIntosh, A. M., Lyuksyutova, O. I., Zipfel, W., Webb, W. W., and Schroeder, F. (2004) Liver fatty acid-binding protein gene ablation inhibits branched-chain fatty acid metabolism in cultured primary hepatocytes. *J. Biol. Chem.* **279**, 30954–65

207. Xie, Y., Newberry, E. P., Kennedy, S. M., Luo, J., and Davidson, N. O. (2009) Increased susceptibility to diet-induced gallstones in liver fatty acid binding protein knockout mice. *J. Lipid Res.* **50**, 977–87

208. Stubbins, R. E., Holcomb, V. B., Hong, J., and Núñez, N. P. (2012) Estrogen modulates abdominal adiposity and protects female mice from obesity and impaired glucose tolerance. *Eur. J. Nutr.* **51**, 861–70

209. Stubbins, R. E., Najjar, K., Holcomb, V. B., Hong, J., and Núñez, N. P. (2012) Oestrogen alters adipocyte biology and protects female mice from adipocyte inflammation and insulin resistance. *Diabetes. Obes. Metab.* **14**, 58–66

210. Atshaves, B. P., Martin, G. G., Hostetler, H. A., McIntosh, A. L., Kier, A. B., and Schroeder, F. (2010) Liver fatty acid-binding protein and obesity. *J. Nutr. Biochem.* **21**, 1015–32

211. Kahn, C. R., Bezy, O., Usar, S., Griffin, N. W., and Gordon, J. I. in *Keystone Symposia: Diabetes-New Insights into Mechanisms of Disease and its Treatment* p. 42, Keystone Symposia, Keystone, CO

212. Agellon, L. B., Li, L., Luong, L., and Uwiera, R. R. E. (2006) Adaptations to the loss of intestinal fatty acid binding protein in mice. *Mol. Cell. Biochem.* **284**, 159–66

213. Sugiyama, M. G., Hobson, L., Agellon, A. B., and Agellon, L. B. (2012) Visualization of sex-dimorphic changes in the intestinal transcriptome of Fabp2 gene-ablated mice. *J. Nutrigenet. Nutrigenomics* **5**, 45–55

214. Krempler, F., Hell, E., Winkler, C., Breban, D., and Patsch, W. (1998) Plasma Leptin Levels : Interaction of Obesity With a Common Variant of Insulin Receptor Substrate-1. *Arterioscler. Thromb. Vasc. Biol.* **18**, 1686–1690

215. Considine, R. V, Sinha, M. K., Heiman, M. L., Kriauciunas, a, Stephens, T. W., Nyce, M. R., Ohannesian, J. P., Marco, C. C., McKee, L. J., and Bauer, T. L. (1996) Serum immunoreactive-leptin concentrations in normal-weight and obese humans. *N. Engl. J. Med.* **334**, 292–5

216. Van Heek, M., Compton, D. S., France, C. F., Tedesco, R. P., Fawzi, a B., Graziano, M. P., Sybertz, E. J., Strader, C. D., and Davis, H. R. (1997) Diet-induced obese mice develop peripheral, but not central, resistance to leptin. *J. Clin. Invest.* **99**, 385–90

217. Douglass, J. D., Malik, N., Chon, S.-H., Wells, K., Zhou, Y. X., Choi, A. S., Joseph, L. B., and Storch, J. (2012) Intestinal mucosal triacylglycerol accumulation secondary to decreased lipid secretion in obese and high fat fed mice. *Front. Physiol.* **3**, 25

218. Lambert, D. M., and Fowler, C. J. (2005) The endocannabinoid system: drug targets, lead compounds, and potential therapeutic applications. *J. Med. Chem.* **48**, 5059–87

219. Storr, M. A., and Sharkey, K. A. (2007) The endocannabinoid system and gut-brain signalling. *Curr. Opin. Pharmacol.* **7**, 575–82

220. Di Marzo, V., and Matias, I. (2005) Endocannabinoid control of food intake and energy balance. *Nat. Neurosci.* **8**, 585–9

221. Burdyga, G., Lal, S., Varro, A., Dimaline, R., Thompson, D. G., and Dockray, G. J. (2004) Expression of cannabinoid CB1 receptors by vagal afferent neurons is inhibited by cholecystokinin. *J. Neurosci.* **24**, 2708–15

222. Izzo, A. A., Piscitelli, F., Capasso, R., Aviello, G., Romano, B., Borrelli, F., Petrosino, S., and Di Marzo, V. (2009) Peripheral endocannabinoid dysregulation in obesity: relation to intestinal motility and energy processing induced by food deprivation and re-feeding. *Br. J. Pharmacol.* **158**, 451–61

223. DiPatrizio, N. V, Joslin, A., Jung, K.-M., and Piomelli, D. (2013) Endocannabinoid signaling in the gut mediates preference for dietary unsaturated fats. *FASEB J.* **27**, 2513–20

224. Leamy, L. J., Kelly, S. A., Hua, K., and Pomp, D. (2012) Exercise and diet affect quantitative trait loci for body weight and composition traits in an advanced intercross population of mice. *Physiol. Genomics* **44**, 1141–53

225. Primeau, V., Coderre, L., Karelis, a D., Brochu, M., Lavoie, M.-E., Messier, V., Sladek, R., and Rabasa-Lhoret, R. (2011) Characterizing the profile of obese patients who are metabolically healthy. *Int. J. Obes. (Lond).* **35**, 971–81

226. Dill, M. J., Shaw, J., Cramer, J., and Sindelar, D. K. (2013) 5-HT1A receptor antagonists reduce food intake and body weight by reducing total meals with no conditioned taste aversion. *Pharmacol. Biochem. Behav.* **112**, 1–8

227. Shaughnessy, S., Smith, E. R., Kodukula, S., Storch, J., and Fried, S. K. (2000) Adipocyte metabolism in adipocyte fatty acid binding protein knockout mice (aP2-/-) after short-term high-fat feeding: functional compensation by the keratinocyte [correction of keritinocyte] fatty acid binding protein. *Diabetes* **49**, 904–11

228. Maeda, K., Cao, H., Kono, K., Gorgun, C. Z., Furuhashi, M., Uysal, K. T., Cao, Q., Atsumi, G., Malone, H., Krishnan, B., Minokoshi, Y., Kahn, B. B., Parker, R. a, and Hotamisligil, G. S. (2005) Adipocyte/macrophage fatty acid binding proteins control integrated metabolic responses in obesity and diabetes. *Cell Metab.* **1**, 107–19

229. Bass, N. (1990) Fatty acid-protein expression in the liver: its regulation and relationship to the zonation of fatty acid metabolism. *Mol. Cell. Biochem.* **98**, 167–176

230. Sweetser, D. A., Birkenmeier, E. H., Hoppe, P. C., McKeel, D. W., and Gordon, J. I. (1988) Mechanisms underlying generation of gradients in gene expression within the intestine: an analysis using transgenic mice containing fatty acid binding protein-human growth hormone fusion genes. *Genes Dev.* **2**, 1318–32

231. Kazantzis, M., and Stahl, A. (2012) Fatty acid transport proteins, implications in physiology and disease. *Biochim. Biophys. Acta* **1821**, 852–7

232. Kohsaka, A., Laposky, A. D., Ramsey, K. M., Estrada, C., Joshu, C., Kobayashi, Y., Turek, F. W., and Bass, J. (2007) High-fat diet disrupts behavioral and molecular circadian rhythms in mice. *Cell Metab.* **6**, 414–21

233. Pan, X., and Hussain, M. M. (2009) Clock is important for food and circadian regulation of macronutrient absorption in mice. *J. Lipid Res.* **50**, 1800–13

234. Oishi, K., Shirai, H., and Ishida, N. (2005) CLOCK is involved in the circadian transactivation of peroxisome-proliferator-activated receptor α (PPAR α) in mice. **581**, 575–581

235. Chen, L., and Yang, G. (2014) PPARs Integrate the Mammalian Clock and Energy Metabolism. *PPAR Res.* **2014**, 1–6

236. Glatz, J. F., Baerwaldt, C. C., Veerkamp, J. H., and Kempen, H. J. (1984) Diurnal variation of cytosolic fatty acid-binding protein content and of palmitate oxidation in rat liver and heart. *J. Biol. Chem.* **259**, 4295–300

237. Masuda, D., Hirano, K., Oku, H., Sandoval, J. C., Kawase, R., Yuasa-Kawase, M., Yamashita, Y., Takada, M., Tsubakio-Yamamoto, K., Tochino, Y., Koseki, M., Matsuura, F., Nishida, M., Kawamoto, T., Ishigami, M., Hori, M., Shimomura, I., and Yamashita, S. (2009) Chylomicron remnants are increased in the postprandial state in CD36 deficiency. *J. Lipid Res.* **50**, 999–1011

238. Ho, S.-Y., Delgado, L., and Storch, J. (2002) Monoacylglycerol metabolism in human intestinal Caco-2 cells: evidence for metabolic compartmentation and hydrolysis. *J. Biol. Chem.* **277**, 1816–23

239. Hubbell, T., Behnke, W. D., Woodford, J. K., and Schroeder, F. (1994) Recombinant liver fatty acid binding protein interacts with fatty acyl-coenzyme A. *Biochemistry* **33**, 3327–34

240. Hostetler, H. A., Balanarasimha, M., Huang, H., Kelzer, M. S., Kaliappan, A., Kier, A. B., and Schroeder, F. (2010) Glucose regulates fatty acid binding protein interaction with lipids and peroxisome proliferator-activated receptor α. *J. Lipid Res.* **51**, 3103–16

241. Huang, H., Starodub, O., McIntosh, A., Atshaves, B. P., Woldegiorgis, G., Kier, A. B., and Schroeder, F. (2004) Liver fatty acid-binding protein colocalizes with peroxisome proliferator activated receptor alpha and enhances ligand distribution to nuclei of living cells. *Biochemistry* **43**, 2484–500

242. Petrescu, A. D., Huang, H., Martin, G. G., McIntosh, A. L., Storey, S. M., Landrock, D., Kier, A. B., and Schroeder, F. (2012) Impact of L-FABP and Glucose on Polyunsaturated Fatty Acid Induction of PPARα Regulated β-oxidative Enzymes. *Am. J. Physiol. Gastrointest. Liver Physiol.*

243. Desvergne, B., and Wahli, W. (1999) Peroxisome proliferator-activated receptors: nuclear control of metabolism. *Endocr. Rev.* **20**, 649–88

244. Karimian Azari, E., Leitner, C., Jaggi, T., Langhans, W., and Mansouri, A. (2013) Possible role of intestinal fatty acid oxidation in the eating-inhibitory effect of the PPAR-α agonist Wy-14643 in high-fat diet fed rats. *PLoS One* **8**, e74869

245. Oishi, K., Shirai, H., and Ishida, N. (2005) CLOCK is involved in the circadian transactivation of peroxisome-proliferator-activated receptor α (PPAR α) in mice. **581**, 575–581

246. Hotamisligil, G. S., Johnson, R. S., Distel, R. J., Ellis, R., Papaioannou, V. E., and Spiegelman, B. M. (1996) Uncoupling of obesity from insulin resistance through a targeted mutation in aP2, the adipocyte fatty acid binding protein. *Science* **274**, 1377–9

247. Furuhashi, M., Tuncman, G., Görgün, C. Z., Makowski, L., Atsumi, G., Vaillancourt, E., Kono, K., Babaev, V. R., Fazio, S., Linton, M. F., Sulsky, R., Robl, J. A., Parker, R. A., and Hotamisligil, G. S. (2007) Treatment of diabetes and atherosclerosis by inhibiting fatty-acid-binding protein aP2. *Nature* **447**, 959–65

248. Fu, Y., Luo, N., Lopes-Virella, M. F., and Garvey, W. T. (2002) The adipocyte lipid binding protein (ALBP/aP2) gene facilitates foam cell formation in human THP-1 macrophages. *Atherosclerosis* **165**, 259–69

249. Makowski, L., Boord, J. B., Maeda, K., Babaev, V. R., Uysal, K. T., Morgan, M. A., Parker, R. A., Suttles, J., Fazio, S., Hotamisligil, G. S., and Linton, M. F. (2001) Lack of macrophage fatty-acid-binding protein aP2 protects mice deficient in apolipoprotein E against atherosclerosis. *Nat. Med.* **7**, 699–705

250. Layne, M. D., Patel, A., Chen, Y. H., Rebel, V. I., Carvajal, I. M., Pellacani, A., Ith, B., Zhao, D., Schreiber, B. M., Yet, S. F., Lee, M. E., Storch, J., and Perrella, M. A. (2001) Role of macrophage-expressed adipocyte fatty acid binding protein in the development of accelerated atherosclerosis in hypercholesterolemic mice. *FASEB J.* **15**, 2733–5

251. Maeda, K., Uysal, K. T., Makowski, L., Görgün, C. Z., Atsumi, G., Parker, R. A., Brüning, J., Hertzel, A. V., Bernlohr, D. a, and Hotamisligil, G. S. (2003) Role of the fatty acid binding protein mal1 in obesity and insulin resistance. *Diabetes* **52**, 300–7

252. Cao, H., Maeda, K., Gorgun, C. Z., Kim, H.-J., Park, S.-Y., Shulman, G. I., Kim, J. K., and Hotamisligil, G. S. (2006) Regulation of metabolic responses by adipocyte/macrophage Fatty Acid-binding proteins in leptin-deficient mice. *Diabetes* **55**, 1915–22

253. Tan, N., Shaw, N. S., Vinckenbosch, N., Liu, P., Yasmin, R., Desvergne, B., and Wahli, W. (2002) Selective Cooperation between Fatty Acid Binding Proteins and Peroxisome Proliferator-Activated Receptors in Regulating Transcription Selective Cooperation between Fatty Acid Binding Proteins and Peroxisome Proliferator-Activated Receptors in Regulating T.

254. Heck, A. M., Yanovski, J. A., and Calis, K. A. (2000) Orlistat, a new lipase inhibitor for the management of obesity. *Pharmacotherapy* **20**, 270–9

255. Ahnen, D. J., Guerciolini, R., Hauptman, J., Blotner, S., Woods, C. J., and Wargovich, M. J. (2007) Effect of orlistat on fecal fat, fecal biliary acids, and colonic cell proliferation in obese subjects. *Clin. Gastroenterol. Hepatol.* **5**, 1291–9

256. Brooks, G. A., and Mercier, J. (1994) Balance of carbohydrate and lipid utilization during exercise: the "crossover" concept. *J. Appl. Physiol.* **76**, 2253–61

257. Liou, J., Tuazon, M. A., Burdzy, A., and Henderson, G. C. (2013) Moderate compared to low dietary intake of trans-fatty acids impairs strength of old and aerobic capacity of young SAMP8 mice in both sexes. *Lipids* **48**, 1135–43

258. Rosenkilde, M., Nordby, P., Nielsen, L. B., Stallknecht, B. M., and Helge, J. W. (2010) Fat oxidation at rest predicts peak fat oxidation during exercise and metabolic phenotype in overweight men. *Int. J. Obes. (Lond).* **34**, 871–7

259. Stringer, W., Wasserman, K., and Casaburi, R. (1995) The VCO2/VO2 relationship during heavy, constant work rate exercise reflects the rate of lactic acid accumulation. *Eur. J. Appl. Physiol. Occup. Physiol.* **72**, 25–31

260. Garland, T., Schutz, H., Chappell, M. A., Keeney, B. K., Meek, T. H., Copes, L. E., Acosta, W., Drenowatz, C., Maciel, R. C., van Dijk, G., Kotz, C. M., and Eisenmann, J. C. (2011) The biological control of voluntary exercise, spontaneous physical activity and daily energy expenditure in relation to obesity: human and rodent perspectives. *J. Exp. Biol.* **214**, 206–29

261. Garcia-Valles, R., Gomez-Cabrera, M. C., Rodriguez-Mañas, L., Garcia-Garcia, F. J., Diaz, A., Noguera, I., Olaso-Gonzalez, G., and Viña, J. (2013) Life-long spontaneous exercise does not prolong lifespan but improves health span in mice. *Longev. Heal.* **2**, 14

262. Minokoshi, Y., Kim, Y.-B., Peroni, O. D., Fryer, L. G. D., Müller, C., Carling, D., and Kahn, B. B. (2002) Leptin stimulates fatty-acid oxidation by activating AMP-activated protein kinase. *Nature* **415**, 339–43

263. Gibala, M. (2009) Molecular responses to high-intensity interval exercise. *Appl. Physiol. Nutr. Metab.* **34**, 428–32

264. Gibala, M. J., Little, J. P., Macdonald, M. J., and Hawley, J. A. (2012) Physiological adaptations to low-volume, high-intensity interval training in health and disease. *J. Physiol.* **590**, 1077–84